



Hochschule
Zittau/Görlitz
UNIVERSITY OF APPLIED SCIENCES



Europäische Union

Europa fördert Sachsen.



Europäischer Sozialfonds

Final Report on the Research Project:

**Thermal storage processes around borehole heat exchangers
for heating and cooling of the building with heat pumps**

Chapter A: Numerical Building and System Simulation

M.Sc. Prasanth Subramani

Faculty of Business Administration and Engineering

SUBRAMANI, P. (2021): Numerical Building and System Simulation. – in: GERSCHEL, A.; HERLING, M.; SCHÄFER, T.; STÖCKMANN, L.; SUBRAMANI, P.; WALTER, T.; SCHÜTTE, T.; KRIMMLING, J. & MEINERT, J. (2021): Thermal storage processes around borehole heat exchangers for heating and cooling of the building with heat pumps. – Final Report, HSZG (eds.), **2767**: 7-88; Zittau.

Contents

List of Figures	10
List of Tables	12
List of Symbols	13
List of Abbreviations	16
1 Introduction	17
2 Methodology	18
3 Simulation model in TRNSYS	19
3.1 Building.....	19
3.2 Heating and cooling system.....	21
3.2.1 <i>Heat pump</i>	22
3.2.2 <i>Floor heating system</i>	23
3.2.3 <i>Double depressurized differential manifold (DDV)</i>	23
3.2.4 <i>Chilled ceiling</i>	24
3.2.5 <i>Mixer coupled with PID (Cooling circuit)</i>	24
3.2.6 <i>Ventilation system</i>	25
3.2.7 <i>Control strategy</i>	25
3.2.7.1 <i>Heating</i>	25
3.2.7.2 <i>Cooling</i>	27
3.3 Borehole heat exchanger.....	27
3.4 Simulation period and time step.....	30
3.5 Evaluation criteria	30
3.6 Evaluation boundaries and functions	31
3.7 Intermediate results	33
4 Subtasks	36
4.1 Pressure drop calculation	36
4.1.1 <i>Pressure drop calculation in BHE Field</i>	36
4.1.2 <i>Hydraulic balancing of connecting pipes in BHE field</i>	38
4.1.3 <i>Temperature dependent properties</i>	40
4.1.4 <i>Pressure drop calculation in primary circuit</i>	41
4.2 Double depressurized differential manifold (DDV).....	44
4.3 Automation of parameter variation	45
4.4 Inverter heat pump.....	47

4.4.1	<i>Introduction</i>	47
4.4.2	<i>Simulative analysis of optimization potential</i>	48
4.4.3	<i>Experimental validation of optimization potential by IVHP</i>	49
4.4.4	<i>Validation of optimization potential – Literature analysis</i>	50
4.4.5	<i>Mathematical modelling</i>	50
4.4.6	<i>Summary</i>	51
4.5	Heating / cooling demand variation	51
4.5.1	<i>Introduction</i>	51
4.5.2	<i>Building with predominant heating demand</i>	52
4.5.3	<i>Building with predominant cooling demand</i>	52
4.5.4	<i>Building with equal heating and cooling demand</i>	58
5	Parameter studies	64
5.1	Parameter studies 1	64
5.1.1	<i>Variant matrix</i>	64
5.1.2	<i>Results</i>	65
5.2	Parameter studies 2	73
5.2.1	<i>Variant matrix</i>	73
5.2.2	<i>Results</i>	74
5.3	Parameter studies 3	79
5.3.1	<i>Variant matrix</i>	79
5.3.2	<i>Results</i>	79
6	Conclusion	87
	Literature	88

List of Figures

Fig. A-2.1	Constructive parameter of BHE field (Earth Energy Designer Vers. 3.22).....	18
Fig. A-3.1	Office building 3D sketch.....	19
Fig. A-3.2	Substitute building for simulation.....	20
Fig. A-3.3	Heating and cooling system schema.....	21
Fig. A-3.4	Characteristic curve for heat pump SmartHeat Titan 274 BW.....	22
Fig. A-3.5	Mixer circuit used for cooling.....	25
Fig. A-3.6	Monthly energy demand and peak load.....	28
Fig. A-3.7	Balance boundaries for the performance analysis.....	31
Fig. A-3.8	Total primary energy consumption – borehole length 4,000 m.....	34
Fig. A-3.9	Comparison of first year and 15-year simulation results.....	35
Fig. A-4.1	The resistance of BHEs.....	37
Fig. A-4.2	Divider / mixer (WAGNER 2012).....	38
Fig. A-4.3	Connecting pipes in BHE field.....	39
Fig. A-4.4	Length and pressure drop of connecting pipes in BHE.....	39
Fig. A-4.5	Hydraulic balancing of connecting pipes in BHE field.....	40
Fig. A-4.6	Primary circuit of heat pump.....	42
Fig. A-4.7	DDV circuit.....	44
Fig. A-4.8	Macros in excel to create batch file.....	46
Fig. A-4.9	Batch file 1.....	46
Fig. A-4.10	Batch file 2.....	46
Fig. A-4.11	Batch file 3.....	47
Fig. A-4.12	Macros in excel to arrange deck file.....	47
Fig. A-4.13	Demonstration of cyclic losses through simulative analysis.....	48
Fig. A-4.14	Experimental validation of optimization potential by IVHP.....	49
Fig. A-4.15	Characteristic curve field for Hoval UltraSource T comfort (13).....	51
Fig. A-4.16	Monthly energy demand and peak load.....	53
Fig. A-4.17	Characteristic curve of heat pump variant SmartHeat Titan 115 BW R.	54
Fig. A-4.18	Monthly energy demand and peak load.....	58
Fig. A-4.19	Characteristic curve of heat pump variant SmartHeat Titan 139 BW R.	59
Fig. A-5.1	Total primary energy consumption $Q_{P,tot}$ for parameter studies 1 (4,000 m vs. 5,000 m).....	65

Fig. A-5.2	Total primary energy consumption $Q_{P,tot}$ for parameter studies 1 (Total BHE length 5,000 m).	66
Fig. A-5.3	$Q_{P,tot}$ vs. $Q_{P,H}$ vs. $Q_{P,C}$ for parameter studies 1 (5,000 m, 0.03 K/m).	67
Fig. A-5.4	$Q_{P,H}$ vs. $\bar{T}_{out,BHE,H}$ for parameter studies 1 (5,000 m, 0.03 K/m).	68
Fig. A-5.5	$Q_{P,C}$ vs. $\bar{T}_{out,BHE,H}$ for parameter studies 1 (5,000 m, 0.03 K/m).	69
Fig. A-5.6	$\bar{T}_{out,BHE,H}$ (15-year average) for parameter studies 1 (5,000 m).	70
Fig. A-5.7	$\bar{T}_{out,BHE,H}$ (annual average) for parameter studies 1 (5,000 m).	71
Fig. A-5.8	Bivalent point vs. operation period of auxiliary heater/cooler (parameter studies 1).	72
Fig. A-5.9	$Q_{P,tot}$ for parameter studies 2 (3,000 m).	74
Fig. A-5.10	$Q_{P,tot}$ vs. $Q_{P,H}$ vs. $Q_{P,C}$ for parameter studies 2 (3,000 m, 0.065 K/m).	75
Fig. A-5.11	$\bar{T}_{out,BHE,H}$ (15-year average) for parameter studies 2 (3,000 m).	76
Fig. A-5.12	$\bar{T}_{out,BHE,C}$ (15-year average) for parameter studies 2 (3,000 m).	77
Fig. A-5.13	$\bar{T}_{out,BHE,C}$ (annual average) for parameter studies 2 (3,000 m).	77
Fig. A-5.14	Bivalent point vs. operation period of auxiliary heater / cooler (parameter studies 2).	78
Fig. A-5.15	$Q_{P,tot}$ for parameter studies 3 (4,000 m).	80
Fig. A-5.16	$Q_{P,tot}$ vs. $Q_{P,H}$ vs. $Q_{P,C}$ for parameter studies 3 (4,000 m, 0.065 K/m).	81
Fig. A-5.17	$\bar{T}_{out,BHE,H}$ (15-year average) for parameter studies 3 (4,000 m).	82
Fig. A-5.18	$\bar{T}_{out,BHE,C}$ (15-year average) for parameter studies 3 (4,000 m).	83
Fig. A-5.19	$\bar{T}_{out,BHE,C}$ (annual average) for parameter studies 3 (4,000 m, 0.01 K/m vs. 0.03 K/m).	84
Fig. A-5.20	$\bar{T}_{out,BHE,C}$ (annual average) for parameter studies 3 (4,000 m, 0.065 K/m vs. 0.09 K/m).	84
Fig. A-5.21	Bivalent point vs. operation period of auxiliary heater / cooler (parameter studies 3).	85

List of Tables

Tab. A-3.1	Building envelope and U-Value.....	20
Tab. A-3.2	Peak load and total energy demand of the building.	20
Tab. A-3.3	Correction factor calculation.	20
Tab. A-3.4	Floor heating system design parameter.	23
Tab. A-3.5	Mass flow rate calculation.....	23
Tab. A-3.6	Chilled ceiling design parameters.	24
Tab. A-3.7	Mass flow rate calculation.....	24
Tab. A-3.8	EED design parameters and results.	29
Tab. A-3.9	SPF as efficient criteria.	30
Tab. A-3.10	Variant matrix for initial parameter studies.	33
Tab. A-4.1	Drag coefficient of components.	42
Tab. A-4.2	Parameters and inputs required in Type1994 TRNSYS.	43
Tab. A-4.3	Building envelope and U-Value with passive house standard.	52
Tab. A-4.4	Energy demand and correction factor.	53
Tab. A-4.5	Floor heating system design parameter.	55
Tab. A-4.6	Mass flow rate calculation.....	55
Tab. A-4.7	Chilled ceiling system design parameter.....	55
Tab. A-4.8	Mass flow rate calculation.....	56
Tab. A-4.9	Properties of refrigerant and boreholes with simulation results.	57
Tab. A-4.10	Building envelope and U-Value with KfW55 standard.	58
Tab. A-4.11	Building envelope and U-Value with passive house standard.	59
Tab. A-4.12	Floor heating system design parameter.	60
Tab. A-4.13	Mass flow rate calculation.....	60
Tab. A-4.14	Chilled ceiling system design parameter.....	61
Tab. A-4.15	Mass flow rate calculation.....	61
Tab. A-4.16	Properties of refrigerant and boreholes with simulation results.	62
Tab. A-5.1	Variant matrix for parameter studies 1.	64
Tab. A-5.2	Variant matrix for parameter studies 2.	73
Tab. A-5.2	Variant matrix for parameter studies 3.	79

List of Symbols

Symbol	Parameter	Unit
α	Angle between divider and connection pipe	[°]
A_a	Cross sectional area of connection pipe	[m ²]
A_s	Cross sectional area of the mixer	[m ²]
A_O	Cross sectional area of the divider inlet	[m ²]
A_v	Cross sectional area of the divider	[m ²]
$CS_{Aux,C}$	Control signal for operation of the auxiliary cooler	[-]
$CS_{Aux,H}$	Control signal for operation of the auxiliary heater	[-]
CS_{HP}	Control signal for heat pump operation	[-]
$CS_{P,C}$	Control signal for passive cooling system operation	[-]
CS_{PID}	Control signal by PID controller	[-]
$CS_{PID,C}$	Control signal by PID controller for cooling	[-]
$CS_{PID,H}$	Control signal by PID controller for heating	[-]
$CS_{R,Set}$	Control signal to maintain the return flow temperature in setpoint value	[-]
d_v	Diameter of divider	[m]
D	Diameter	[m]
G	Glycol content in heat carrier fluid	[%]
f_P	Primary energy factor for electricity	[-]
k	Roughness of pipe	[mm]
λ	Friction number	[-]
L	Length	[m]
μ	Dynamic viscosity	[Pa·s]
\dot{m}	Minimum mass flow	[kg/h]
m_{1-4}	Mass flow	[kg/h]
m_{HP}	Mass flow to the condenser side of heat pump	[kg/h]
m_R	Return mass flow from distribution system	[kg/h]
m_S	Supply mass to the distribution system	[kg/h]
n	Number of boreholes (= total borehole length / borehole depth)	[-]
N	Total number of variants	[-]
N_1	Total number of variants with gradient 0.01 K/m	[-]
N_2	Total number of variants with gradient 0.03 K/m	[-]
N_3	Total number of variants with gradient 0.065 K/m	[-]
N_4	Total number of variants with gradient 0.09 K/m	[-]
ρ	Density	[kg/m ³]

Symbol	Parameter	Unit
ρ_{brine}	Density of brine	[kg/m ³]
Δp	Pressure drop	[bar or kPa]
Δp_a	Pressure drop in all component in between divider and mixer	[bar or kPa]
$\Delta p_{vs,z}$	Pressure drop of all components including divider and mixer	[bar or kPa]
$P_{Aux,C}$	Energy consumption by the auxiliary cooler	[kWh]
$P_{Aux,H}$	Energy consumption by the auxiliary heater	[kWh]
P_{comp}	Energy consumption by compressor	[kWh]
$P_{P,brine,C}$	Energy consumption by refrigerant circulation pump for cooling	[kWh]
$P_{P,brine,H}$	Energy consumption by refrigerant circulation pump for heating	[kWh]
$P_{P,DDV}$	Energy consumption by circulation pump between DDV and Heat pump	[kWh]
$P_{P,dist,C}$	Energy consumption by circulation pump for cooling energy distribution	[kWh]
$P_{P,dist,H}$	Energy consumption by circulation pump for heat distribution	[kWh]
Q_E	End energy consumption	[kWh]
$Q_{E,C}$	End energy consumption for cooling	[kWh]
$Q_{E,H}$	End energy consumption for heating	[kWh]
$Q_{E,tot}$	Total end energy consumption	[kWh]
Q_{Use}	Energy consumed by user in form of heat or cold	[kWh]
$Q_{Use,C}$	Heat extracted from the building	[kWh]
$Q_{Use,H}$	Heat supplied to the building	[kWh]
Q_P	Primary energy consumption	[kWh]
$Q_{P,C}$	Primary energy consumption for cooling	[kWh]
$Q_{P,C,min}$	Minimum primary energy consumption for cooling	[kWh]
$Q_{P,H}$	Primary energy consumption for heating	[kWh]
$Q_{P,H,min}$	Minimum primary energy consumption for heating	[kWh]
$Q_{P,tot}$	Total primary energy consumption	[kWh]
$Q_{P,tot,min}$	Minimum total primary energy consumption	[kWh]
R	Resistance	[kg/m ⁷]
R_{tot}	Resistance to flow by whole BHE field	[kg/m ⁷]
Re	Reynolds number	[-]
SPF_C	Seasonal performance factor for cooling	[-]
SPF_H	Seasonal performance factor for heating	[-]
SPF_{tot}	Total seasonal performance factor	[-]
T_a	Outside air temperature	[°C]

Symbol	Parameter	Unit
$T_{a,mov,avg}$	24-h moving average of outside air temperature	[°C]
T_R	Temperature of the fluid returning from the distribution system	[°C]
$T_{R,Set}$	Maximum allowed return fluid temperature from heat distribution system	[°C]
T_S	Supply fluid temperature	[°C]
ΔT	Temperatur difference	[K]
T_f	Temperature of the fluid in primary circuit of heat pump	[°C]
$T_{out,BHE}$	Fluid outlet temperature from BHE	[°C]
$T_{out,BHE,C}$	BHE field fluid outlet temperature during heat supply to ground	[°C]
$\bar{T}_{out,BHE,C}$	BHE field fluid outlet temperature averaged over the heat supply period	[°C]
$T_{out,BHE,H}$	BHE field fluid outlet temperature during heat extraction from the ground	[°C]
$\bar{T}_{out,BHE,H}$	BHE field fluid outlet temperature $\mu\mu$ averaged over the heat extraction period	[°C]
μ_k	Kinematic viscosity	[m ² /s]
v	Fluid velocity	[m/s]
V	Volumetric flow of complete system	[m ³ /s]
$Var1$	Total borehole length	[m]
$Var2$	Borehole depth	[m]
$Var3$	Borehole spacing	[m]
$Var4$	Hydraulic connection of BHEs	[-]
$Var5$	Geothermal Gradient	[K/m]
\dot{V}_0	Volume flow at divider inlet	[m ³ /s]
w_a	Velocity of fluid in connection pipe	[m/s]
w_0	Fluid velocity at divider inlet	[m/s]
ζ	Drag coefficient	[-]
ζ_a	Total drag coefficient of all components in between divider and mixer	[-]
$\zeta_{o,vs,z}$	Drag coefficient of divider/mixer and all components in between them	[-]

List of Abbreviations

Abbreviation	Wording
BB 1-4	Balance boundary 1-4
BHE	Borehole Heat Exchanger
COP	Coefficient of performance
DDV	Double depressurized differential manifold
EED	Earth Energy Designer
HSZG	Hochschule Zittau / Görlitz, University of Applied Sciences
IVHP	Inverter Heat Pump
NWFG	Junior Research Group (Nachwuchsforschergruppe)
PEC	Primary energy consumption
PID	Proportional-integral-derivative
SPF	Seasonal performance factor
TABS	Thermally activated building system

1 Introduction

Geothermal energy is a reliable source for the combined heating and cooling application because of its less fluctuating temperature. Though it is an efficient source, there exist complication in designing a larger borehole heat exchanger field for the combined application of heating and cooling. Thus, an analysis of Borehole Heat Exchanger (BHE) for the combined application of heating and cooling of the building was carried out in F-W HSZG from 2013 to 2014. As a follow-up, Promotion Haack worked on the constructive design of the BHE field for the combined application of heating and cooling of an office building. In 2017, an interdisciplinary research group with four work packages containing five young researchers (NWFG Erdwärme) from various backgrounds was formed at F-W HSZG. The aim of this research group is to analyse the thermal storage process around BHE for the combined application of heating and cooling. The primary responsibility of this work is carrying out simulative analysis for such purpose. With the aid of previous results and resources, the research work is continued. For common research goals, resources and information are exchanged mutually with Promotion Haack.

Multiple researchers worked earlier on the optimizing of the BHE field for combined application with analytical models. These optimization works ignored the transient effect mostly. Hence, there is a requirement for optimizing the constructive design of the BHE field with transient simulations. For this purpose, a research concept was developed in Promotion Haack. The concept involves pre-examination of optimization potential by constructive design, development of transient simulation model in TRNSYS replicating real-time behaviour of system and building, and parameter studies with the simulation model. Preliminary investigations have shown significant optimization potential. For further investigation with TRNSYS, multiple components were modelled for completion of the simulation model. Additionally, multiple subtasks essential for validating the simulation model and widening the research scope were worked out. Finally, various parameter studies were carried out with this simulation model to provide a generalized solution for designing a borehole heat exchanger.

In addition to the constructive design of BHEs, energy optimization potential through Inverter Heat Pump (IVHP) were explored. During the research, it was observed that the efficiency of the system could be improved further by using IVHP. The efficiency potential of IVHP, with air as a source, has been answered already. Meanwhile, satisfactory answers are not provided with the ground as a source. Besides, there exists no commercial model for IVHP in TRNSYS. Though the final goal of the task cannot be reached during the project period, preliminary investigations have shown successful potential for optimization. This preliminary investigation will be used to generate a follow-up project at the Zittau/Görlitz University of Applied Science.

2 Methodology

Optimization of the constructive design of BHEs for the combined application of heating and cooling of the building is carried out through simulative analysis using transient system simulation tool TRNSYS. This research work focuses on larger systems (> 30 kW), which require a larger BHE field. For this purpose, a non-residential building is designed. Initially, the research concept was developed. Then suitable heat/cold generation and distribution systems were planned, designed, and sized. After that, a simulation model was developed in TRNSYS. Here, the system components unavailable for our research work are developed within the research group. Finally, various parameter studies were carried out with the help of server technologies specially designated for NWFG Erdwärme in Zittau/Görlitz University of applied science. The crucial parameter varied in simulation analysis are

- (1) **Use energy ratio:** In combined applications, the use energy ratio (ratio of heat energy demand by building to cooling demand) plays a vital role in designing BHEs. Hence, to provide a generalized solution, three-building models with different ratios (equal heating and cooling demand, predominant heating demand, and predominant cooling demand) were designed. All building model has the same envelope but varies in standard and occupancy density.
- (2) **Location dependent properties:** Multiple location-dependent properties influence the design criteria and operational efficiency. The scope of this research work is limited to the geothermal gradient since it is the parameter that influences the tendency of design criteria.
- (3) **Constructive design** (Fig. A-2.1): This work intends to find the optimum construction parameter. Hence, all possible construction parameters (Number of boreholes, depth, spacing, borehole pipe diameter, hydraulic connections of BHEs in the field) are varied in parameter studies.

All the simulated variants are evaluated under ecological, energetic, and economic criteria. At this moment, an energetic evaluation is carried out. This approach has to be implemented in the simulation model and evaluated.

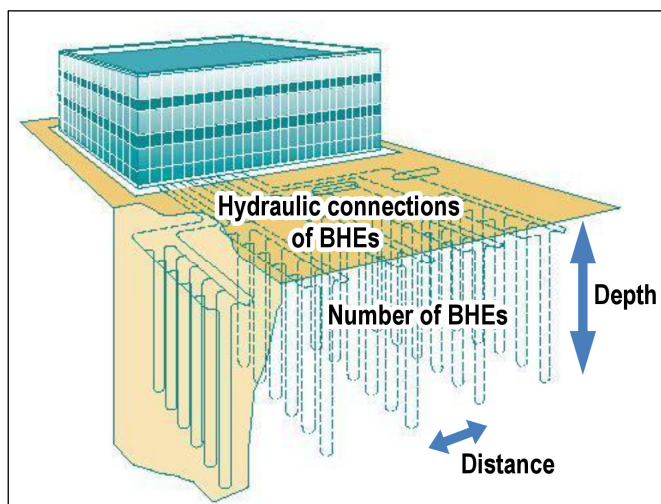


Fig. A-2.1
Constructive parameter of BHE field
(Earth Energy Designer Vers. 3.22).

3 Simulation model in TRNSYS

A simulation model replicating real-time operation is essential for the optimization of the constructive design of BHE fields. A commercial transient system simulation tool TRNSYS is used for this simulative analysis. TRNSYS has enormous pre-modelled components, the possibility for performing parameter studies, and provides an environment to model new components. Hence, it is the perfect choice for our research. The model developed in TRNSYS simulates the working of individual components and their interaction with the surrounding system and environment. Every model (called as types in TRNSYS) is parameterized to replicate the behaviour of specific systems/components. Hence, it is necessary to have details of each system before modelling. In this section, system design, information of each component, and its implementations in TRNSYS are explained.

3.1 Building

An L-shaped office building with six floors (Fig. A-3.1), each height of 3.65 m, is designed for this analysis. The building is sketched in Google SketchUp, and its properties / usage are defined in TRNBuild. Building standard is chosen according to EnEV 2013. Building usage, occupation profile/density, and ventilation are defined according to DIN V 18599. Thickness and U-Value of the critical building structure are listed in Tab. A-3.1. Type56 model the building's thermal behaviour in TRNSYS using the building description file generated by TRNBuild. For thermal energy calculation, the complete building is grouped into 18 zones (twelve big zones and six small zones). Every big zone has a floor area of 360 m² (12 m x 30 m) and 31 windows. Each small zone has a floor area of 144 m² (12 m x 12 m) and 10 windows. Default weather data from TRNSYS for the location Potsdam, Germany, is used for this calculation. Results of thermal energy demand calculation are listed in Tab. A-3.2.

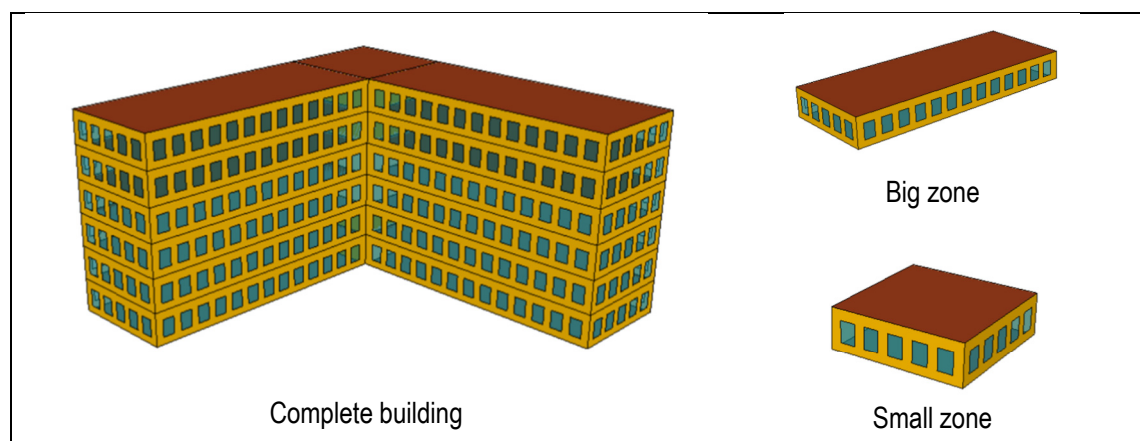


Fig. A-3.1 Office building 3D sketch.

Tab. A-3.1 Building envelope and U-Value.

Parameter	Unit	Ground floor	Outer wall	Inner wall	Ceiling	Roof
Thickness	[m]	0.38	0.455	0.126	0.38	0.485
U-Value	[W/m ² ·K]	0.354	0.287	0.358	0.354	0.207

Tab. A-3.2 Peak load and total energy demand of the building.

	Peak load [kW]	Total energy [kWh]	Ratio [%]
Heating	239.04	231,286.5	79
Cooling	136.5	62,802	21

As this research work involves a massive number of parameter studies, simulation of a complete system with such a large building needs much computational effort. Building and distribution system significantly influences computational time compared to other components in the simulation model. Hence, the computational effort is reduced by scaling down the building and distribution system to a single floor, as shown in the Fig. A-3.2 (only 3rd floor). The correction factor, which is the ratio of the sum of the peak load of a similar zone on all floors to the peak load in the respective zone on the 3rd floor, is introduced to alter the inlet and outlet mass flow rate of the building distribution system. In this way, heat generation systems work at their full potential, but the distribution system's size is reduced. Correction factor for three blocks (a group of similar zones on all floor) for heating and cooling operation is shown in Tab. A-3.3.

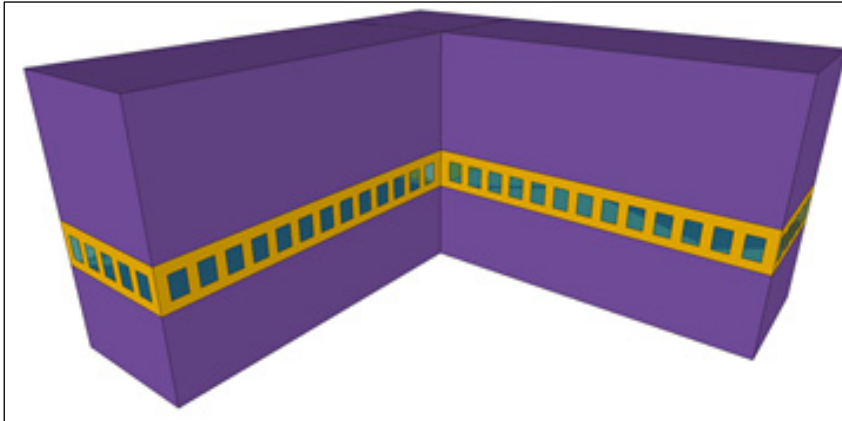


Fig. A-3.2 Substitute building for simulation.

Tab. A-3.3 Correction factor calculation.

Parameter	Unit	Block A		Block B		Block C	
		$Q_{Use,H}$	$Q_{Use,C}$	$Q_{Use,H}$	$Q_{Use,C}$	$Q_{Use,H}$	$Q_{Use,C}$
Q_{Use} floor 3	[kW]	6.4769	4.0477	15.984	9.0205	16.146	10.904
Sum of Q_{Use} of all six floors	[kW]	40.096	22.912	98.992	51.051	99.95	62.537
Correction factor	[-]	6.19	5.66	6.19	5.66	6.19	5.74

3.2 Heating and cooling system

Once building and its energy demand are known, it is necessary to choose appropriate heat generation and distribution system. Thermally activated building system (TABS), by integrating building structures as a thermal energy storage, have proven to be economically efficient system. Main disadvantage is slow reaction for sudden fluctuation in load (For example: unexpected gathering of large group of people). As rapid change of usage profile in office buildings are less expected, TABS can be an efficient system for this purpose.

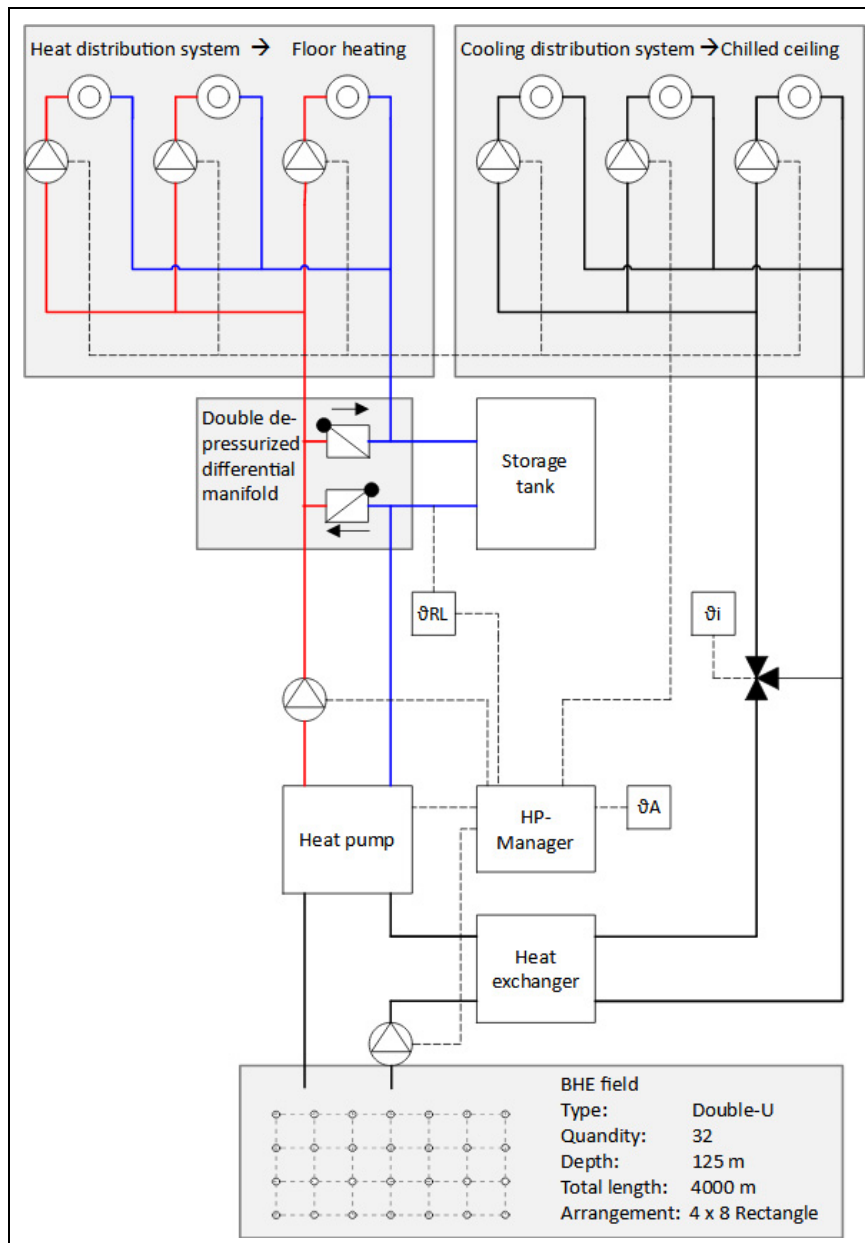


Fig. A-3.3
Heating and cooling
system schema.

Floor heating and the chilled ceiling are commonly used as a heat and cold distribution system, respectively, in TABS. Less operating temperature for heating and higher operating temperature for cooling (mostly passive cooling) improves the efficiency of the complete system. A ground-coupled heat pump is selected as a heat generation system. Cooling

of the building is carried out by coupling the chilled ceiling directly with BHE through a heat exchanger. The schema of the complete heating and cooling system is shown in Fig. A-3.3. The system design is carried out based on the initial energy demand calculated by TRNSYS. The design of each component and modelling of components in TRNSYS is explained in the upcoming section.

3.2.1 Heat pump

As our focus is on a monovalent heating system, the heat pump capacity should be larger than or equal to the building peak load (239.04 kW). Hence, heat pump SmartHeat Titan 274 BW with a nominal capacity of 269.39 kW and COP of 4.36 (at B0/W35) is chosen (Fig. A-3.4).

The heat pump is modelled using Type401 in TRNSYS. It maps the heat pump based on the manufacture provided characteristic curves for heating capacity and electric power. These curves depict heating capacity and electric power as a function of evaporator inlet temperature and condenser outlet temperature. Coefficients of the biquadratic polynomial have to be calculated using these curves. A separate excel file is provided by the developer along with Type401 for this purpose. These coefficients are feed to Type401 through a text file. This polynomial function represents steady-state behaviour. Other factors like cyclic losses, frosting and defrosting losses, etc., are modelled in Type401. In our analysis, frosting and defrosting losses are neglected. Type401 describes the cyclic losses using an exponential function, which requires two parameters: heating (3 minutes) and cooling (5 minutes) constant.

Our design criteria for the BHE field design is that evaporator inlet temperature is not supposed to fall below $-5\text{ }^{\circ}\text{C}$. In parameter studies, multiple variants fall in this category. The heat generation system is also equipped with an auxiliary heater (COP = 1), which supplies required heat if the evaporator inlet temperature falls below $-5\text{ }^{\circ}\text{C}$. The intention of this auxiliary heater is to identify the variants with which monovalent heating is not possible.

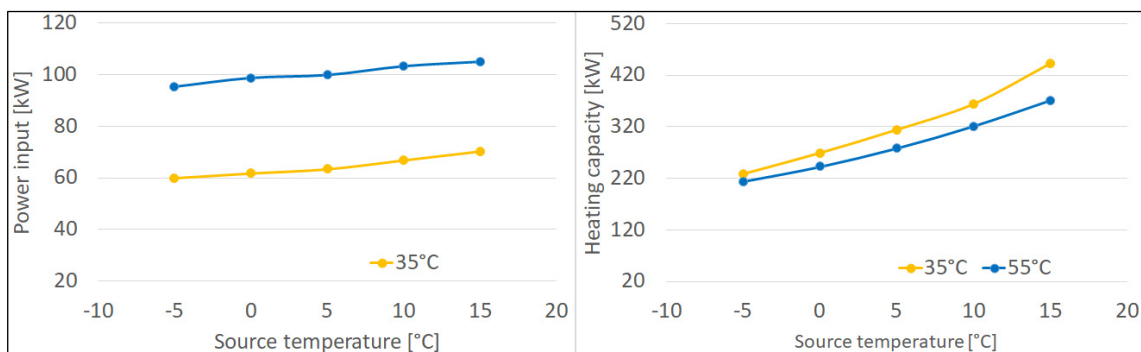


Fig. A-3.4 Characteristic curve for heat pump SmartHeat Titan 274 BW.

3.2.2 Floor heating system

The primary advantage of using a floor heating system is its low operating temperature and high comfortability. It also offers a high degree of design freedom. Even though installation cost is higher than the conventional system, energy bill saving is significant. The initial design of the floor heating system is carried out in TGA-Heizung by Hottgenroth Software. The floor heating system in TRNSYS is modelled according to TGA-Heizung. Design parameters used for modelling floor heating system is listed in Tab. A-3.4. Fluid flow rate and temperature are varied to maintain the room temperature at the expected level. Mass flow rate to individual zone calculated using peak load, power consumption by the circulation pump, and ΔT is listed in Tab. A-3.5. The fluid flow rate for every zone is varied using an individual PID controller. Power consumption at maximum flow rate is calculated using pressure drop, which is varied linearly for variable mass flow rate. Supply temperature is controlled using the return flow control method suggested by DIMPLEX (explained in section 3.2.6).

Tab. A-3.4 Floor heating system design parameter.

Design Parameter	Unit	Value
Pipe spacing (center to center)	[m]	0.15
Pipe outside diameter	[m]	0.014
Pipe wall thickness	[m]	0.002
Pipe wall conductivity	[KJ/(h·m·K)]	1.26

Tab. A-3.5 Mass flow rate calculation.

Parameter	Unit	Block A	Block B	Block C
Peak load of floor 3	[kW]	7.1	17.65	17.65
Fluid heat capacity	[kJ/kg]	4.19	4.19	4.19
ΔT	[K]	7	7	7
Maximum mass flow rate	[kg/h]	871	2,166	2,166
Maximum power consumption by the circulation pump	[W]	133	506	506

3.2.3 Double depressurized differential manifold (DDV)

DDV is used for hydraulic decoupling of the heat generation unit with a distribution circuit with a variable mass flow rate. Conventional heating systems with buffer storage have a higher operating temperature, which negatively influences energetic efficiency, which can be avoided by using buffer storage in return flow with DDV to decouple heat generation and distribution unit. Hydraulic decoupling is essential because of the different mass flow in the heat generation unit and distribution system (mass flow is variable in our model). A mathematical model for DDV was not available for TRNSYS. Hence, a new TRNSYS model (Type1991) is created. The modelling approach is explained in section 4.2. The storage tank in the return flow is sized as 7.5 m³.

3.2.4 Chilled ceiling

Chilled ceiling coupled with BHEs (passive cooling) proved to be delivering high comfort at reduced running cost. Hence, the chilled ceiling is chosen as a cooling distributing system. Design parameters for the chilled ceiling are shown in Tab. A-3.6. Pipe spacing is chosen based on the “*Leistungskalkulator Flächenkühlung*” tool developed by PURMO. It calculates the specific cooler power (W/m^2) based on pipe spacing, the difference between room and fluid temperature, and thermal resistance. Power calculation in this tool is carried out as per DIN EN 1264-5:2020-02. During the cooling period, the room temperature is controlled by variable mass flow combined with a constant supply setpoint temperature of 19 °C. Mass flow to each zone is controlled by an individual PID controller. The maximum flow rate is chosen based on the peak load of the building (Tab. A-3.7). Power consumption at maximum flow rate is calculated using pressure drop, which is varied linearly for variable mass flow rate.

Tab. A-3.6 Chilled ceiling design parameters.

Design Parameter	Unit	Value
Pipe spacing	[m]	0.15
Pipe inside diameter	[m]	0.0136
Specific norm mass flow	[kg/(h·m ²)]	19.5
Specific norm power	[KJ/(h·m ²)]	136.1

Tab. A-3.7 Mass flow rate calculation.

Parameter	Unit	Block A	Block B	Block C
Peak load	[kW]	4.04	9.02	10.9
Fluid heat capacity	[kJ/kg]	4.19	4.19	4.19
ΔT	[K]	2	2	2
Required mass flow rate	[kg/h]	1,738	3,875	4,684
Maximum power consumption by the circulation pump	[W]	260	1,800	2,341

3.2.5 Mixer coupled with PID (Cooling circuit)

As explained in the previous section, the supply temperature is supposed to be maintained at 19 °C. The BHE field is mostly colder than 19 °C, which reflects in fluid temperature as well. Hence, to maintain 19 °C supply fluid temperature, mixing circuit as shown in Fig. A-3.5 is used in between the chilled ceiling and heat exchanger. PID controller is used to quantifying mass flow diversion to supply flow (m_2). The control variable of the PID controller is the supply fluid temperature (T_s) with setpoint 19 °C. This circuit controls the mass flow through the heat exchanger so that the temperature of fluid after mixing is

19 °C. The circuit is implemented in TRNSYS by connecting the already available components divider (type11h), mixer (type11f), and heat exchanger (type5). Divider and mixer are just a couple of tee pieces that divide fluid flow into multiple or combine multiple flows. A counter-flow heat exchanger with a high overall heat transfer coefficient (70,000 W/K) is used.

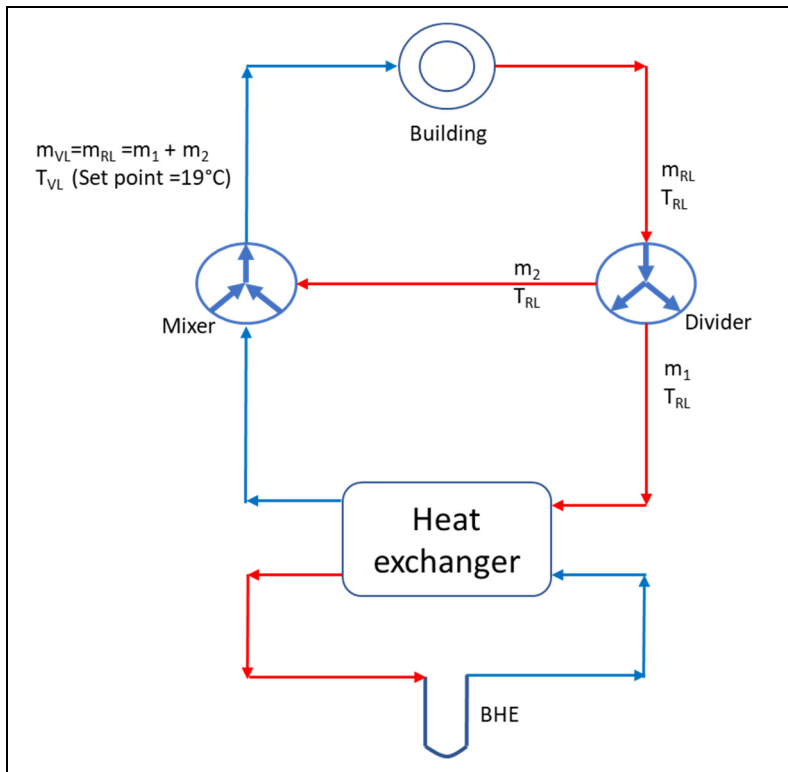


Fig. A-3.5
Mixer circuit used for cooling.

3.2.6 Ventilation system

For the selected energy standards, mechanical air ventilation was not necessary. Hence only free air ventilation at the rate of 0.67 1/h, which fulfils the minimum air exchange rate requirements by DIN EN 15251:2012-12, is used. During weekends the air exchange rate is reduced to 0.57 1/h.

3.2.7 Control strategy

For efficient heating / cooling, it is necessary to choose the right control strategy. Room temperatures in office buildings should be maintained at 21 °C during the heating period and 24 °C during the cooling period.

3.2.7.1 Heating

Room temperature is controlled by varying the mass flow rate and temperature of the heating fluid. The mass flow rate of the floor heating system in each room is controlled using a separate PID-Controller, with room temperature as the control variable and 21 °C

as the setpoint. The mass flow rate is allowed to fluctuate between 15 % and 100 % of the designed value. To mathematically represent this in TRNSYS, every PID controller provides the control signal CS_{PID} varies between 1 to 0. Maximum mass flow is required if the signal is 1, and 0 represents no real heat demand from the respective zone. If any of the PID signals is greater than 0, heat energy is required from the heat generation circuit.

Fluid temperature is varied by controlling maximum return fluid temperature through a polynomial function. A polynomial function is derived by a heating curve provided by DIMPLEX.

$$T_{R,Set} = -0.0061 \cdot T_{a,mov,avg}^2 - 0.5247 \cdot T_{a,mov,avg} + 32.904 \quad (A.1)$$

Heat generator (heat pump and auxiliary heater) are regulated so that return-fluid temperature from the floor heating unit is maintained under TR, set by polynomial function A.1. $CS_{R,Set}$ is defined in TRNSYS, which denotes that fluid needs to be heated. $CS_{R,Set}$ is set to zero when the fluid temperature reaches $T_{R,Set}$ and set back to 1 when fluid cools down 2 K less than $T_{R,Set}$. The above-described control signal is generated in TRNSYS using Type165b.

The heat generator system has to be switched on if there is heat demand from any zone and the fluid return temperature from the floor heating system is not in the defined range. Additional safety parameter ($T_{a,mov,avg}$) is introduced in the generation control signal for the heat generation unit because the heat generation system is not supposed to react to minute fluctuations in room temperature in summer. The heat generator is supposed to work only if $T_{a,mov,avg}$ is less than 14°C. This can be mathematically expressed as

$$T_{a,mov,avg} < 14 \quad \& \quad \sum_1^3 CS_{PID,H}(i) > 0 \quad \& \quad CS_{R,Set} = 1 \quad (A.2)$$

Besides, it is necessary to decide which of the heat generator supply required heat. Fluid outlet temperature from BHE ($T_{out,BHE}$) decides whether the heat pump should generate the required heat or the auxiliary heater. When $T_{out,BHE} > -5$ °C, the heat pump supplies the heat demand. Once this limit is reached, the heat pump is switched off, and the auxiliary heater supplies the required heat. The heat pump remains switched-off until $T_{out,BHE}$ reaches -4 °C with a minimum of 18 minutes. Control signals CS_{HP} and $CS_{Aux,H}$ are generated in TRNSYS by using Type40 and Type911.

So, the heat pump is switched-on ($CS_{HP} = 1$) if

$$T_{a,mov,avg} < 14 \quad \& \quad \sum_1^3 CS_{PID,H}(i) > 0 \quad \& \quad CS_{R,Set} = 1 \quad \& \quad CS_{Aux,H} = 1 \quad (A.3)$$

The auxiliary heater is switched-on ($CS_{Aux,H} = 1$) if

$$T_{a,mov,avg} < 14 \quad \& \quad \sum_1^3 CS_{PID,H}(i) > 0 \quad \& \quad CS_{R,Set} = 1 \quad \& \quad CS_{HP} = 1 \quad (A.4)$$

3.2.7.2 Cooling

The room temperature during the cooling period is controlled by variable mass flow combined with a constant supply setpoint temperature of 19 °C. Mass flow to each zone is controlled by an individual PID controller. The mixing circuit, explained in section 3.2.5, is used to maintain a 19 °C supply temperature.

The design criteria for the BHE field is that the fluid outlet temperature does not exceed 20 °C. Due to parameter variation, multiple variants exist where fluid outlet temperature from BHEs is greater than 20 °C. In this case, the auxiliary cooler cools the fluid to 19 °C. This auxiliary cooler intends to identify construction by which monovalent cooling is not possible. The complete cooling unit is switched off if 24 h moving average of outside air temperature ($T_{a,mov,avg}$) is less than 14 °C.

So, the cooling system is on ($CS_{P,C} = 1$) if

$$T_{a,mov,avg} > 14 \quad \& \quad \sum_{i=1}^3 CS_{PID,C}(i) > 0 \quad (A.5)$$

The auxiliary cooler is on ($CS_{Aux,C} = 1$) if

$$T_{a,mov,avg} > 14 \quad \& \quad \sum_{i=1}^3 CS_{PID,C}(i) > 0 \quad \& \quad T_{out,BHE} > 20 \quad (A.6)$$

3.3 Borehole heat exchanger

In parameter studies, constructive design parameter is varied to find the optimum construction possibilities. For the initial design of the BHE field, the optimization tool EED was used, which determined the optimal design for combined heating and cooling operation for criteria such as the number of BHES, arrangement, borehole spacing, depth of the borehole, total length BHEs, and area of the BHE field. Following constraints were used in EED to list the optimum construction.

- Temperature limits of the average fluid temperature were set at -5 °C for heating operation and 19 °C for cooling operation. The average operating temperature over the considered period (50 years) should be within this limit.
- The geothermal probes are hydraulically connected in parallel.
- Minimum mass flow in individual BHE is limited to ensure turbulent flow, i. e. \dot{m} ($Re = 2,300$).

From the variants suggested by EED, a constructive design with a minimum total length of BHE and rectangular arrangement is chosen, which is used as a base constructive-design for the parameter studies in TRNSYS. Information required for designing of BHE field in EED are

- Monthly load and a peak load of the building, calculated in TRNSYS (Fig. A-3.6).

- 25 % Ethylene Glycol and 75 % water mixture is used as a refrigerant in the BHE circuit. Properties are listed in the Tab. A-3.8.
- Seasonal performance factor (SPF) of the heat pump (4.36).
- Type of BHE and its geometry and properties (Tab. A-3.8).
- Location dependent soil properties and geothermal gradient (Tab. A-3.8).
- Simulation period, which is the design period of the system (50 years).

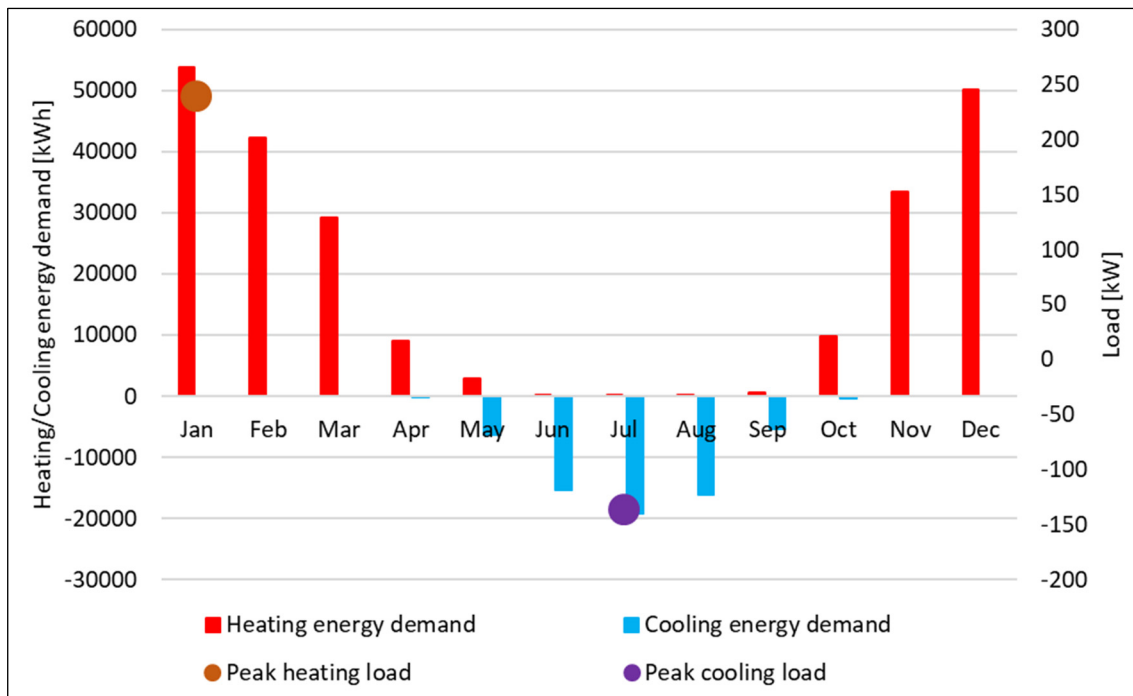


Fig. A-3.6 Monthly energy demand and peak load.

BHE fields are modelled in TRNSYS using the Type557a. With Type557, the BHE field with vertical BHEs (u-pipe 1 to 10, concentric tube) can be simulated. This model is chosen primarily because of the possibility of simulating the BHE field, which lacks other commercially available models. The model assumes that the boreholes are placed uniformly within a cylindrical storage volume of ground. Heat transfer is solved in the model by splitting into simple problems and superimposing it using the linearity of the heat conduction equation. The ground temperature is calculated by the superimposition of three parts; a global temperature, a local solution, and a steady-flux solution. The global and local problems are solved using the explicit finite difference method. The steady flux solution is obtained analytically. Heat transfer between the circulating fluid and the ground is modelled using an analytical, which is then used as a boundary condition in the local problem. Some of the limitations of Type 557 are listed down.

- *BHEs are assumed to be placed uniformly in a cylindrical form. Hence, the arrangement of BHEs cannot be varied. Since research work does not intend to optimize the BHE field arrangement, this limitation will not influence our research work.*

- *The thermal capacity of the borehole and dead time efforts of fluid flow are excluded in the simulation model. This influences the short-term behaviour of BHEs.*

Tab. A-3.8 EED design parameters and results.

	Parameter	Unit	Value
Ground	Ground thermal conductivity	[W/(m·K)]	2.1
	Ground heat capacity	[MJ/(m ³ ·K)]	2.3
	Ground surface temperature	[°C]	8.7
	Geothermal heat flux	[W/m ²]	0.07
Borehole	Configuration	334 ("32 : 4 x 8 rectangle")	
	Borehole depth	[m]	125
	Borehole spacing	[m]	9
	Borehole installation	[-]	Doppel-U
	Borehole diameter	[mm]	152.4
	U-pipe diameter	[mm]	32
	U-pipe thickness	[mm]	2.9
	U-pipe thermal conductivity	[W/(m·K)]	0.4
	U-pipe shank spacing	[mm]	85
	Filling thermal conductivity	[W/(m·K)]	2
	Contact resistance pipe / filling	[(m·K)/W]	0
Thermal resistances	Borehole thermal resistance, fluid/ground	[(m·K)/W]	0.06772
	Borehole thermal resistance, internal	[(m·K)/W]	0.23
Heat carrier fluid	Thermal conductivity	[W/(m·K)]	0.48
	Specific heat capacity	[J/(kg·K)]	3,795
	Density	[kg/m ³]	1,052
	Viscosity	[kg/(m·s)]	0.0052
	Freezing point	[°C]	-14
	Flow rate per borehole	[l/s]	0.52
Base load	Seasonal performance factor (heating)	[-]	4.36
	Seasonal performance factor (cooling)	[-]	1.00E+05

3.4 Simulation period and time step

During simulative analysis, it was observed that long-term simulation is essential to predict the optimization potential by constructive design. For example, dominant heat extraction from the ground leads to continuous cooling of the ground and vice versa. This source temperature reduction decreases the efficiency of the heating system. Also, at some point, the fluid temperature might fall below the minimum requirement. Hence, to provide a plausible suggestion, long term simulation is essential. System design duration of 50 years is perfect for this case. But, simulating all variants for 50 years needs intensive computational effort. During analysis, it was also observed that the stationary BHE field temperature would be reached after 15 years by most variants. Hence, all variants are simulated for 15 years. For convergence of all components in the model, a smaller simulation time step is essential. For example, in our simulation model, pipe volume should be greater than the volumetric flow rate multiplied by the simulation time step. To fulfil this criterion, 5 minutes time step is chosen by trial-and-error method.

3.5 Evaluation criteria

Regarding the task of energetic optimization of the constructive design of the BHE field, there is a question of criteria for optimization. Two factors that decide the energetic efficiency of the system are the SPF and primary energy consumption (PEC). SPF is the ratio of heat supplied to the building to the electrical energy required by the complete system. Q_p is the multiplication of primary energy factors for electricity (f_p) and electrical energy consumption by the system (Q_E). Choosing SPF as evaluation criteria may lead to misinterpretation. This is explained with a fictive example.

As shown in Tab. A-3.9, when SPF is used as evaluation criteria, old building with SPF = 5 sounds better. But, in the perspective of the energy turnaround, a renovated building is efficient because of less energy consumption, which eventually leads to less CO₂ emission. Besides, energy saving cannot be quantified with SPF. For example, when SPF changes from 1 to 2, the change in energy consumption is 100 %, whereas 4 to 5 is only 25 %. For this reason, the evaluation is carried out based on primary energy consumption. Besides, primary energy consumption provides direct information regarding CO₂ emissions.

Tab. A-3.9 SPF as efficient criteria.

Change in SPF [-]	Change in SPF [%]	Change in Q_E [%]	Parameter	Unit	Old building	Renovated building
1 → 2	50	-100	Q_{Use}	[kWh/a]	12,500	8,000
2 → 3	33	-50	Q_E	[kWh/a]	2,500	2,000
3 → 4	25	-33	SPF	[-]	5	4
4 → 5	20	-25				
5 → 6	17	-20				

3.6 Evaluation boundaries and functions

Primary energy consumption (Q_p) of the complete system (BG4) is influenced by factors like heat/cold generator, distribution system, the energy required to extract the heat/cold, etc. The construction with minimum electrical energy required by the circulation pump to extract heat/cold (BG1) need not be efficient construction at BG4 (total energy consumption). But it influences total primary energy consumption. For evaluation purposes, different boundary conditions are created, as shown in Fig. A-3.7. Balance boundary 1 includes just BHE and circulation pumps. In balance boundary-2, heat/cold generator and heat exchanger are added up. Balance boundary 4 includes all the components in the simulation model. Different balance boundaries are chosen for evaluation, depending on the requirement.

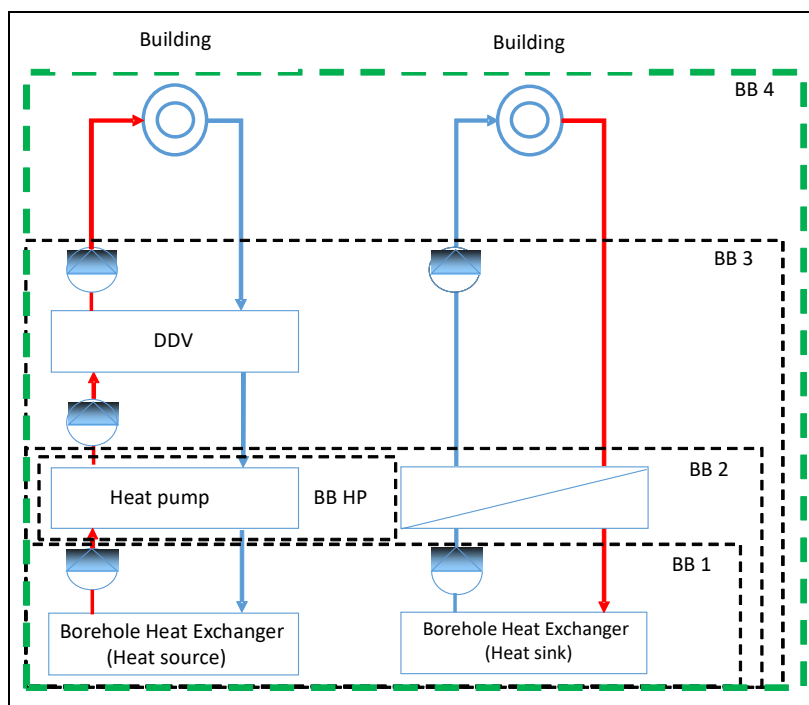


Fig. A-3.7
Balance boundaries for the performance analysis.

The basic formula for calculation of primary energy consumption Q_p and SPF are

$$Q_p = Q_E \cdot f_p \quad \& \quad SPF = \frac{Q_{Use}}{Q_E} \quad (A.7)$$

In this work, primary energy consumption for a complete system (BB4) is evaluated predominantly. Hence, the formula to calculate **different primary energy consumption at balance boundary 4** is listed down. A constant primary energy factor ($f_p = 1.8$) is used to calculate primary energy from end energy.

$$Q_{E,H}(BB4) = P_{comp} + P_{P,brine,H} + P_{P,DDV} + P_{P,dirst,H} + P_{Aux,H} \quad (A.8)$$

$$Q_{P,H}(BB4) = Q_{E,H}(BB4) \cdot f_p \quad (A.9)$$

$$Q_{E,C}(BB4) = P_{P,brine,C} + P_{P,dist,C} + P_{Aux,C} \quad (A.10)$$

$$Q_{P,C}(BB4) = Q_{E,C}(BB4) \cdot f_P \quad (A.11)$$

$$Q_{E,tot}(BB4) = Q_{E,H}(BB4) + Q_{E,C}(BB4) \quad (A.12)$$

$$Q_{P,tot}(BB4) = Q_{P,H}(BB4) + Q_{P,C}(BB4) \quad (A.13)$$

$$SPF_H(BB4) = \frac{Q_{Use,H}}{Q_{E,H}(BB4)} \quad (A.14)$$

$$SPF_C(BB4) = \frac{Q_{Use,C}}{Q_{E,C}(BB4)} \quad (A.15)$$

$$SPF_{tot}(BB4) = \frac{Q_{Use,H} + Q_{Use,C}}{Q_{E,tot}(BB4)} \quad (A.16)$$

With the simulation model, multiple parameters studies were carried out. These parameter studies intend to find the variant with minimum primary energy consumption. Hence, the **minimum value search function** is defined as follows.

$$Q_{P,tot}(i) = (Q_{P,H}(i) + Q_{P,C}(i)) : i = 1, 2 \dots N_j \quad j = 1, 2, 3, 4 \quad (A.17)$$

$$Q_{P,tot,min} = \min(\{Q_{P,tot}(i) : i = 1, 2 \dots N_j\}) \quad j = 1, 2, 3, 4 \quad (A.18)$$

$$Q_{P,H,min} = \min(\{Q_{P,H}(i) : i = 1, 2 \dots N_j\}) \quad j = 1, 2, 3, 4 \quad (A.19)$$

$$Q_{P,C,min} = \min(\{Q_{P,C}(i) : i = 1, 2 \dots N_j\}) \quad j = 1, 2, 3, 4 \quad (A.20)$$

Several **evaluation functions** were used to present the results as a graph. These evaluation functions are listed below. Evaluation function #1 (A.21) evaluates the ratio of total primary energy consumption of the current variant to the minimum primary energy consumption in the respective gradient. Evaluation function #2 (A.22) evaluates the ratio of primary energy consumption for heating of the current variant to the minimum primary energy consumption for heating in the respective gradient. Evaluation function #3 (A.23) evaluates the ratio of primary energy consumption for cooling of the current variant to the minimum primary energy consumption for cooling in the respective gradient.

$$\# 1 = \frac{Q_{P,tot}^j(i)}{Q_{P,tot,min}^j} \quad i = 1, 2 \dots N_j ; j = 1, 2, 3, 4 \quad (A.21)$$

$$\# 2 = \frac{Q_{P,H}^j(i)}{Q_{P,H,min}^j} \quad i = 1, 2 \dots N_j ; j = 1, 2, 3, 4 \quad (A.22)$$

$$\# 3 = \frac{Q_{P,C}^j(i)}{Q_{P,C,min}^j} \quad i = 1, 2 \dots N_j ; j = 1, 2, 3, 4 \quad (A.23)$$

The average fluid outlet temperature of the BHE field during the heating/period is evaluated to present the results of parameter studies. Formula to calculate this average temperature is presented in down.

$$\bar{T}_{out,BHE,H} = \frac{\sum_{i=1}^n T_{out,BHE,H}(i) * CS_{HP}(i)}{\sum_{i=1}^n CS_{HP}(i)}, n = \text{number of timestep} \quad (\text{A.24})$$

$$\bar{T}_{out,BHE,C} = \frac{\sum_{i=1}^n T_{out,BHE,C}(i) * CS_{P,Cool}(i)}{\sum_{i=1}^n CS_{P,Cool}(i)}, n = \text{number of timestep} \quad (\text{A.25})$$

3.7 Intermediate results

Parameter studies were carried out with the simulation model with constructive parameters, geothermal gradient, and hydraulic connections in the circuit as variables. The intention of this parameter-study is to find energetically optimum constructions for various locations (geothermal gradients). Hence, the primary energy consumption of the complete system (Q_p for balance boundary 4) was evaluated predominantly. Further evaluations are carried out depending on the requirement to explain the other thesis. Initial parameter studies with base constructive-design of BHE carried out using EED are presented in this section. The variant matrix used for initial parameter-studies is shown in Tab. A-3.10. The total number of variants is 240.

Total number of variants (N) and variants in every gradient (N_j)

$$N_1 = N_2 = N_3 = N_4 = Var1 \cdot Var2 \cdot Var3 \cdot Var4 = 1 \cdot 6 \cdot 10 \cdot 1 = 60 \quad (\text{A.26})$$

$$N = N_1 + N_2 + N_3 + N_4 = 60 + 60 + 60 + 60 = 240$$

Tab. A-3.10 Variant matrix for initial parameter studies.

Parameter	Unit	Value										
Total BHE length	[m]	4,000										
Number of BHEs n	[-]	20	32	40	80	160	200					
Depth of BHEs	[m]	200	125	100	50	25	20					
Borehole spacing	[m]	1	2	3	4	5	6	8	7	8	9	10
Geothermal gradient	[K/100 m]	1										
		3	The average value for Germany									
		6,5	At Zittau									
		9										
Hydraulic connections of BHEs in field		parallel										
Basic construction design from EED		32 x 125 m BHEs										

Fig. A-3.8 depicts the ratio of primary energy consumption of a particular variant to the minimum primary energy consumption from all variants in the respective gradient (A.21) for one year (Y-axis). Four graphs represent four gradients. The X-axis represents borehole depth and the corresponding number of boreholes n . Curve parameters are borehole spacing. Value 1 represents minimum primary energy consumption ($Q_{P,tot,min}$) in the respective gradient. Value 1.05 represents 5 % more $Q_{P,tot}$ than $Q_{P,tot,min}$ in respective gradient. Variants with borehole spacing 1m and 2m are excluded to avoid inconsistencies in evaluation.

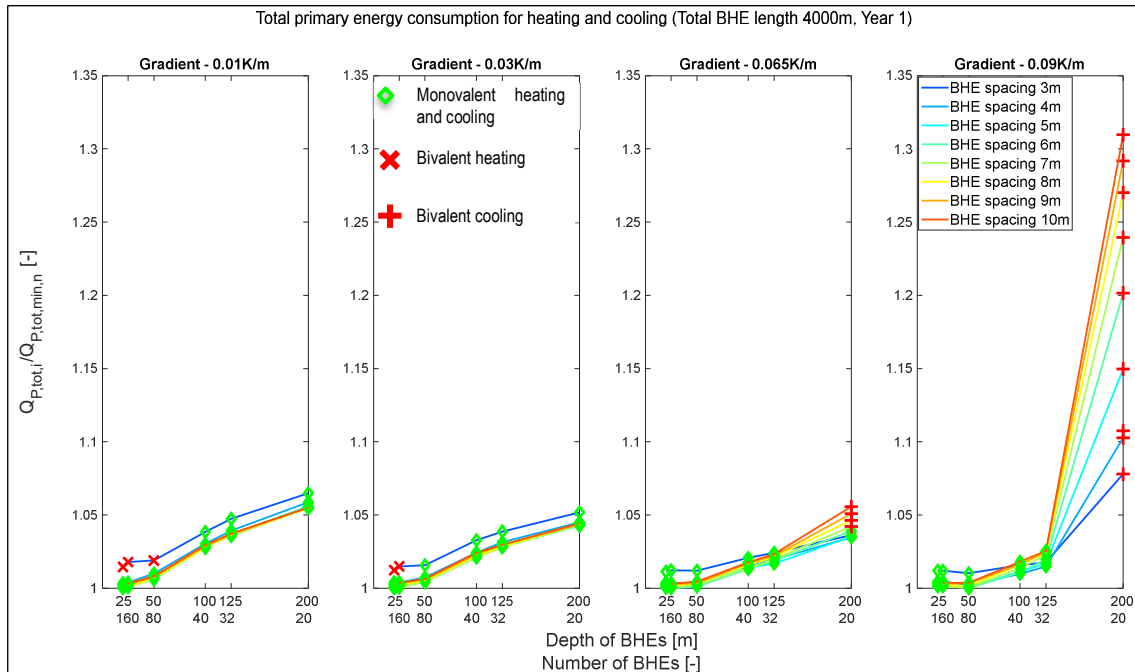


Fig. A-3.8 Total primary energy consumption – borehole length 4,000 m.

Fig. A-3.8 shows that total primary energy consumption ($Q_{P,tot}$) is less when BHE is not deeper than 50 m. $Q_{P,tot}$ increases by deeper borehole because of higher electrical energy consumption by circulation pump resulted from higher pressure drop. Though deeper BHEs have a favourable operating temperature for the heat pump, the influence of pressure drop dominates. Besides, higher operating temperature with deeper BHEs during cooling prolongs the cooling system's operation or sometimes demands energy from an external source (auxiliary cooler in this case).

Demand from auxiliary cooler can be seen by 200 m deep BHEs at gradient 0.065 K/m and 0.09 K/m, significantly influencing $Q_{P,tot}$. This overlapped effect of higher pressure drops, prolonged operation of the cooling system, and the possibility of using auxiliary cooler by deeper BHEs make it insignificant variant. Before concluding optimization potential, there exists a question of the representative year for the constructive design of the BHE field. Because systems with BHEs are planned for a more extended period, predominant heat extraction leads to continuous cooling down of the ground over the year. There exists a possibility of reaching minimum temperature in heat pump operation if analysed for a more extended period. For this purpose, the simulation period is increased

to 15 years. Year 15 is chosen because observation made during parameter studies shows that most variants reach stationary operating temperature after this period.

Fig. A-3.9 depicts the ratio of primary energy consumption of the particular variant to the minimum primary energy consumption from all variants (A.21) in the respective gradient (Y-axis). The first two graphs show first-year and 15-year results for gradient 0.03 K/m. The third and fourth graphs show first-year and 15-year results for gradient 0.065 K/m. The X-axis represents borehole depth and the corresponding number of boreholes n . Curve parameters are borehole spacing.

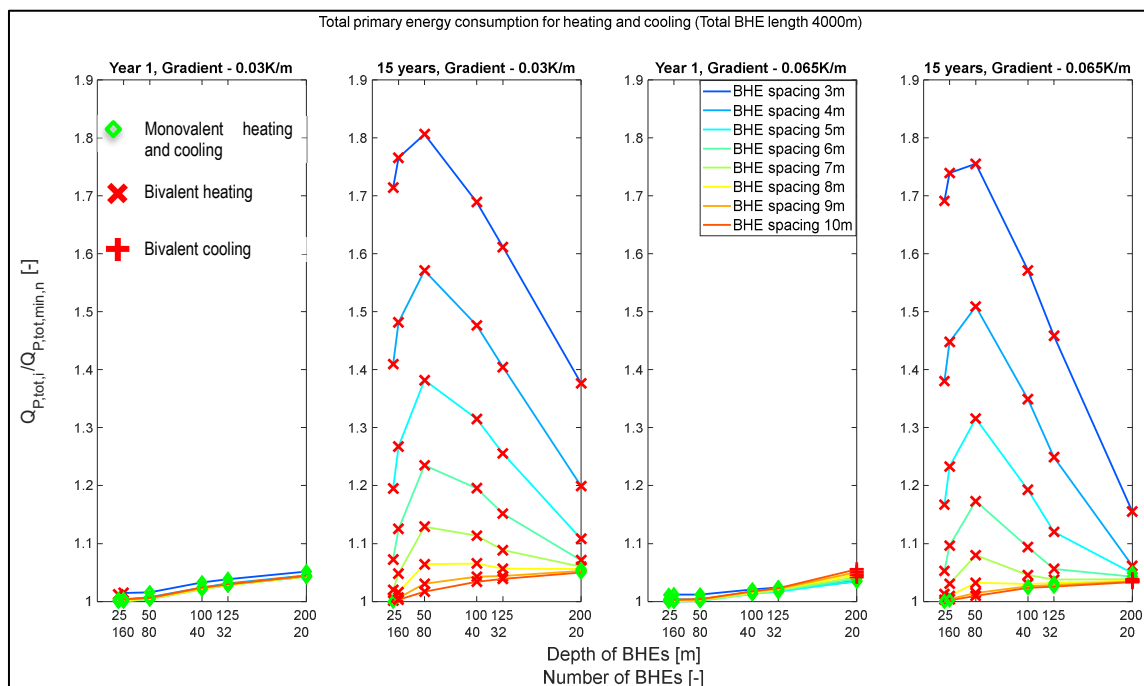


Fig. A-3.9 Comparison of first year and 15-year simulation results.

By comparing first-year results and results over 15 years (in Fig. A-3.9), it can be realized that multiple variants cannot be monovalent for heating in the long term. This means that the heat pump reaches the minimum source side operating temperature limit ($-5\text{ }^{\circ}\text{C}$) during heat supply, which leads to the operation of a secondary heat supply system (auxiliary heater). 80 % increment in $Q_{P,tot}$ can be interpreted that aid of the auxiliary heater is required for a more extended period. Very few variants with BHE spacing more or equal to 8m can be monovalent. Since most of the constructive design falls below the operating temperature limit of the heat pump ($-5\text{ }^{\circ}\text{C}$), there is the uncertainty of the rest of the variants falling into this category during a more extended period. This uncertainty can be solved by increasing the total length of BHEs. Further parameter studies with a total BHE length of 5,000 m are carried out, explained in section 5.

4 Subtasks

4.1 Pressure drop calculation

The energy demand by the circulation pump depends on the pressure drop in the circuit. In the primary circuit of the heat pump, the energy-demand / pressure-drop varies depending on the constructive design of BHEs. To automate the pressure-drop/energy-demand by circulation pump calculation in parameter studies, a mathematical model is developed with the help of WAGNER (2012), and implemented in TRNSYS as Type1994. This model is developed focusing primarily this parameter studies. Hence, alteration might be essential if applied for other purposes. The mathematical model is explained in this section. The primary side of the heat pump contains not only BHEs but also multiple other components and pipes, which are connected in series. Pressure drops in individual elements in the circuit are required to calculate total pressure drop (Δp). The pressure drop calculation procedure is different for straight pipes, components, and divider/mixer. Hence, the initial procedure is explained. Then, pressure drop calculation for the primary circuit is demonstrated with an example circuit.

4.1.1 Pressure drop calculation in BHE Field

Straight pipes: Pressure drop in straight pipes can be calculated using the formula (A.27). R is resistance to flow by pipe, which can be calculated using the formula A.28.

$$\Delta p = R \cdot V^2 \quad (\text{A.27})$$

$$R = \frac{\lambda \cdot L \cdot \rho \cdot 8}{D^5 \cdot \pi^5} \quad (\text{A.28})$$

Friction number (λ) in equation (A.28) depends on nature of flow (turbulent or laminar). Nature of flow can be decided using Reynolds number ($Re < 2,300$ Laminar, $Re > 2,300$ turbulent). Reynolds number can be calculated using equation A.29.

$$Re = \frac{\rho \cdot v \cdot D}{\mu_k} \quad (\text{A.29})$$

Friction number in case of laminar flow: $Re < 2,300$

$$\lambda = \frac{64}{Re} \quad (\text{A.30})$$

Friction number in case of laminar flow: $Re > 2,300$

$$\frac{1}{\sqrt{\lambda}} = -2 \cdot \log \left(\frac{2.51}{Re \cdot \sqrt{\lambda}} + \frac{k}{D} \cdot 0.269 \right) \quad (\text{A.31})$$

Pressure drops in all pipes can be calculated using the formula A.32. Here, R_{tot} is total resistance offered by all pipes combined. To calculate R_{tot} , resistance (R) in all individual pipes has to be calculated initially using formula A.28.

$$\Delta p = R_{tot} \cdot V^2 \quad (A.32)$$

Before calculating total resistance (R_{tot}) offered by all pipes from individual resistances (R), understanding the hydraulic connections of pipes in BHE field is essential. Hydraulic connections of pipe can be serial, parallel, or mixes. An example of the mixed arrangement, which has n number of rows with m number of pipes in each row is shown in Fig. A-4.1. It is not necessary to have m pipes in each row.

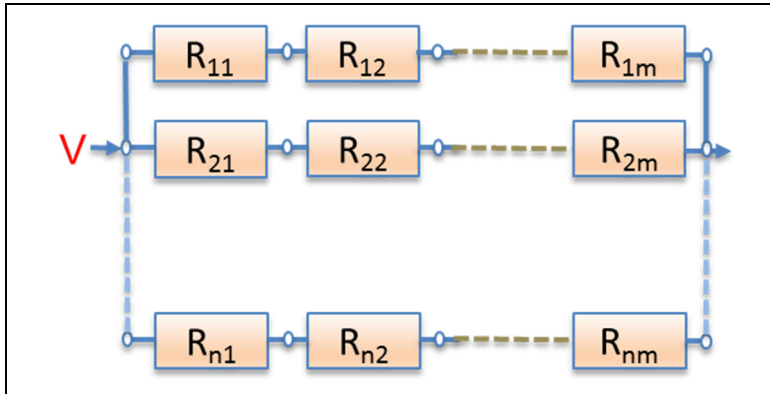


Fig. A-4.1
The resistance of BHEs.

For the depicted example, resistance by pipes in each row (R_1, R_2, \dots, R_n) can be calculated using A.33. Once the resistance of each row is known, total resistance can be calculated using A.34. With this resistance, the total pressure drop in the BHE field can be calculated.

$$R_1 = R_{11} + R_{12} + \dots + R_{1m}, \dots \quad (A.33)$$

$$R_{tot} = \frac{1}{\left(\frac{1}{\sqrt{R_1}} + \frac{1}{\sqrt{R_2}} + \dots + \frac{1}{\sqrt{R_n}} \right)^2} \quad (A.34)$$

Pressure drop in components: Apart from BHEs and connecting pipes, there exist multiple small components circuit. Pressure drops in these components can be calculated using equation A.35. Drag coefficient and fluid velocity of individual components are required for pressure drop calculation.

$$\Delta p = \frac{\zeta \cdot \rho_{brine} \cdot v^2}{2} \quad (A.35)$$

Pressure drop in divider/mixer: By using the method explained in WAGNER (2012), the total pressure drops of divider, mixer, all elements in between them can be calculated. Therefore, the total pressure drop of all components between divider and mixer must be calculated initially. From the total pressure drop, the total zeta value can be calculated using equation A.37. Finally, total pressure drops (divider + mixer + elements in between them) can be calculated using equation A.36. This calculation procedure is valid only if the form of divider / mixer depicted in Fig. A-4.2 is used. Hence, it is assumed that this form of divider / mixer is used irrespective of number of BHEs.

$$\Delta p_{vs,z} = \zeta_{o,vs,z} \cdot \frac{\rho}{2} \cdot w_0^2 \quad (\text{A.36})$$

$$\zeta_{o,vs,u} = \frac{1}{0.692 \cdot K_0 + 0.128 \cdot \frac{A_v}{A_s} - 0.424 \cdot K_0 \cdot \frac{A_v}{A_s} - 0.013} \quad (\text{A.37})$$

$$K_0 = \frac{\sum A_a}{A_0} \cdot \frac{1}{\sqrt{0.6 + 1 + \zeta_a}} \quad (\text{A.38})$$

$$\zeta_a = \frac{\Delta p_a}{\frac{\rho}{2} \cdot w_a^2} \quad (\text{A.39})$$

$$w_a = \frac{\dot{V}_0}{\sum A_a} \quad (\text{A.40})$$

Valid for $\alpha = 90^\circ$, $\frac{L}{d_v} \leq 50$, $0.5 \leq \frac{A_v}{A_s} \leq 1$, $Re = \frac{w_0 \cdot d_v}{\nu} \geq 10^4$ and $0.54 \leq K_0 \leq 1.6$.

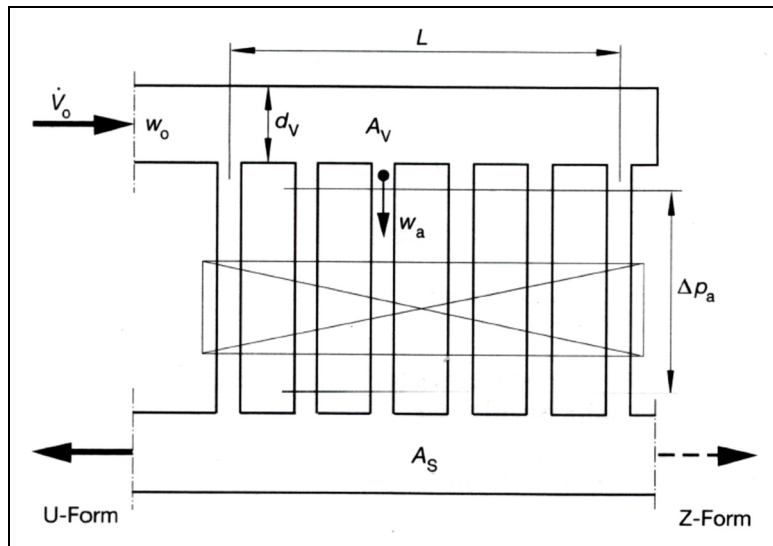


Fig. A-4.2
Divider / mixer (WAGNER 2012).

4.1.2 Hydraulic balancing of connecting pipes in BHE field

BHEs in the field are connected with divider/mixer through connecting pipes. The length of the connecting pipe varies depending on the constructive design of the BHE field, and hence pressure drop along with it. This influences the mass flow rate through individual pipes / BHEs. According to VDI 4640-2:2015-05, hydraulic balancing is necessary if the smallest and longest connecting pipe differs in length by more than 15 %. In parameter studies, BHEs are assumed to be arranged in rectangular form, as shown in Fig. A-4.3. In this example, 32 BHEs are arranged in rectangular form (4 x 8), connected in parallel.

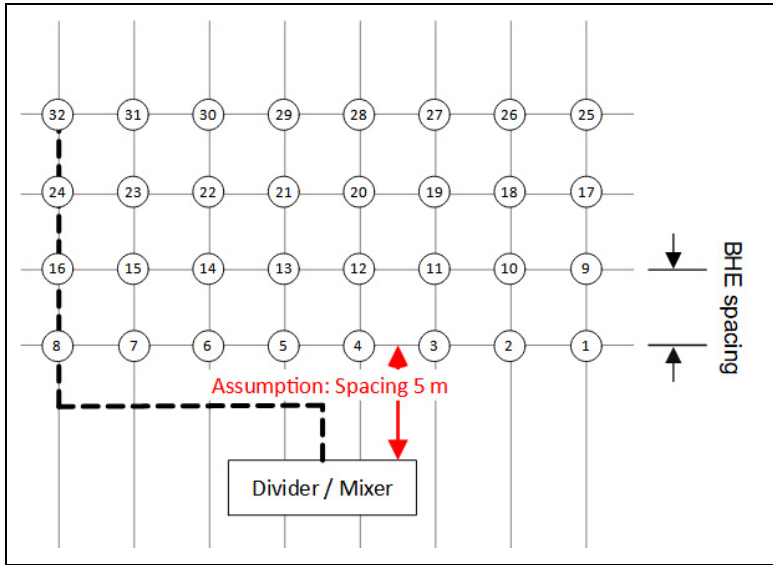


Fig. A-4.3
Connecting pipes in BHE field.

To ease the calculation, BHEs and divide/mixer is assumed to be always placed in front of the BHE field as shown in Fig. A-4.3. Here, connecting pipes are assumed to be laid as represented in the dotted line. In this case, the length of connection pipes depends on bore-hole spacing, number of BHEs. For a borehole spacing of 10 m, each pipe's length and its pressure drop are depicted in Fig. A-4.4. Pressure drops in the individual connecting pipe is calculates using A.27. Note: Volumetric flow rate in this formula is for a single pipe, not for the whole system. For 10 m spacing, the difference in length between the smallest and longest pipe is almost 86 %. Hence, hydraulic balancing is essential for this BHE field. Hydraulic balancing required for individual BHE is depicted in Fig. A-4.5.

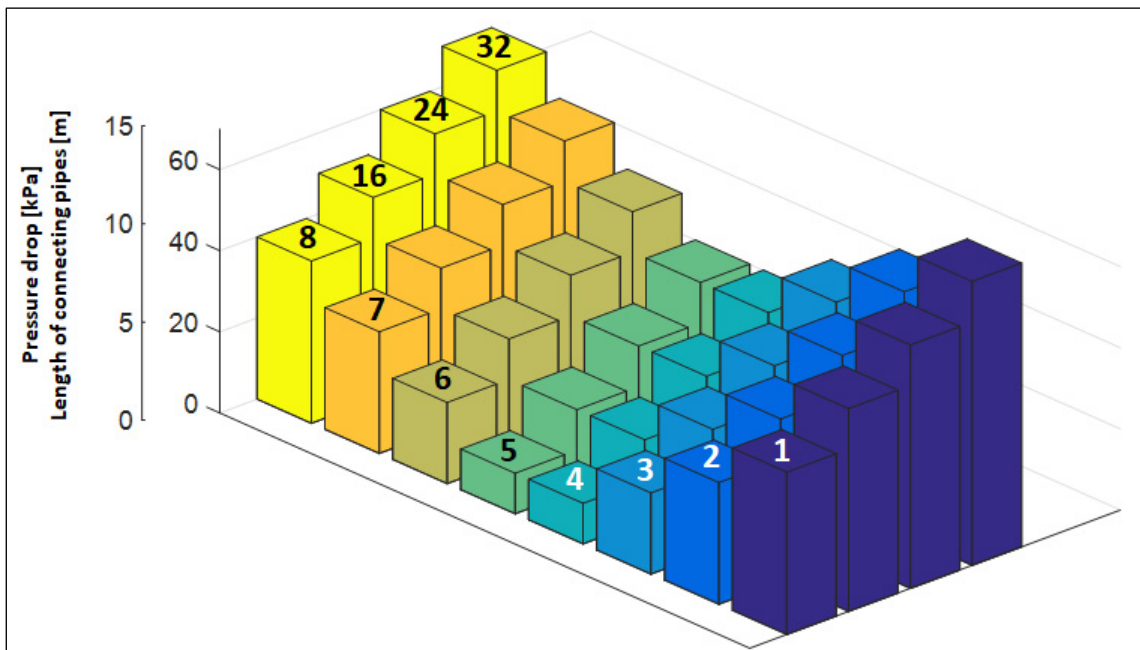


Fig. A-4.4 Length and pressure drop of connecting pipes in BHE.

In the case of 1 m spacing, the difference in length between the smallest and longest pipe is almost 51 %. The difference is more than 15 % irrespective of the number of BHEs and borehole spacing. Hence, hydraulic balancing is always essential. In conclusion, it is sufficient to calculate the pressure drop in the longest connecting pipe.

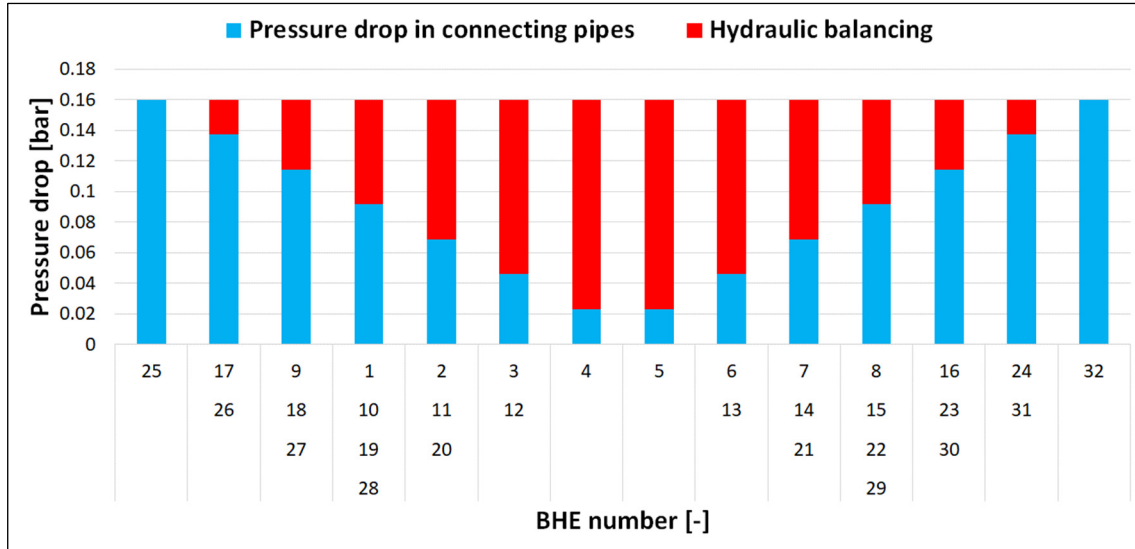


Fig. A-4.5 Hydraulic balancing of connecting pipes in BHE field.

4.1.3 Temperature dependent properties

A mixture of ethylene glycol and water is used as a heat carrier fluid on the primary side of the heat pump. Ethylene glycol content in fluid varies from 25 to 40 %. The heat carrier fluid temperature varies significantly during the simulation, hence properties like density, dynamic viscosity. This has a strong influence on pressure drop calculation. Hence, density and dynamic viscosity are calculated every time step. To do so, polynomial functions were generated from the data provided by the manufacturer. Polynomial functions for density and dynamic viscosity are shown in equation A.41 and A.42, respectively. These polynomial functions are valid for fluid temperatures from -20 to +40 °C and ethylene glycol mixture from 25 to 40 %.

$$\begin{aligned}
 \rho(T_f) = & 129.1757 \cdot G - 6.018965 \cdot G^2 + 0.1250608 \cdot G^3 - 0.950696 \cdot T_f \\
 & + 0.05691005 \cdot T_f \cdot G - 0.001865357 \cdot T_f \cdot G^2 \\
 & + 0.00001835942 \cdot T_f \cdot G^3 - 0.002437507 \cdot T_f^2 \\
 & - 0.00007813298 \cdot G \cdot T_f^2 + 0.000002941503 \cdot T_f^2 \cdot G^2 \\
 & + 0.00009292929 \cdot T_f^3 - 0.000002444962 \cdot T_f^3 \cdot G \\
 & - 9.364531 \cdot 10^{-19} \cdot T_f^4 - 0.0009651998 \cdot G^4
 \end{aligned} \tag{A.41}$$

$$\begin{aligned}
\mu(T) = & 0.0003573 \cdot G - 0.000015406 \cdot G^2 + 0.0000003809 \cdot G^3 \\
& - 0.00012575 \cdot T_f + 0.0000048402 \cdot T_f \cdot G - 0.00000027626 \cdot T_f \\
& \cdot G^2 + 0.0000000011628 \cdot T_f \cdot G^3 - 0.0000017801 \cdot T_f^2 \\
& + 0.0000001914 \cdot T_f^2 \cdot G + 0.0000000029715 \cdot T_f^2 \cdot G^2 \\
& + 0.0000000016999 \cdot T_f^3 - 0.0000000056577 \cdot T_f^3 \cdot G + 0 \cdot 1 \\
& + 0.000000001877 \cdot T_f^4 - 0.0000000029834 \cdot G^4
\end{aligned} \tag{A.42}$$

4.1.4 Pressure drop calculation in primary circuit

In parameter studies, the primary circuit varies depending on the BHE field. Hence, to automate pressure drop calculation, understanding of circuit connection is essential. Here, the procedure is explained with an example of two BHEs with two U-tubes connected in parallel, as shown in Fig. A-4.6. In the circuit, multiple elements are connected in serial. Hence, the total pressure drop is the sum of pressure drops in every component. The pressure drop in individual elements must be calculated carefully because of complex hydraulic connections in the BHE field. The procedure is explained step by step.

- Here, the evaporator of the heat pump is connected to the divider/mixer through a connecting pipe. The pressure drop in the evaporator is almost constant, and the manufacturer provides the data. Hence, this value is added to the total pressure drop at the end.
- Connecting pipes between evaporator and divider / mixer (both supply and return pipes) are straight pipes. Hence, the pressure drop in these pipes is calculated using formula A.27.
- Pressure drop calculation for divider / mixer is explained in section 4.1.1. Initially, pressure drops in the elements in between divider and mixer have to be calculated. From that total pressure drop can be calculated.
- Every BHEs are connected with a divider and mixer through connecting pipes. As explained in section 4.1.3, hydraulic balancing is always essential for our parameter studies. After hydraulic balancing, every connecting pipes has same pressure drop. Hence, the longest connecting pipe in BHE field is identified, and pressure drop in it is calculated using equation A.27.
- As shown in Fig. A-4.6, connecting pipes and U-tubes in BHE are coupled with the aid of multiple components. For example, reducer and Y-piece (flow divider) in forward flow, Y-piece (flow mixer) and expansion in return flow. The number of these components is equal to the number of BHEs in the case of parallel connections. These components are not necessary if a single U-tube is used. Also, in the pressure drop calculation of BHEs, a straight pipe is assumed. This ignores the significant pressure drops in the U-bend at the bottom of the BHEs. Hence, pressure drops in these U-bends are calculated separately and added to the total pressure drop. The procedure is already explained in section 4.1.1. Zeta values used for calculation in parameter studies are listed in Tab. A-4.1.
- BHEs are nothing but pipes connected in serial or parallel. Pressure drop for the entire BHE field can be calculated using the formula A.32. As explained earlier, resistance to flow by every pipe has to be calculated using formula A.28. Then

total resistance to the BHE field flow is calculated by using A.33 and A.34. In our example, two BHEs with two U-tubes in each are connected parallel. Hence, it is simplified as four straight pipes, and the procedure mentioned above is used to calculate the total pressure drop.

- Once all individual pressure drops are calculated, the total pressure drop is the sum of pressure drops in the evaporator, connecting pipes between evaporator and divider / mixer, divider / mixer (which includes pressure drops in element between them).
- This calculation procedure is implemented in TRNSYS as Type1994. Parameters and inputs required for pressure drop calculation are depicted in Tab. A-4.2.

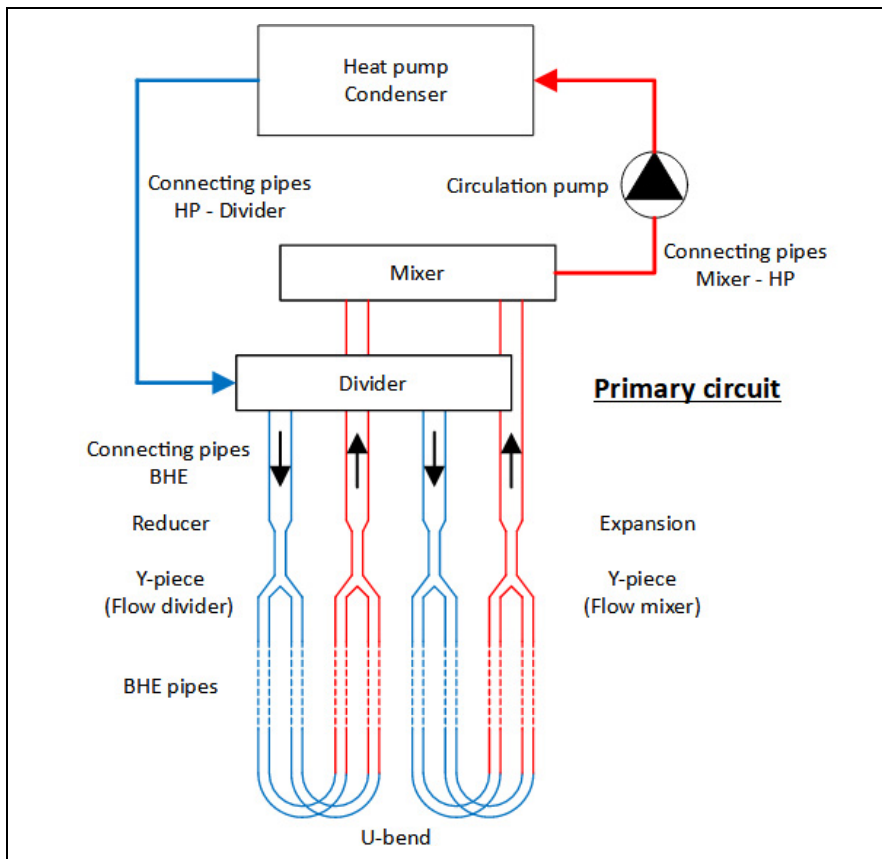


Fig. A-4.6
Primary circuit of
heat pump.

Tab. A-4.1 Drag coefficient of components.

Component	Drag coefficient ζ [-]
Valve forward flow	7.38
Reducer	0.25
Y-piece (Flow divider)	0.7
U-bend	0.83
Y-piece (Flow mixture)	0.543
Expansion	0.14
Valve return flow	7.38

Tab. A-4.2 Parameters and inputs required in Type1994 TRNSYS.

(A) Parameter	Unit
Diameter of U-pipe	[m]
Roughness of pipe (k in A.14)	[mm]
Number of U-Tubes	[-]
BHE depth	[m]
Number of BHEs in series	[-]
Number of rows of BHEs	[-]
Total pump efficiency (varies from 0 to 1)	[-]
Glycol content in fluid in primary circuit	[%]
Alpha (angle between connecting pipes and divider/mixer)	[°]
Length of divider/mixer	[m]
Diameter of divider/mixer	[m]
Diameter of connection pipes in BHE field	[m]
Length of longest connecting pipes in BHE field	[m]
Diameter of pipe connecting evaporator and divider/mixer	[m]
Length of pipe connecting evaporator and divider/mixer	[m]
Number of components (It is 6 in depicted circuit in Fig.. A-4.1)	2
Diameter of the component-1	[m]
Diameter of the component-2	[m]
Mass flow rate in components-1	[kg/h]
Mass flow rate in components-2	[kg/h]
Zeta value of components-1	[-]
Zeta value of components-2	[-]
Multiplication factor for components-1	[-]
Multiplication factor for components-2	[-]
(B) Input	Unit
Mass flow rate in BHE field	[kg/h]
Inlet temperature to BHE field	[kg/h]

4.2 Double depressurized differential manifold (DDV)

Double depressurized differential manifold (DDV) is a combined assembly of two stop-cocks, two bypass lines with return flow prevention, a safety module with a pressure gauge, and a connection option for expansion valve. It acts as an interface between a heat pump, heat distribution circuit, and a buffer storage tank. The heating system planned for simulation analysis has a variable mass flow rate in the distribution system and constant but different mass flow rates in the heat pump system. In a conventional heating system, buffer storage acts as an interface between heat generation and distribution systems. Higher operating temperature requirement by such systems has negative impacts on energy efficiency. Direct coupling of a heat pump with distribution is also inefficient because of higher load fluctuation. Hence, an input / output puffer-storage in return flow with DDV as an interface between heat generation and distribution system is used in our simulation model. This avoids a higher operating temperature problem without increasing the cyclic operation of the heat pump significantly. But there exists no mathematical model to represent working DDV. Hence, a mathematical model was developed by Promotion Haack in Excel. TRNSYS and Excel interaction is again time-consuming. Therefore, the mathematical model is implemented as a new TRNSYS Type1991. Circuit diagram representing the working of DDV is depicted in Fig. A-4.7.

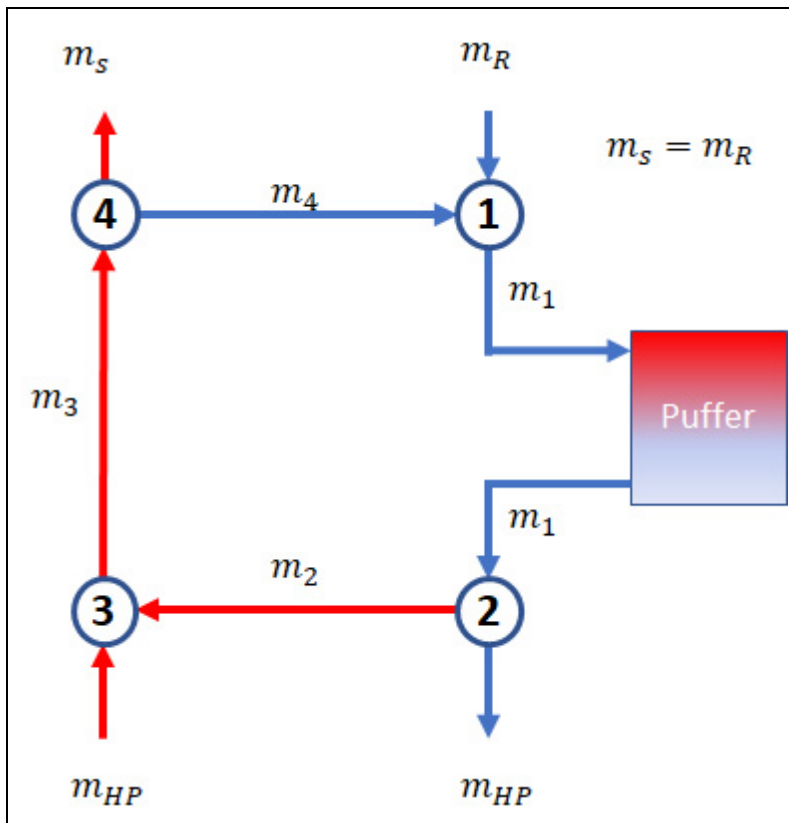


Fig. A-4.7
DDV circuit.

DDV controls the direction and quantity of mass flow depending on the pressure difference between heat distribution and generation circuits. It maintains a constant mass flow rate in the heat generation circuit and watches out the fluid returns from the distribution system

goes back to it. This process has to be mathematically modelled in TRNSYS. Since the size of DDV is small dead time effects in the pipe are less. Hence, it can be ignored in modelling. In this model, DDV operation is modelled with conditional equations and adjusting fluid temperatures when required (for example, mixing two fluid streams with different temperatures).

Depending on the control system design, there exist three different possibilities of mass flow:

- **Case 1:** When both heat generation and distribution system are working (m_R and $m_{HP} > 0$). Bypassed fluid from point 4 (m_4) mixes with return fluid from the distribution system (m_R) at point 1. This fluid then passes through puffer storage, then pumped to higher temperature by heat pump. At point 4, $m_S (= m_R)$ is supplied to the distribution system and m_4 is diverted back to point 1.

$$\text{Here } m_1 = m_4 + m_R, m_2 = 0, m_{HP} = m_1, m_3 = m_{HP}, m_R = m_3 - m_S$$

- **Case 2:** When heat generation system is off and distribution system is working ($m_R > 0$ and $m_{HP} = 0$). In this case, return fluid from distribution system pass through puffer storage, diverted at point 2 avoiding heat pump. Complete fluid goes back to distribution system again.

$$\text{Here } m_1 = m_R, m_2 = m_1, m_{HP} = 0, m_3 = m_2, m_S = m_3$$

- **Case 3:** When heat generation system is on and distribution system is off ($m_S = 0$ and $m_{HP} > 0$). This case is rare possibility as heat generation is turned on only when there is demand. Complete fluid coming from the heat pump is diverted from point 4 to point 1, where it passes through puffer storage and goes back to the heat pump again. The cycle goes on until the heat pump is switched off.

$$\text{Here } m_1 = m_4, m_2 = 0, m_{HP} = m_1, m_3 = m_{HP}, m_4 = m_3, m_S = m_R = 0$$

4.3 Automation of parameter variation

Parameter studies for this work are carried out with server technologies specially designated for this purpose at the Zittau/Görlitz University of Applied Science. There exist multiple servers with various numbers of kernels. The number of simulations carried out parallelly depends on the number of kernels in a particular server. Both TRNSYS 17 and TRNSYS 18 offer the possibility to perform parameter studies but have their limitations in both versions. Hence, parameter studies were controlled using deck files (*.dck) and batch files (*.bat). Deck file is a script file created by TRNSYS (in TRNEdit), and the batch file is a script file created in Notepad for windows. To automate the generation of the batch file, a macros program was created in excel. The batch files generated by this macros program control how variants are simulated and starts / stops simulations. Parameter required for this macro is depicted with example in Fig. A-4.8. In this example, four variants are simulated with two kernels. This macros program creates three batch files, as shown in Fig. A-4.9 to Fig. A-4.11.

4.4.2 Simulative analysis of optimization potential

Cyclic loss decreases the efficiency of the on-off heat pump, which can be reduced in IVHP. Additionally, demand relevant heat extraction in IVHP increases the operating temperature and energy efficiency. These two effects are explained through simulative analysis with two heat pumps of capacity 270 kW and 135 kW. Both the heat pumps are coupled with 40 BHEs each of 100 m deep. The condenser inlet temperature is assumed to be constant at 28 °C, so that sink side temperature is at the same level for all variants. 135 kW heat pump works continuously (operation time 168 h), whereas the 270-kW heat pump works in cyclic mode (operation time 84 h, idle time 84 h). The cyclic intervals are varied as 0.5 h, 1 h, 2 h, 4 h, 84 h (Note: All variants have the same operating and idle time). In case of inadequate heat supply (< 26,947 kWh) in 168 h, the pump runs continuously after that till predefined energy (26,947 kWh) is supplied. The experiment is repeated, assuming no cyclic losses (Heating constant and cooling constant is set near zero in TRNSYS Type401). In Fig. A-4.13, electrical energy required by the pump to supply heat of 26,947 kWh and average operating temperature by all variants are presented.

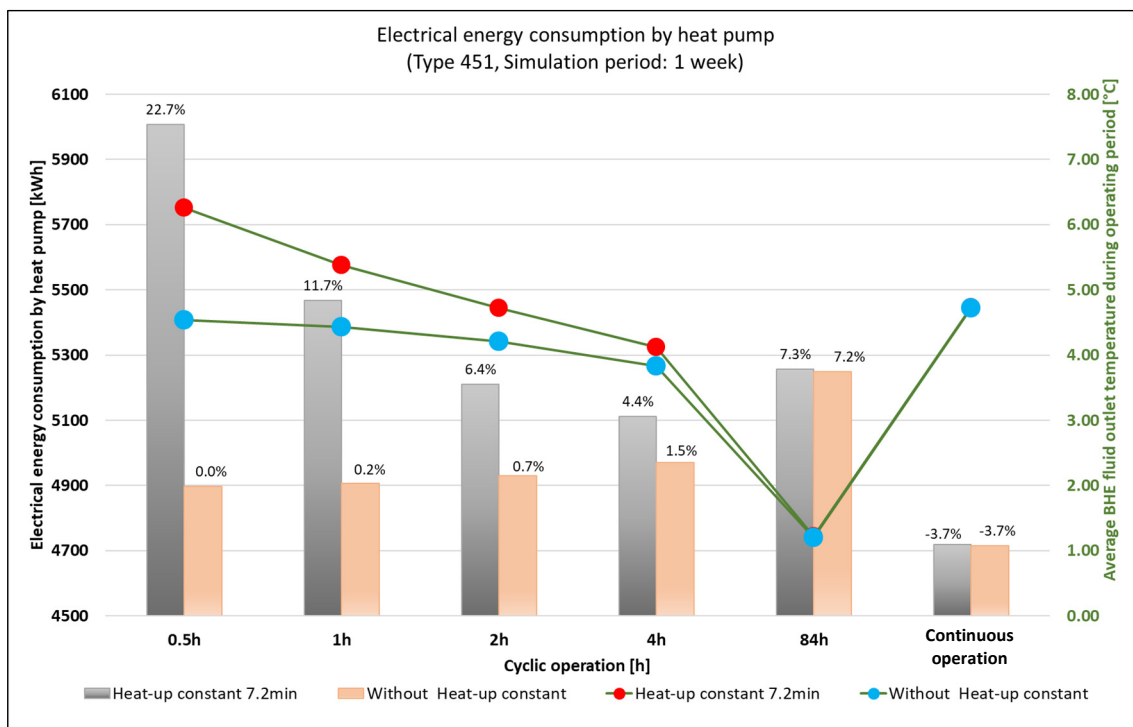


Fig. A-4.13 Demonstration of cyclic losses through simulative analysis.

Considering the variants with cyclic losses, the average operating temperature decreases and electrical energy consumption increases with cycle time. When the electric energy consumption trend without cyclic losses is observed, the variant with less cycle has better operating temperature and less energy consumption than the variant with higher cycle time. It can be summarized that variants with repeated cycles have a better operating temperature, but cyclic losses make it inefficient. On the other hand, the continuously operating variant with a 135-kW heat pump has a better operating temperature and minimal electrical energy consumption (Note: Same total energy supply by all variants).

Hence, IVHP that extracts heat from the source depending on demand should have better operating-temperature. Prolonged operation by IVHP also reduces the number of cycles (reduces related cyclic losses). Both reduced cyclic losses and improved operating temperature increase the overall efficiency of the inverter heat pump.

4.4.3 Experimental validation of optimization potential by IVHP

The tendency of the above-explained temperature behaviour for the different cyclic operations is validated with an experimental investigation over 24 h. A 100 m BHE located at F-W, HSZG is subjected to extract heat at the rate of 5 kW in a cyclic operation (0.125 h, 0.25 h, 0.5 h, 4 h, 12 h) and the rate of 2.5 kW in a continuous operation. Average fluid outlet temperature and total heat extracted are plotted in Fig. A-4.14.

It can be observed that the variant with less cycle time has a better operating temperature. Here, the variant with the continuous operation is more or less equal operating temperature as the smallest cycle. The trend is the same as that of simulative analysis in the previous section. It can be seen that heat extracted is not constant in experiments as in the simulative analysis. It is challenging to maintain the exact heat extraction rate in experimental analysis. But total heat extraction varies from 58 to 61 kWh, which is 5 % approximately. This deviation is expected to have the least impact on the tendency of the curve. Hence it can be concluded that demand relevant heat extraction has a better operating temperature.

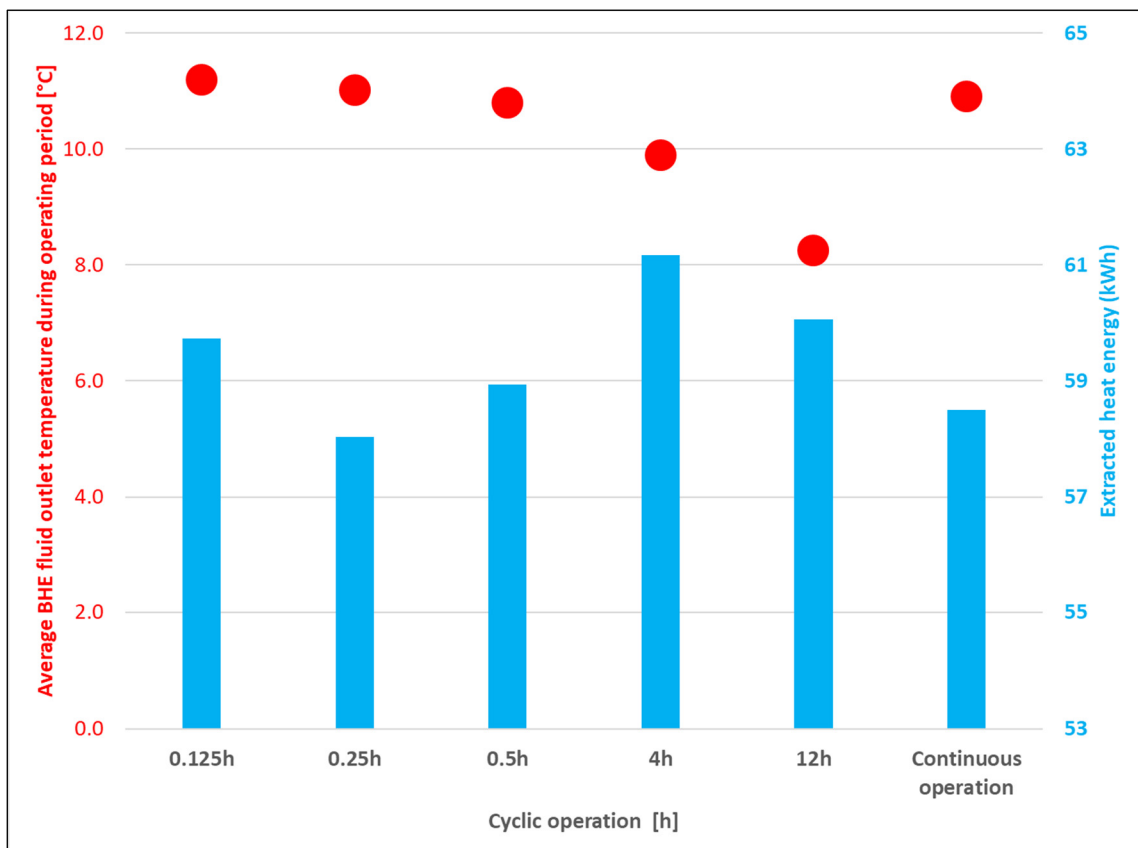


Fig. A-4.14 Experimental validation of optimization potential by IVHP.

4.4.4 Validation of optimization potential – Literature analysis

BAGARELLA et al. (2016) compared air sourced on-off heat pump with inverter heat pump. It concluded that depending upon the sizing of the heat pump, 12.3-16.2 % of energy-saving is possible with IVHP. MERKER et al. (2014) compared the effect of heating and cooling constants on Seasonal Performance Factor (SPF) for varying total borehole length. It concluded that the heating constant has a significant influence on the SPF of the total system irrespective of borehole length. This experiment didn't quantify the optimization potential by IVHP but explained the significance of cyclic losses. MADANI et al. (2011) made a direct comparison of ground-source on-off and variable speed heat pumps. It concludes that on-off heat pump sized more than 86 % of the peak load of the building has almost similar energy consumption as IVHP. But in this research, the influence of cyclic losses is ignored. As cyclic losses are significant in the on-off heat pump, simulative analysis considering this effect is essential for the conclusion.

GASSER et al. (2017) has theoretically and experimentally shown that capacity-controlled heat pump has energy-saving potential, depending on operating conditions. It is shown that for a heating water supply temperature of 46 °C and a BHE temperature of 6 °C, the examined capacity-controlled heat pump is 5 % more efficient than the on / off heat pump. For a heating water supply temperature of 30 °C and a BHE temperature of 13 °C, the capacity-controlled heat pump is 11 % more efficient.

4.4.5 Mathematical modelling

As theoretical optimization potential is validated through various methods, detailed simulative analysis is essential to quantify optimization potential. Hence, a character curve based mathematical modelling of IVHP (Hoval UltraSource T comfort (13)) is initiated during the project period. The manufacturer provided characteristics field of the heat pump variant Hoval UltraSource T comfort (13) is shown in Fig. A-4.15. Here, the X-axis represents source temperature, the Y-axis represents heat pump outlet temperature, and the Z-axis represents heat supplied by the condenser. Three different planes in the figure represent data at the maximum frequency (100 %), design frequency (41 %), and minimum frequency (20 %). This data is interpolated to form planes at the interval of every 0.1 % of frequencies. These planes are then converted into polynomial functions using the curve fitting option in MATLAB. These polynomial functions are used to model the steady-state behaviour of the heat pump in the TRNSYS model. Cyclic losses are introduced then as a correction factor to calculate actual performance. Transient and cyclic losses are modelled in analogous to Type401 (Single-stage heat pump). The stationary performance calculation of the model is validated. But validation of transient behaviour of the model is essential. For this purpose, an experimental setup is essential. Due to lack of resources and time during the current project, it is planned to create a follow-up project on this topic. The initial idea is to create a generic mathematical, which can be used in the simulative investigation to quantify optimization potential.

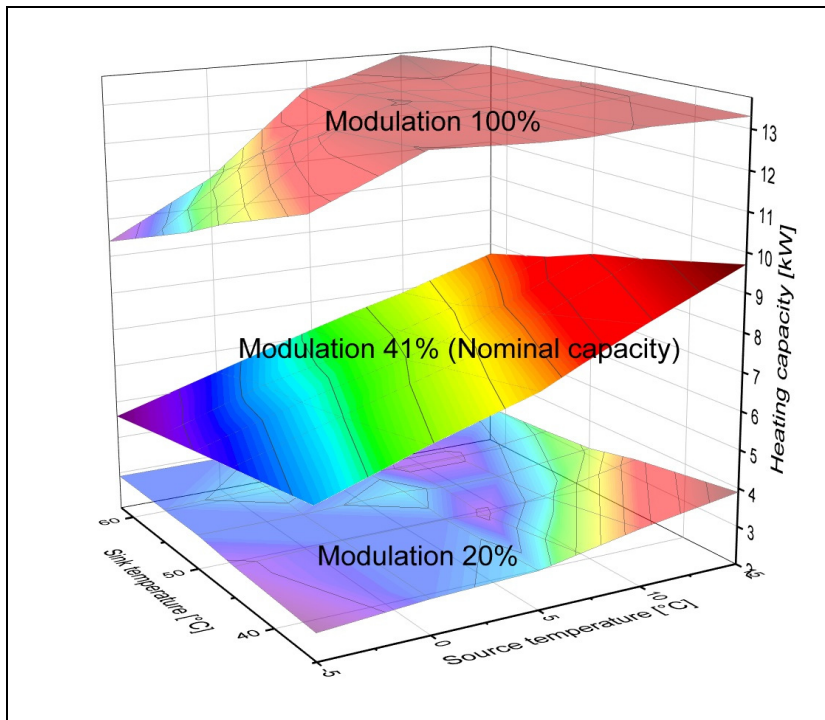


Fig. A-4.15
Characteristic curve field
for Hoval UltraSource T
comfort (13).

4.4.6 Summary

As discussed earlier, reduced cyclic losses and improved operating temperature increase the overall efficiency of IVHP. But to quantify optimization potential in real-time applications, detailed transient system simulation is essential. Quantification with simulation studies for air sourced IVHP has been carried out by multiple researchers already. But satisfactory conclusions are not made with ground sourced heat pump. For simulative studies, IVHP modelling is essential. Modelling and validation are not possible with available resources within this research project. Hence, it is planned to generate a follow-up project on this topic.

4.5 Heating / cooling demand variation

4.5.1 Introduction

In the framework of constructive design of BHEs for the combined application of heating and cooling, there exists a subtask of heating and cooling energy demand variation in the building. The objective of this task is to find office-building with the following energy demand structure

- Building with predominant heating demand
- Building with predominant cooling demand
- Building with almost similar heating and cooling demand

Building energy demand depends on various factors like energy-standard, building usage, HVAC system, etc. Maintaining the minimum energy standard for newly constructed buildings in Germany is mandatory. As building energy-standard improves over time, multiple building standards exist parallelly. Energy demand structure also varies for these

buildings. For example, cooling demand increases in passive houses because of less heat transfer to the surroundings. Hence, initially, existing valid energy standards for office buildings are analysed. To obtain the energy demand ratios mentioned above, demand profile, building standard, occupation density/profile, and ventilation heat recovery efficiency are varied for the building structure shown in Fig. A-3.1. Energy demand for various buildings is calculated using TRNSYS and IDA-ICE (Trial version). Buildings with above explained demand profile are explained in the following section along with their system design, and simulation model development. System and simulation models are designed analogous to the simulation model created by Promotion Haack.

4.5.2 Building with predominant heating demand

The building model (Fig. A-3.1) used in the base simulation model (section 3) has a use-energy demand ratio of 79/21. The building is designed according to EnEV 2013, and building usage, occupation profile/density, and ventilation are defined according to DIN V 18599. Energy demand calculation, HVAC system design, and implementation in TRNSYS have been explained already in section 3. Initial parameter studies carried out using this building model is explained in section 3.7. Further parameter studies are explained in section 5.1.

4.5.3 Building with predominant cooling demand

Building constructed in passive house standard with ventilation heat recovery system of efficiency 80 %, occupation density of 12 m²/person, and full occupancy from 8:00 to 17:00 including weekends has predominant cooling demand. Total heating and cooling energy demands are 30,102 kWh and 100,210 kWh, respectively (heating/cooling-ratio of 23/77). U-value of important building structures is listed in Tab. A-4.3. Monthly energy demand and peak load are depicted in Fig. A-4.16.

Tab. A-4.3 Building envelope and U-Value with passive house standard.

Parameter	Unit	Ground floor	Outer wall	Inner wall	Ceiling	Roof
Thickness	[m]	0.42	0.43	0.126	0.41	0.45
U-Value	[W/(m ² ·K)]	0.12	0.12	0.358	0.351	0.10

Substitute model: As explained in section 3, only the third floor is simulated in parameter studies to reduce computational effort. Correction factors are calculated: the ratio of the sum of the energy demand of the similar zone on all floors to the energy demand of the respective zone on stock 3. Energy demand and correction factors are shown in Tab. A-4.4. These factors are used to correct the fluid mass flow entering and coming out of the distribution system and to calculate total energy consumption.

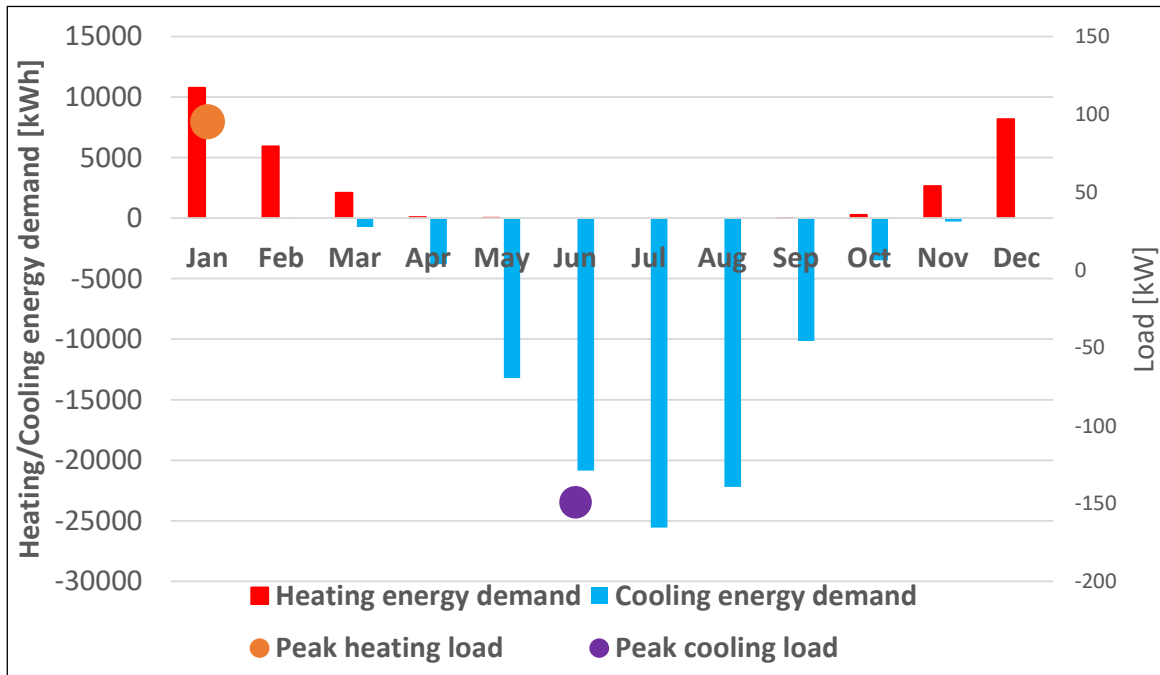


Fig. A-4.16 Monthly energy demand and peak load.

Tab. A-4.4 Energy demand and correction factor.

Parameter	Unit	Block A		Block B		Block C	
		$Q_{Use,H}$	$Q_{Use,C}$	$Q_{Use,H}$	$Q_{Use,C}$	$Q_{Use,H}$	$Q_{Use,C}$
Q_{Use} floor 3	[kW]	615	2,537	1,487	7,052	1,691	8,678
Sum of Q_{Use} of all six floors	[kW]	4,848	13,926	11,478	38,869	13,776	49,276
Correction factor	[-]	7.88	5.49	7.72	5.51	8.15	5.68

Ventilation and heat recovery system: An air exchange rate of 0.67 1/h with the weekend reduction to 0.57 1/h (similar to base simulation model), that fulfils the minimum requirements by DIN EN 15251:2012-12, is used. But unlike the base simulation mode, a heat recovery system with efficiency of 80 % is used in the simulation model (passive house standard demands a minimum heat recovery of about 75 %). According to LfU (2008), specific electrical energy consumption for the ventilation system with heat recovery is 0.4 W/m³h. This value is used to calculate the total electrical energy consumption of the ventilation unit. The operation of the heat recovery system has to be controlled to improve the efficiency of the overall system. In the recovery system, inlet air either passes through a heat exchanger where it exchanges thermal energy from exhaust air or bypasses it. During the heating period, heat recovery is essential if inlet air is cooler than exhaust air and vice versa during the cooling period. The heating or cooling period cannot be directly defined. Hence, a temperature-based control technique is developed using multiple Type 911 in TRNSYS. These types generate a control signal based on room temperature and outer air temperature, which decides if inlet air needs to pass through the exchanger or bypass it.

The bypass valve opens if the exhaust air temperature reaches +23 °C or the outer air temperature rises more than +21 °C. Once opened bypass valve closes back if exhaust air temperature reduces to +22 °C or outer air temperature reduces to +20.8 °C. This process is controlled by two type911 units, which represents the heating period.

The bypass valve closes if room temperature goes more than +23.5 °C or exhaust air temperature goes more than +24 °C. The bypass valve opens back if exhaust air goes back to +22 °C or air temperature goes below +23 °C. This process is controlled by two type911 units, which represent the cooling period.

Heat pump and storage tank: For this simulation, heat pump SmartHeat Titan 115 BW R, which has a nominal capacity of 111.65 kW with COP 4.3 at B0/W35, is chosen. The manufacturer provided characteristics are depicted in Fig. A-4.17. The heat pump model is implemented in TRNSYS through type 401, as explained in section 3.2.1.

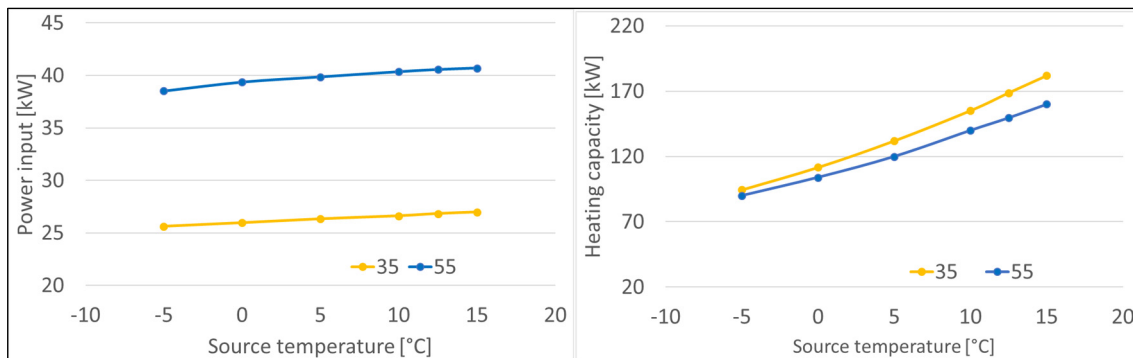


Fig. A-4.17 Characteristic curve of heat pump variant SmartHeat Titan 115 BW R.

Our design criteria for the BHE field design is that evaporator inlet temperature is not supposed to fall below -5 °C. In parameter studies multiple variants fall in this category. Hence, the heat generation system is also equipped with an auxiliary heater, which supplies the required heat if the evaporator temperature falls below -5 °C. The intention of this auxiliary heater is to identify the variants with which monovalent heating is not possible.

As in the base simulation model, the heat pump and heat distribution system are coupled through a double depressurized differential manifold (DDV) and storage tank in return flow. The tank is sized to a volume of 4.6 m³ (1000 l / 25 kW).

Floor heating system: Floor heating system analogous to the base simulation model is used. Pipe spacing is decided based on the *Schnellauslegung Flächenheizung und Heizkörper* program by Purmo. It calculates the specific heating power [W/m²] based on pipe spacing, the difference between room and fluid temperature, and thermal resistance. Power calculation in this tool is carried out as per DIN EN 1264-5:2020-02. Criteria for design and parameters are listed in Tab. A-4.5. Pipe spacing with specific heating power more than peak load should be chosen. Fluid flow rate and temperature are varied to maintain the room temperature at the expected level. Fluid flow for every zone is varied using an individual PID controller. Supply temperature is controlled using the return flow control method suggested by Dimplex. Energy demand by circulation pump at maximum flow rate is calculated, which is then varied linearly according to flow rate.

Tab. A-4.5 Floor heating system design parameter.

	Parameter	Unit	Value
Design criteria	Supply temperature	[°C]	35
	Return temperature	[°C]	28
	Specific peak load	[W/m ²]	18.38
Design parameter	Pipe spacing (centre to centre)	[m]	0.3
	Pipe outside diameter	[m]	0.014
	Pipe wall thickness	[m]	0.002
	Pipe wall conductivity	[kJ/(h·m·K)]	1.26

Tab. A-4.6 Mass flow rate calculation.

Parameter	Unit	Block A	Block B	Block C
Peak load on floor 3	[kW]	2.25	5.79	6.03
Fluid heat capacity	[kJ/kg]	4.19	4.19	4.19
ΔT	[K]	7	7	7
Required mass flow rate	[kg/h]	276	710	740
Maximum power consumption by the circulation pump	[W]	42	166	173

Chilled ceiling: As like the base simulation model, pipe spacing is chosen based on the “*Leistungskalkulator Flächenkühlung*” tool developed by PURMO. Design criteria and parameters for the chilled ceiling are shown in Tab. A-4.7. During the cooling period, the room temperature is controlled by variable mass flow combined with a constant supply setpoint temperature of 19 °C. Mass flow to each zone is controlled by an individual PID controller. Again, energy demand by circulation pump at maximum flow rate is calculated, which is then varied linearly according to flow rate.

Tab. A-4.7 Chilled ceiling system design parameter.

	Parameter	Unit	Value
Design criteria	Supply temperature	[°C]	19
	Specific peak load	[W/m ²]	28.75
Design parameter	Pipe spacing (centre to centre)	[m]	0.05
	Pipe inside diameter	[m]	0.014
	Specific norm mass flow	[kg/(h·m ²)]	19.5
	Specific norm power	[kg/(h·m ²)]	163.1

Tab. A-4.8 Mass flow rate calculation.

Parameter	Unit	Block A	Block B	Block C
Peak load of floor 3	[kW]	3.80	9.01	10.53
Fluid heat capacity	[kJ/kg]	4.19	4.19	4.19
ΔT	[K]	2	2	2
Required mass flow rate	[kg/h]	1,633	3,873	4,523
Maximum power consumption by the circulation pump	[W]	244	1,799	2,261

Borehole heat exchanger: As in the base simulation model, the basic design of the BHE field is carried out using EED simulation. EED simulation lists possible variants, which has fluid operating temperature during the heating period greater than $-5\text{ }^{\circ}\text{C}$ and less than $+20\text{ }^{\circ}\text{C}$ during the cooling period. One among the listed variants is chosen as base construction for parameter studies. Properties of BHE, the refrigerant used in EED simulation, and selected construction variants are listed in Tab. A-4.9. Monthly energy demand and peak load used for this EED simulation are shown in Fig. A-4.16.

Control strategy for heating: Here, the PID controllers vary the mass flow rate between 0 to 100 % and 24 h moving average temperature below which the heating system supposed to be active is reduced to $+11\text{ }^{\circ}\text{C}$. The remaining control strategy is almost similar to that of the base simulation model.

So, the heat pump is switched-on if

$$T_{a,mov,avg} < 11 \quad \& \quad \sum_1^3 CS_{PID,H}(i) > 0 \quad \& \quad CS_{R,Set} = 1 \quad \& \quad CS_{HP} = 1 \quad (\text{A.43})$$

The auxiliary heater is switched-on if

$$T_{a,mov,avg} < 11 \quad \& \quad \sum_1^3 CS_{PID,H}(i) > 0 \quad \& \quad CS_{R,Set} = 1 \quad \& \quad CS_{Aux,H} = 1 \quad (CS_{HP} = 0) \quad (\text{A.44})$$

Control strategy for cooling: Control strategy for cooling is again similar to the base simulation model except that the 24 h moving average above which the cooling system can be active is reduced to $+2\text{ }^{\circ}\text{C}$.

So, the cooling system is on if

$$T_{a,mov,avg} > 2 \quad \& \quad \sum_1^3 CS_{PID,H}(i) > 0 \quad (\text{A.45})$$

The auxiliary cooler is on if

$$T_{a,mov,avg} > 2 \quad \& \quad \sum_1^3 CS_{PID,H}(i) > 0 \quad \& \quad T_{out,BHE} > 20 \quad (A.46)$$

Tab. A-4.9 Properties of refrigerant and boreholes with simulation results.

	Parameter	Unit	Value
Ground	Ground thermal conductivity	[W/(m·K)]	2.1
	Ground heat capacity	[MJ/(m ³ ·K)]	2.3
	Ground surface temperature	[°C]	8.7
	Geothermal heat flux	[W/m ²]	0.065
Borehole	Configuration	384 ("60 : 5 x 12 rectangle")	
	Borehole depth	[m]	49.73
	Borehole spacing	[m]	10
	Borehole installation	[-]	Doppel-U
	Borehole diameter	[mm]	152.4
	U-pipe diameter	[mm]	32
	U-pipe thickness	[mm]	2.9
	U-pipe thermal conductivity	[W/(m·K)]	0.4
	U-pipe shank spacing	[mm]	85
	Filling thermal conductivity	[W/(m·K)]	2
	Contact resistance pipe / filling	[(m·K)/W]	0
Thermal resistances	Borehole thermal resistance, fluid/ground	[(m·K)/W]	0.06772
	Borehole thermal resistance, internal	[(m·K)/W]	0.23
Heat carrier fluid	Thermal conductivity	[W/(m·K)]	0.48
	Specific heat capacity	[J/(kg·K)]	3,795
	Density	[kg/m ³]	1,052
	Viscosity	[kg/(m·s)]	0.0052
	Freezing point	[°C]	-14
	Flow rate per borehole	[l/s]	0.52
Base load	Seasonal performance factor (heating)	[-]	4.36
	Seasonal performance factor (cooling)	[-]	1.00E+05

4.5.4 Building with equal heating and cooling demand

Building constructed in KfW55 standard, with heat recovery ventilation system of efficiency of 65 %, occupation density of 15 m²/person, and full occupation from 8:00 to 16:00 including weekends has almost equal heating and cooling demand. U-value of important building structures is listed in Tab. A-4.10. Monthly energy demand and peak load are depicted in Fig. A-4.18. Total heating and cooling energy demands are 74,642 kWh and 77,237 kWh, respectively, which accounts for a heating/cooling energy demand ratio of 49/51.

Tab. A-4.10 Building envelope and U-Value with KfW55 standard.

Parameter	Unit	Ground floor	Outer wall	Inner wall	Ceiling	Roof
Thickness	[m]	0.41	0.41	0.126	0.41	0.49
U-Value	[W/(m ² ·K)]	0.246	0.208	0.358	0.351	0.145

Substitute model: As explained in section 3, only the third floor is simulated in parameter studies to reduce computational effort. Correction factors are calculated: the ratio of the sum of the energy demand of a similar zone on all floors to the energy demand of the respective zone on stock 3. Energy demand and correction factors are shown in Tab. A-4.11. These factors are used to correct the fluid mass flow entering and coming out of the building and to calculate total energy consumption.

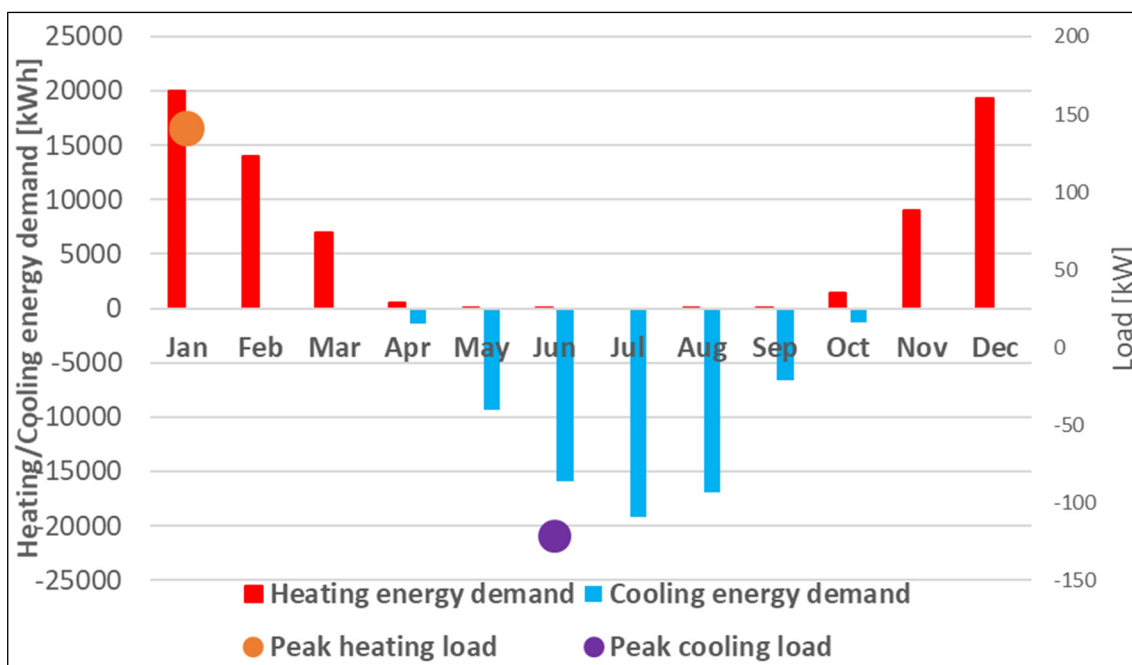


Fig. A-4.18 Monthly energy demand and peak load.

Tab. A-4.11 Building envelope and U-Value with passive house standard.

Parameter	Unit	Block A		Block B		Block C	
		$Q_{Use,H}$	$Q_{Use,C}$	$Q_{Use,H}$	$Q_{Use,C}$	$Q_{Use,H}$	$Q_{Use,C}$
Q_{Use} floor 3	[kW]	1,620	2,092	4,086	5,595	4,358	7,141
Sum of Q_{Use} of all six floors	[kW]	12,172	10,834	30,247	29,089	32,223	37,314
Correction factor	[-]	7.51	5.18	7.40	5.20	7.39	5.23

Ventilation and heat recovery system: An air exchange rate of 0.67 1/h with a weekend reduction to 0.57 1/h, that fulfils the minimum requirements by DIN EN 15251:2012-12, is used. A constant heat recovery rate of 70 % is used in the simulation model (efficiency of available ventilation system varies between 65% to 90%). According to LFU (2008), specific electrical energy consumption for the ventilation system with heat recovery is 0.4 W/m³h. This value is used to calculate the total electrical energy consumption of the ventilation unit. The operation of the heat recovery system has to be controlled to improve the efficiency of the overall system. Heat recovery is controlled in the same way, as explained in section 4.6.3.

The bypass valve is set to open if the exhaust air temperature reaches +23 °C or the outer air temperature rises more than +21 °C. Once opened bypass valve closes back if exhaust air temperature reduces to +22 °C or outer air temperature reduces to +20.8 °C. This process is controlled by two Type911 units, which represents the heating period.

The bypass valve is closed if room temperature goes more than +23.5 °C or exhaust air temperature goes more than +24 °C. The bypass valve opens back if exhaust air goes back to +22 °C, or the air temperature goes below +23 °C. This process is controlled by two Type911 units, which represent the cooling period.

Heat pump and storage tank: For this purpose, heat pump SmartHeat Titan 139 BW R, which has a nominal capacity of 136.16 kW with COP 4.39 at B0/W35, is chosen. The manufacturer provided a characteristic curve is depicted in Fig. A-4.19. The heat pump model is implemented in TRNSYS through Ttype401, as explained in section 3.2.1.

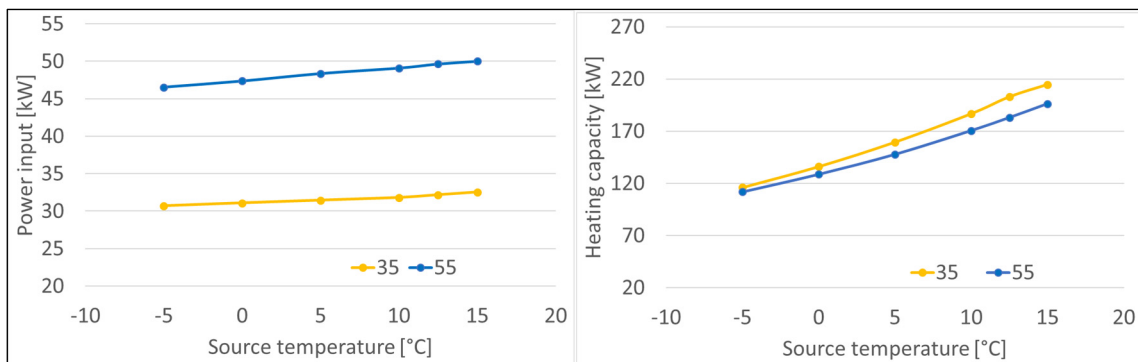


Fig. A-4.19 Characteristic curve of heat pump variant SmartHeat Titan 139 BW R.

Our design criteria for the BHE field design is that evaporator inlet temperature is not supposed to fall below $-5\text{ }^{\circ}\text{C}$. In parameter studies multiple variants fall in this category. Hence, the heat generation system is also equipped with an auxiliary heater, which supplies the required heat if the evaporator temperature falls below $-5\text{ }^{\circ}\text{C}$. The intention of this auxiliary heater is to identify the variants with which monovalent heating is not possible.

As in the base simulation model, the heat pump and heat distribution system are coupled through a double depressurized differential manifold and storage tank in return flow. The tank is sized to a volume of 5.5 m^3 ($1000\text{ l} / 25\text{ kW}$).

Floor heating system: Floor heating system is designed in analogous to previous simulation models. Pipe spacing is decided based on the *Schnellauslegung Flächenheizung und Heizkörper* program by Purmo. It calculates the specific heating power $[\text{W}/\text{m}^2]$ based on pipe spacing, the difference between room and fluid temperature, and thermal resistance. Criteria for design and parameters are listed in Tab. A-4.12. Fluid flow rate and temperature are varied to maintain the room temperature at the expected level. Fluid flow for every zone is varied using an individual PID controller. Supply temperature is controlled using the return flow control method suggested by DIMPLEX (with the help of polynomial function A.1). Energy demand by circulation pump at maximum flow rate is calculated, which is then varied linearly according to flow rate.

Tab. A-4.12 Floor heating system design parameter.

	Parameter	Unit	Value
Design criteria	Supply temperature	$[\text{ }^{\circ}\text{C}]$	35
	Return temperature	$[\text{ }^{\circ}\text{C}]$	28
	Specific peak load	$[\text{W}/\text{m}^2]$	26.37
Design parameter	Pipe spacing (centre to centre)	$[\text{m}]$	0.3
	Pipe outside diameter	$[\text{m}]$	0.014
	Pipe wall thickness	$[\text{m}]$	0.002
	Pipe wall conductivity	$[\text{kJ}/(\text{h}\cdot\text{m}\cdot\text{K})]$	1.26

Tab. A-4.13 Mass flow rate calculation.

Parameter	Unit	Block A	Block B	Block C
Peak load of floor 3	$[\text{kW}]$	3.46	8.85	8.91
Fluid heat capacity	$[\text{kJ}/\text{kg}]$	4.19	4.19	4.19
ΔT	$[\text{K}]$	7	7	7
Required mass flow rate	$[\text{kg}/\text{h}]$	424	1,086	1,094
Maximum power consumption by the circulation pump	$[\text{W}]$	65	254	256

Chilled ceiling: The building is cooled by coupling it directly with BHE through a heat exchanger and mixing circuit. Like the previous simulation model, pipe spacing is chosen based on the “*Leistungskalkulator Flächenkühlung*” tool developed by PURMO. Design criteria and the parameter is shown in Tab. A-4.14. The room temperature is controlled by variable mass flow combined with a constant supply setpoint temperature of 19 °C. Mass flow to each zone is controlled by an individual PID controller. Energy demand by circulation pump at maximum flow rate is calculated, which is then varied linearly according to flow rate.

Tab. A-4.14 Chilled ceiling system design parameter.

	Parameter	Unit	Value
Design criteria	Supply temperature	[°C]	19
	Specific peak load	[W/m ²]	24.48
Design parameter	Pipe spacing (centre to centre)	[m]	0.05
	Pipe inside diameter	[m]	0.014
	Specific norm mass flow	[kg/(h·m ²)]	19.5
	Specific norm power	[kg/(h·m ²)]	163.1

Tab. A-4.15 Mass flow rate calculation.

Parameter	Unit	Block A	Block B	Block C
Peak load of floor 3	[kW]	3.61	8.33	10.0
Fluid heat capacity	[kJ/kg]	4.19	4.19	4.19
ΔT	[K]	2	2	2
Required mass flow rate	[kg/h]	1,550	3,579	4,296
Maximum power consumption by the circulation pump	[W]	232	1,663	2,147

Borehole heat exchanger: The basic design of the BHE field is carried out using EED simulation. EED simulation lists possible variants, which have fluid operating temperature during the heating period greater than -5 °C and less than +20 °C during the cooling period. One among the listed variants is chosen as base construction for parameter studies. Properties of BHE, the refrigerant used in EED simulation, and selected construction variants are listed in Tab. A-4.16. Monthly energy demand and peak load used for this EED simulation are shown in Fig. A-4.18.

Control strategy for heating: Here, the PID controllers vary the mass flow rate between 0 to 100 % and 24 h moving average temperature below which the heating system supposed to be active is reduced to +11 °C. The remaining control strategy is almost similar to that of the base simulation model.

So, the heat pump is switched-on if

$$T_{a,mov,avg} < 11 \quad \& \quad \sum_1^3 CS_{PID,H}(i) > 0 \quad \& \quad CS_{R,Set} = 1 \quad \& \quad CS_{Hp} = 1 \quad (A.47)$$

The auxiliary heater is switched-on if

$$T_{a,mov,avg} < 11 \quad \& \quad \sum_1^3 CS_{PID,H}(i) > 0 \quad \& \quad CS_{R,Set} = 1 \quad \& \quad CS_{Aux,H} = 1 \quad (CS_{Hp} = 0) \quad (A.48)$$

Tab. A-4.16 Properties of refrigerant and boreholes with simulation results.

	Parameter	Unit	Value	
Ground	Ground thermal conductivity	[W/(m·K)]	2.1	
	Ground heat capacity	[MJ/(m ³ ·K)]	2.3	
	Ground surface temperature	[°C]	8.7	
	Geothermal heat flux	[W/m ²]	0.065	
Borehole	Configuration	241 ("20 : 2 x 10 rectangle")		
	Borehole depth	[m]	100.14	
	Borehole spacing	[m]	10	
	Borehole installation	[-]	Doppel-U	
	Borehole diameter	[mm]	152.4	
	U-pipe diameter	[mm]	32	
	U-pipe thickness	[mm]	2.9	
	U-pipe thermal conductivity	[W/(m·K)]	0.4	
	U-pipe shank spacing	[mm]	85	
	Filling thermal conductivity	[W/(m·K)]	2	
	Contact resistance pipe / filling	[(m·K)/W]	0	
	Thermal resistances	Borehole thermal resistance, fluid/ground	[(m·K)/W]	0.06772
		Borehole thermal resistance, internal	[(m·K)/W]	0.23
Heat carrier fluid	Thermal conductivity	[W/(m·K)]	0.48	
	Specific heat capacity	[J/(kg·K)]	3,795	
	Density	[kg/m ³]	1,052	
	Viscosity	[kg/(m·s)]	0.0052	
	Freezing point	[°C]	-14	
	Flow rate per borehole	[l/s]	0.52	
Base load	Seasonal performance factor (heating)	[-]	4.39	
	Seasonal performance factor (cooling)	[-]	1.00E+05	

Control strategy for cooling: Control strategy for cooling is again similar to the base simulation model except that a 24 h moving average above which the cooling system can be active is reduced to +2 °C.

So, the cooling system is on if

$$T_{a,mov,avg} > 2 \quad \& \quad \sum_1^3 CS_{PID,H}(i) > 0 \quad (A.49)$$

The auxiliary cooler is on if

$$T_{a,mov,avg} > 2 \quad \& \quad \sum_1^3 CS_{PID,H}(i) > 0 \quad \& \quad T_{out,BHE} > 20 \quad (A.50)$$

5 Parameter studies

Initial parameter studies carried out with the model explained in section 3 (predominant heating demand) were concluded with uncertainty. Hence, further parameter studies with higher total BHE length is carried out. Besides, parameter studies with two simulation models with different energy consumption ratio (explained in section 4.5) were carried out. With the parameter studies, suggestions for the constructive design of the BHEs field for combined application were summarized.

5.1 Parameter studies 1

5.1.1 Variant matrix

Initial parameter studies explained in section 3 shown that further enhancement of variant matrix is essential for the generalized solution of the constructive design of the BHE field for this building model. Hence, further parameter studies were carried out with an enhanced variant matrix (Tab. A-5.1). Here, the total probe length is increased to 5,000 m. Observations made during these parameter studies are discussed with relevant diagrams.

Tab. A-5.1 Variant matrix for parameter studies 1.

Parameter	Unit	Value					
Total BHE length	[m]	4,000					
Number of BHEs n	[-]	20	32	40	80	160	200
Depth of BHEs	[m]	200	125	100	50	25	20
Borehole spacing	[m]	5, 6, 7, 8, 9, 10					
Total BHE length	[m]	5,000					
Number of BHEs	[-]	25	40	50	100	200	250
Depth of BHEs	[m]	200	125	100	50	25	20
Borehole spacing	[m]	5, 6, 7, 8, 9, 10					
Geothermal gradient	[K/100 m]	1					
		3 The average value for Germany					
		6,5 At Zittau					
		9					
Hydraulic connections of BHEs in field		parallel					
BHE pipe dimension		32 x 2.9 mm			40 x 3.7 mm		

Total number of variants (N) and variants in every gradient (N_j)

$$N_1 = N_2 = N_3 = N_4 = Var1 \cdot Var2 \cdot Var3 \cdot Var4 = 2 \cdot 6 \cdot 6 \cdot 1 = 144$$

$$N = N_1 + N_2 + N_3 + N_4 = 144 + 144 + 144 + 144 = 576$$

(A.51)

5.1.2 Results

Fig. A-5.1 depicts the ratio of primary energy consumption of a particular variant to the minimum primary energy consumption from all variants in the respective gradient (A.21) over 15-years (Y-axis). This illustration aims to compare primary energy consumption by variants with a total borehole length of 4,000 m and 5,000 m. Comparison is made for gradients 0.03 K/m (first two graphs) and 0.065 K/m (third and fourth graphs). The X-axis represents borehole depth and the corresponding number of boreholes n . Curve parameters are borehole spacing. Value 1.05 means that the variant has 5 % more total primary energy consumption ($Q_{P,tot}$) compared to the variant with minimum total primary energy consumption ($Q_{P,tot,min}$) in the respective gradient (both 4,000 m and 5,000 m included; Fig. A-5.1).

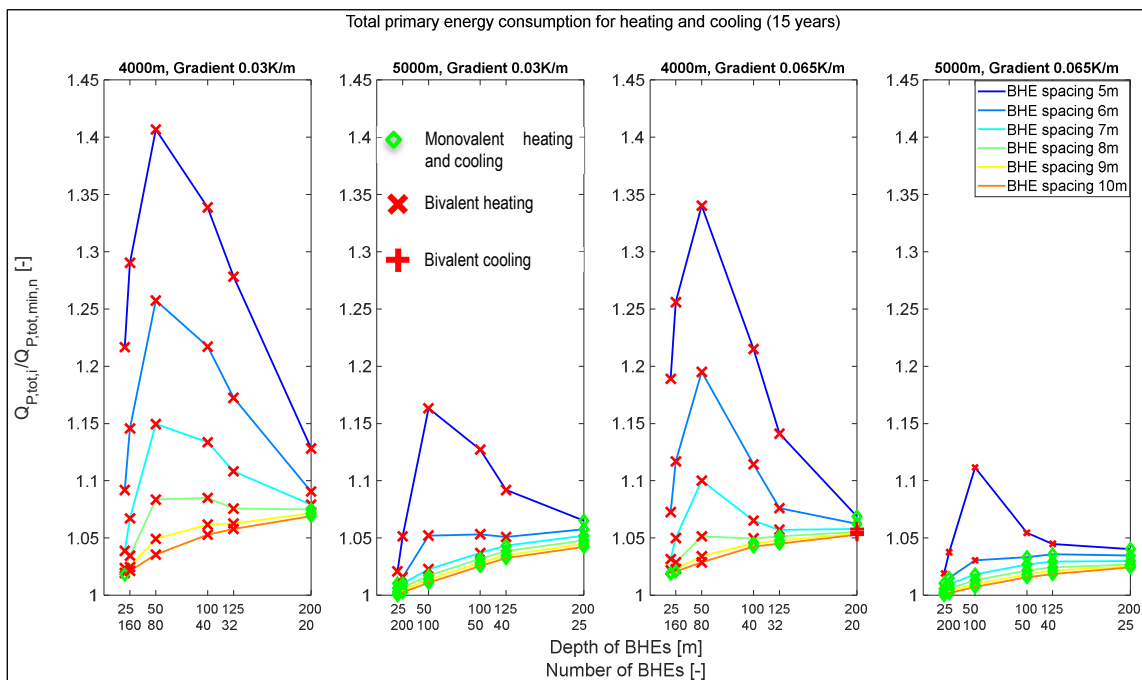


Fig. A-5.1 Total primary energy consumption $Q_{P,tot}$ for parameter studies 1 (4,000 m vs. 5,000 m).

By comparing 4,000 m and 5,000 m, significant variation in primary energy consumption can be observed. Compactly arranged BHEs with a total probe length of 4,000 m demands considerable heat energy from an additional heater, which reflects significantly in $Q_{P,tot}$ (For ex: around 40 % more $Q_{P,tot}$ by 80 BHEs each of 50 m deep for gradient 0.03 K). By increasing the total probe length to 5,000 m, usage of an additional heater can be reduced significantly in a compactly arranged BHE field. Besides, there exist multiple variants with which monovalent heating over 15 years is possible. Monovalent heating is possible if BHEs are arranged with sufficient distance between them (more or equal to 8 m). This comparison clarifies that the total probe length of 5,000 m is required for monovalent heating and cooling of this building using BHEs.

Fig. A-5.2 depicts the ratio of total primary energy consumption ($Q_{P,tot}$) of a particular variant to the minimum primary energy consumption ($Q_{P,tot,min}$) from all 144 variants on respective gradient (A.21) over 15-years (Y-axis). Four graphs represent four gradients. The X-axis represents borehole depth and the corresponding number of boreholes n . Curve parameters are borehole spacing.

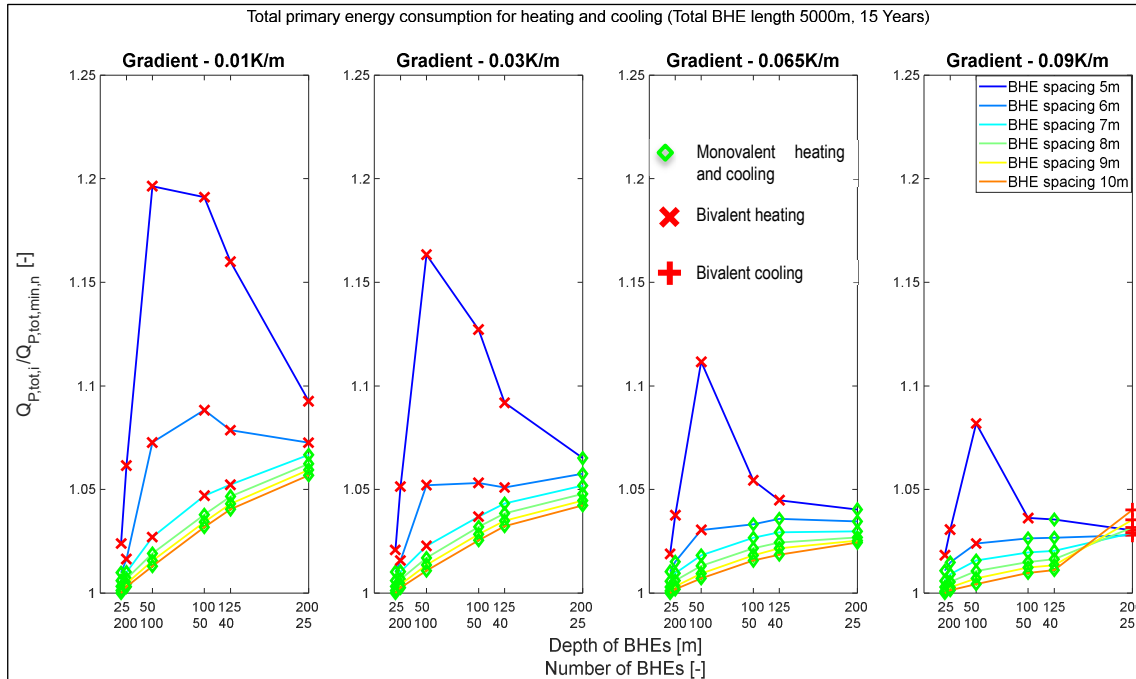


Fig. A-5.2 Total primary energy consumption $Q_{P,tot}$ for parameter studies 1 (Total BHE length 5,000 m).

As shown in the figure, $Q_{P,tot}$ varies up to 20 % when all variants are considered. By considering only monovalent variants, variation in total primary energy consumption depending on constructive design is insignificant (varies 4 to 5 %). The significant variation in $Q_{P,tot}$ are shown by bivalent variants (variants that use the additional heater to supply required heat if the heat pump reaches a minimum source temperature of $-5\text{ }^{\circ}\text{C}$). This deviation could have been reduced using a secondary heating system with a better SPF. As ground sourced heating and cooling system is efficient than most of the concurrent systems, designing monovalent ground sourced heating/cooling system is preferred than choosing better secondary systems. Bivalent systems can be considered in case of other limitations (for example, lack of ground space). This evaluation suggests that designing monovalent variants for heating and cooling should be the primary concern of constructive design. Most of the monovalent variants for heating lies by higher borehole spacing (more or equal to 8 m). Also, 200 m deeper boreholes at gradient 0.09 K/m are bivalent for cooling. Before concluding optimization potential, understanding the following factors is essential: Primary energy consumption for heating/cooling and its reflection in total primary energy consumption; Variation of primary energy consumption for heating and cooling depending on construction parameter. Those factors are explained with relevant diagrams.

Fig. A-5.3 depicts the ratio of primary energy consumption of the variant to minimum energy consumption from all variants in gradient 0.03 K/m over 15 years. Three graphs in the figure represent total primary energy consumption (A.21), primary energy consumption for heating (A.22), and primary energy consumption for cooling (A.23). The X-axis represents borehole depth and the corresponding number of boreholes n . Curve parameters are borehole spacing. Note: Heating and cooling do not necessarily have the same minimum Q point (suits in this evaluation).

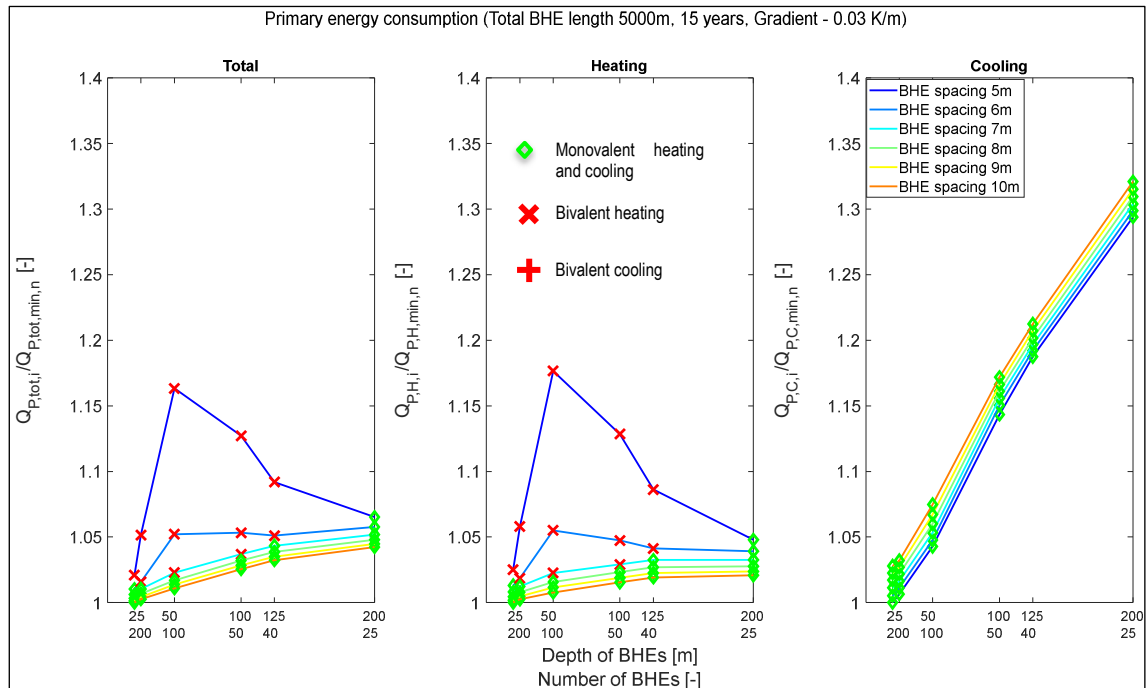


Fig. A-5.3 $Q_{P,tot}$ vs. $Q_{P,H}$ vs. $Q_{P,C}$ for parameter studies 1 (5,000 m, 0.03 K/m).

Considering only the monovalent variant in this gradient, $Q_{P,tot}$ varies 6 % approximately and $Q_{P,H}$ varies 5 % approximately depending on the constructive design. But $Q_{P,C}$ varies more than 30 % depending on the constructive design. Despite huge variation in $Q_{P,C}$, its reflection in $Q_{P,tot}$ is insignificant. This is because of less cooling demand by building and better SPF of the cooling system. $Q_{P,tot}$ varies significantly only if an additional heater is used. This again leads to the previous thesis that designing the variant that assures monovalent heating and cooling for a longer duration should be the primary concern of constructive design of BHEs for this building model. This evaluation explains the variation of total primary energy depending on energy consumption for heating and cooling. As explained earlier, understanding of the variation of energy consumption depending on construction parameter are essential. For this purpose, the following two evaluations were made for heating and cooling separately.

Fig. A-5.4 depicts the ratio of primary energy consumption for heating ($Q_{P,H}$) of a particular variant to the minimum primary energy consumption for heating ($Q_{P,H,min}$) from all variants with a gradient of 0.03 K/m. The second graph depicts the fluid outlet temperature of the BHE field averaged over the heat extraction period in 15 years ($\bar{T}_{out,BHE,H}$). The third graph depicts primary energy consumption by the heating system, excluding the circulation pump on the primary side of the heat pump. The X-axis represents borehole depth and the corresponding number of boreholes n . Curve parameters are borehole spacing.

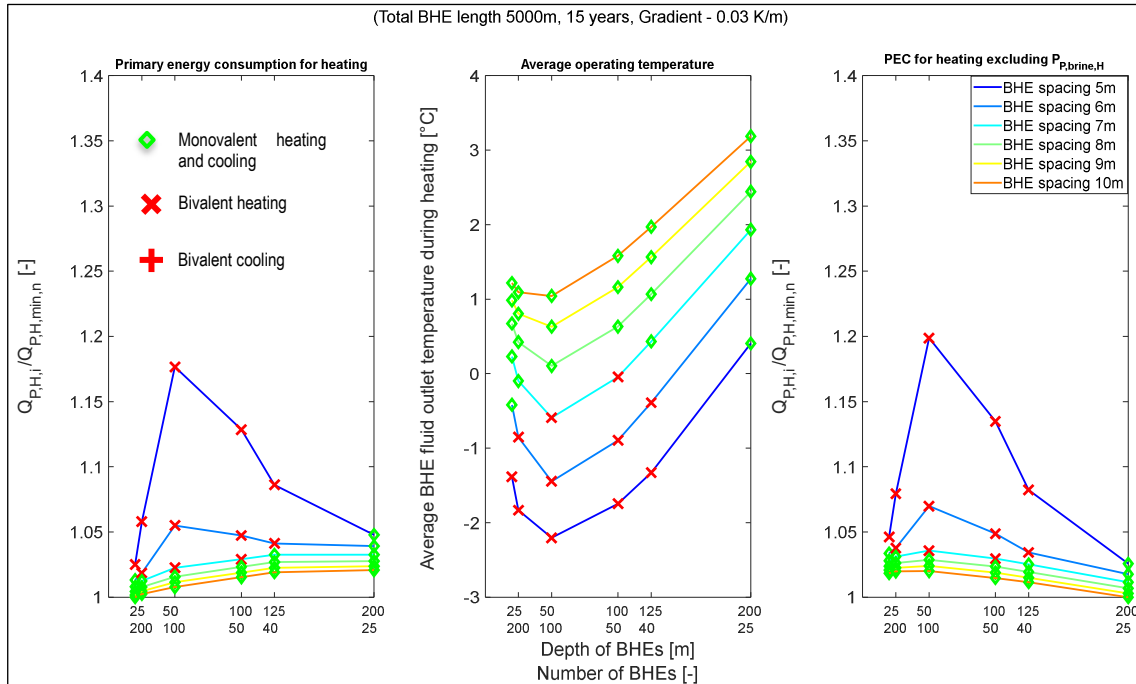


Fig. A-5.4 $Q_{P,H}$ vs. $\bar{T}_{out,BHE,H}$ for parameter studies 1 (5,000 m, 0.03 K/m).

Minimum and maximum $\bar{T}_{out,BHE,H}$ lies at 50 m and 200 m deep BHEs, respectively, whereas minimum primary energy consumption for heating ($Q_{P,H,min}$) lies at 20 m deep BHEs. The main reason for this is the pressure drops in BHEs. More BHEs means less mass flow rate in a single BHE, which leads to less pressure drop and vice versa. Thus, deeper BHEs end up consuming more primary energy despite a favourable operating temperature. This influence can be understood by comparing primary energy for heating with and without the circulation pump (graph 1 and 3). The influence of operating temperature cannot be ignored because it decides the monovalent operation of the heating and cooling system, which is supposed to be a primary concern for constructive design. The second graph of Fig. A-5.4 shows that compactly arranged BHEs low $\bar{T}_{out,BHE,H}$, which used additional heaters during the initial 15 years. This evaluation suggests that borehole spacing of at least 8 m is essential for monovalent operation over 15 years for the selected building model at a location with a gradient of 0.03 K/m. $\bar{T}_{out,BHE,H}$ for all gradients were evaluated in Fig. A-5.6. The variation of energy consumption for cooling depending on construction parameters are explained with the following evaluation.

Fig. A-5.5 depicts the ratio of primary energy consumption for cooling ($Q_{P,C}$) of a particular variant to the minimum primary energy consumption for cooling ($Q_{P,C,min}$) from all variants with a gradient of 0.03 K/m. The second graph depicts the fluid outlet temperature of the BHE field averaged during the heat supply period in 15 years ($\bar{T}_{out,BHE,C}$). The third graph depicts primary energy consumption by the cooling system, excluding the circulation pump on the primary side of the heat pump. The X-axis represents borehole depth and the corresponding number of boreholes n . Curve parameters are borehole spacing.

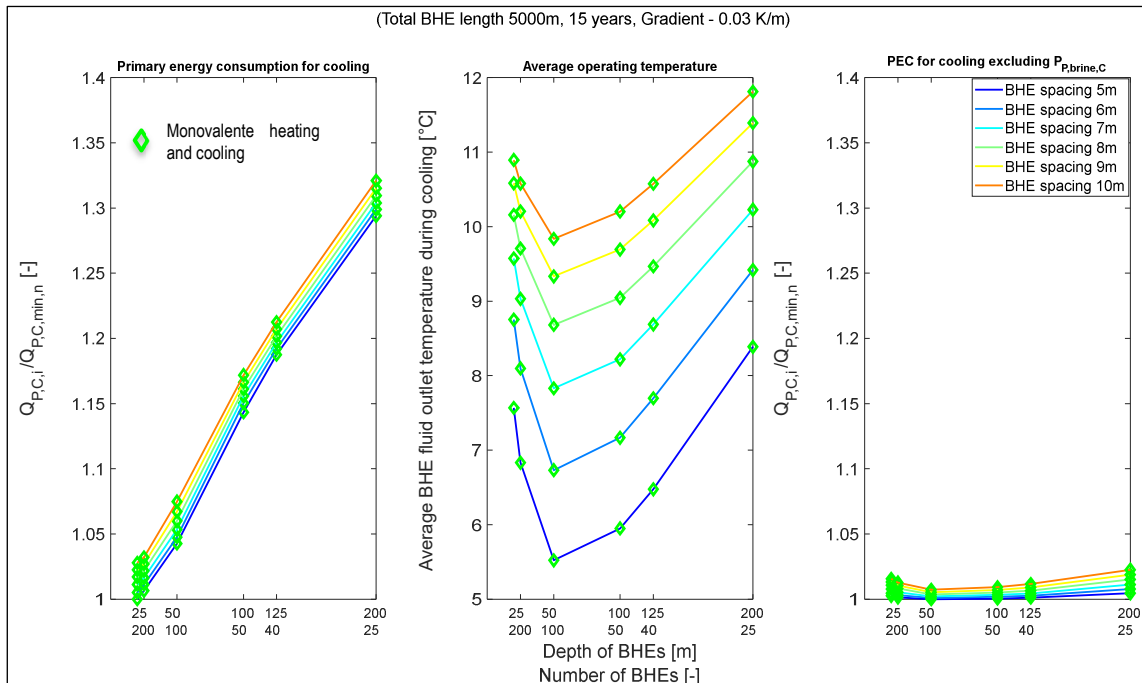


Fig. A-5.5 $Q_{P,C}$ vs. $\bar{T}_{out,BHE,C}$ for parameter studies 1 (5,000 m, 0.03 K/m).

There exists a minimum value for $\bar{T}_{out,BHE,C}$ at 50 m deep boreholes. Compactly arranged BHEs have a favourable operating temperature because dominant heat extraction over a year leads to continuous cooling of ground. But, $\bar{T}_{out,BHE,C}$ has no significant influence on primary energy consumption (can be realized by observing the energy consumption of a cooling system without a circulation pump). Variation of $Q_{P,C}$ is predominantly determined by pressure drops in BHEs and, if applicable, by energy demand from an additional cooler. As explained earlier, though the constructive design of BHEs has a significant influence on $Q_{P,C}$, its reflection on $Q_{P,tot}$ is insignificant. Only if operating temperature increases beyond 19°C, the aid of additional cooler (see 200 m deep BHEs at gradient 0.09 K/m in Fig. A-5.2) is required, which influences $Q_{P,tot}$ significantly.

Furthermore, these variants needed the assistance of an auxiliary cooler only during initial years (ground cooled down after few years). Hence, for buildings with predominant heating demand, choosing monovalent variants for cooling, particularly during initial years of system operation, should be the ultimate concern. It can be summarized that; constructive design should be made so that ground does not cool down fast during heating operation to demand the aid of additional heater and initial ground temperature should not be so high to avoid demand of aid of additional cooler.

Fig. A-5.6 shows fluid outlet temperature of BHE field averaged over the heat extraction period for 15 years ($\bar{T}_{out,BHE,H}$). This evaluation aims to provide an overview of the average source side operating temperature below which aid of additional heater is required. Four graphs represent four gradients. The X-axis represents borehole depth and the corresponding number of boreholes n . Curve parameters are borehole spacing.

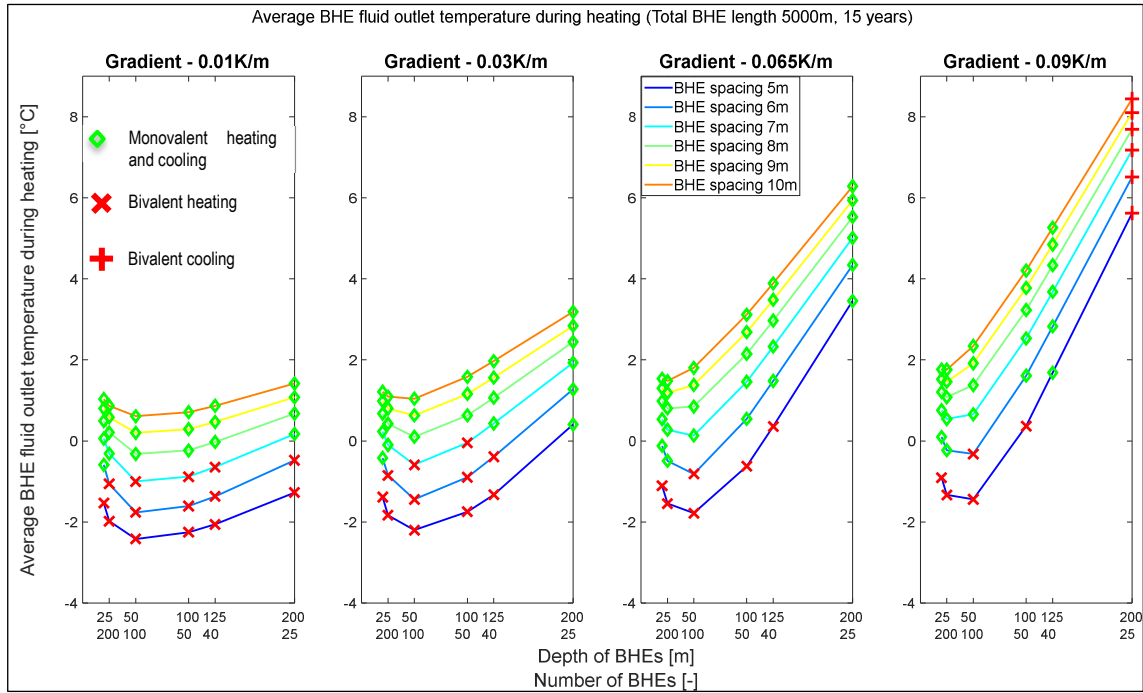


Fig. A-5.6 $\bar{T}_{out,BHE,H}$ (15-year average) for parameter studies 1 (5,000 m).

Fig. A-5.6 shows that sparsely arranged deeper BHEs has a favourable operating temperature over 15 years. Compactly arranged BHEs have a lower operating temperature, indicating that these variants are more likely to fall below the operating temperature limit of $-5\text{ }^{\circ}\text{C}$ for the heat pump. For every evaluated gradient, deeper BHEs (for ex 200 m) have favourable operating temperatures and secure monovalent heating. However, the monovalent operation is secured only for the simulated period. It still fails to explain how fast the constructive design cools down so that monovalent operation can be secured for more extended period. To predict the monovalent operation for more extended period, the annual average operating temperature over 15 years needs to be evaluated. Due to the enormous number of variants, such evaluation is made only for the crucial variants.

Fig. A-5.7 depicts fluid outlet temperature BHE field averaged over the heat extraction period $\bar{T}_{out,BHE,H}$ for every year (total 15 years). Evaluation is made for two borehole spacings (5 m and 10 m) at gradients 0.03 K/m and 0.09 K/m. Curve parameters are borehole depth and the corresponding number of BHEs. As show in Fig. A-5.7, compactly arranged BHE field cools down faster. Hence, source temperature falls below the limit of $-5\text{ }^{\circ}\text{C}$ required for heat pump operation, leading auxiliary heater to supply required heat. 200 m deep BHEs with borehole spacing of 10 m cool down at a slower rate ($\bar{T}_{out,BHE,H}$) around $2\text{ }^{\circ}\text{C}$ for gradient 0.03 K/m and $7\text{ }^{\circ}\text{C}$ for gradient 0.09 K/m after 15 years). The aid of an additional heater is required mostly if $\bar{T}_{out,BHE,H}$ goes below $-2\text{ }^{\circ}\text{C}$. As the variants mentioned above cool at a slower rate and curve flattens already, these variants can be monovalent for heating for a prolonged duration. Though variants with several 20 m or 25 m deep BHEs placed 10 m apart from each other stabilized sooner, these variants are insignificant because of large ground area requirements. It is necessary to note that the aid of an additional cooler is required during initial years for construction with 200 m deep BHEs at gradient 0.09 K/m. But at this location, 125 m deep

BHEs can be chosen because $\bar{T}_{out,BHE,H}$ is still around 4 °C after 15 years, and it is monovalent for cooling. It can be summarized that 25 BHEs each of depth 200 m with bore-hole spacing 10 m is preferred construction for gradients 0.1 K/m, 0.3 K/m, and 0.065 K/m as it secures monovalent heating and cooling for a longer duration. For gradient 0.09 K/m, 40 BHEs each of depth 125 m placed 10 m apart is preferred as it secures monovalent heating and cooling operation. From Fig. A-5.7, it can also be observed that most of the bivalent variant lies below the value -2 °C ($\bar{T}_{out,BHE,H}$) for evaluated variants. Multiple variants were simulated for 15 years in this parameter studies. Hence, to find bivalent points for all simulated variants, the following evaluations were prepared. In Fig. A-5.8, First graph plots: $\bar{T}_{out,BHE,H}$ averaged over 15 years against the total operating period of the additional heater in 15 years; $\bar{T}_{out,BHE,C}$ averaged over 15 years against the total operating period of the additional cooler in 15 years, Second graph plots: $\bar{T}_{out,BHE,H}$ averaged over a year and operating period of the additional heater in the respective year (total 15 years); $\bar{T}_{out,BHE,C}$ averaged for every year and operating period of the additional cooler in the respective year (total 15 years).

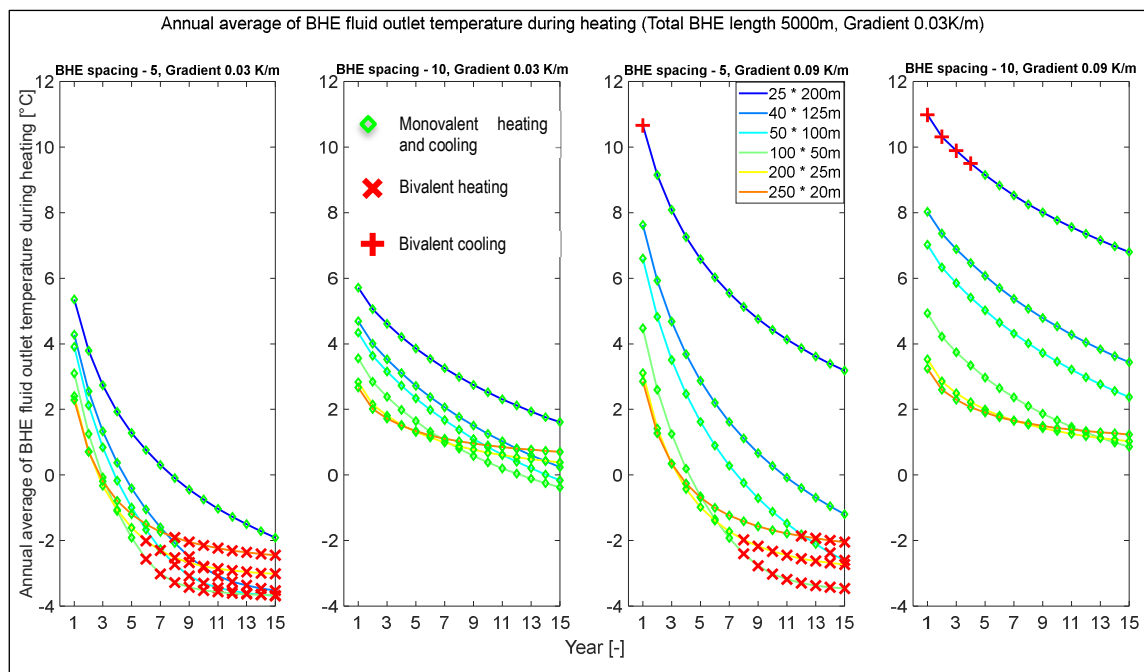


Fig. A-5.7 $\bar{T}_{out,BHE,H}$ (annual average) for parameter studies 1 (5,000 m).

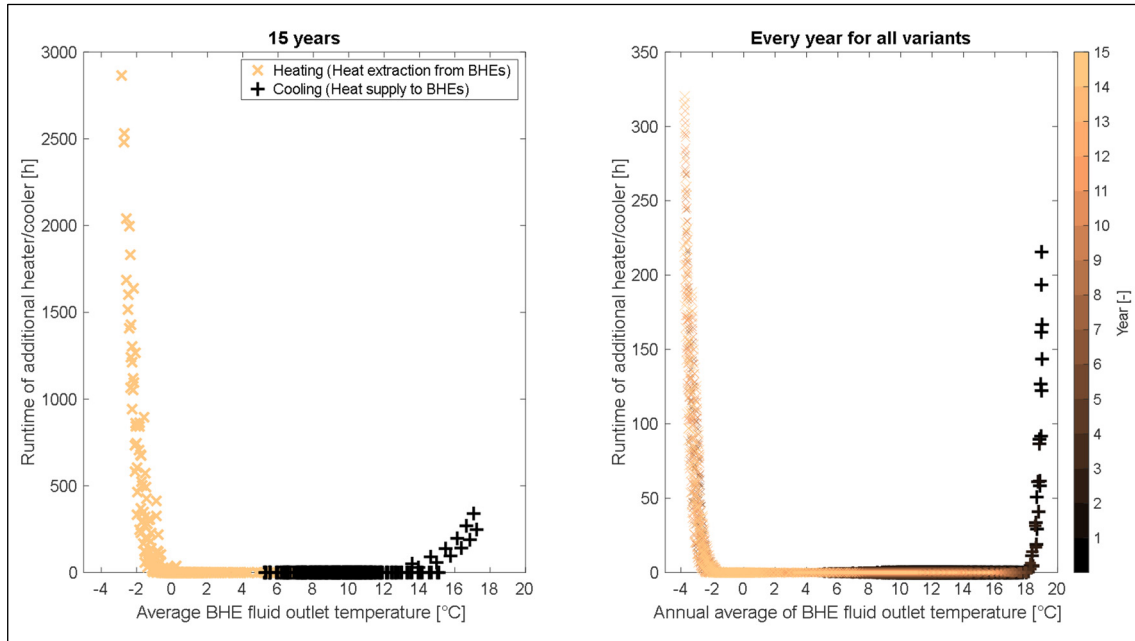


Fig. A-5.8 Bivalent point vs. operation period of auxiliary heater/cooler (parameter studies 1).

This evaluation aims to find the bivalent point as well as $\bar{T}_{out,BHE,H} / \bar{T}_{out,BHE,C}$ dependent operating period of additional heater/cooler. The first graph (averaged over 15 years) shows that demand for additional heaters might arise if $\bar{T}_{out,BHE,H}$ falls below 0°C and its operating period is significant around -2°C . Similarly, demand for additional cooler might arise if $\bar{T}_{out,BHE,C}$ goes beyond 14°C . But 15-year average value cannot be considered for decision making because BHE field temperature changes continuously. Hence, a similar comparison is made with values averaged over the year. The graph shows that demand for auxiliary heaters arises if the annual average source temperature ($\bar{T}_{out,BHE,H}$) falls below -2°C . Also, demand for auxiliary cooler arises if $\bar{T}_{out,BHE,C}$ goes beyond 18°C . The additional heater is required mostly in later years, whereas the additional cooler is required mostly in earlier years. This shows that during the constructive design of BHEs, the initial year has to be focused on cooling and the final year of system design for heating. The operating limit of the heat pump (-5°C) is reached by the variants with an annual average source temperature below -2°C . *Future designing of the BHE field can probably be carried out with simple mathematical models and variants in which $\bar{T}_{out,BHE,H}$ stays above -2°C can be considered monovalent variants. Similarly, the variants with $\bar{T}_{out,BHE,C}$ less than 18°C can be considered monovalent for cooling. But this thesis has to be further analysed to provide plausible conclusions.*

5.2 Parameter studies 2

Second parameter studies have been carried out with the building model with almost equal heating and cooling demand (Building model explained in section 4.5.4). Base constructive design of BHE field is carried out in EED (see section 4.5.4). Initial parameter studies were carried out varying constructive parameters with base design (2,000 m total probe length). Similar to previous parameter studies 1, this parameter studies had shown that most variants are bivalent over the simulation period of 15 years. Hence, further parameter studies with an increased total BHE length of 3,000 m were carried out. Observation made during these parameter studies is explained in this section with relevant diagrams.

5.2.1 Variant matrix

Tab. A-5.2 Variant matrix for parameter studies 2.

Parameter	Unit	Value					
Total BHE length	[m]	3,000					
Number of BHEs n	[-]	15	24	30	60	120	150
Depth of BHEs	[m]	200	125	100	50	25	20
Borehole spacing	[m]	1, 2, 3, 4, 5, 6, 7, 8, 9, 10					
Geothermal gradient	[K/100 m]	1					
		3 The average value for Germany					
		6,5 At Zittau					
		9					
Hydraulic connections of BHEs in field		parallel					
BHE pipe dimension		32 x 2.9 mm					

$$N_1 = N_2 = N_3 = N_4 = Var1 \cdot Var2 \cdot Var3 \cdot Var4 = 1 \cdot 6 \cdot 10 \cdot 1 = 60$$

$$N = N_1 + N_2 + N_3 + N_4 = 60 + 60 + 60 + 60 = 240$$

(A.52)

5.2.2 Results

Fig. A-5.9 depicts the ratio of primary energy consumption of a particular variant to the minimum primary energy consumption from all variants in the respective gradient (A.21) for 15 years (Y-axis). Four graphs represent four gradients. The X-axis represents borehole depth and the corresponding number of boreholes n . Curve parameters are borehole spacing. Value 1.05 represents 5 % more primary energy consumption than the minimum variant. Borehole spacing of 1 m and 2 m are ignored in evaluation to avoid inconsistencies.

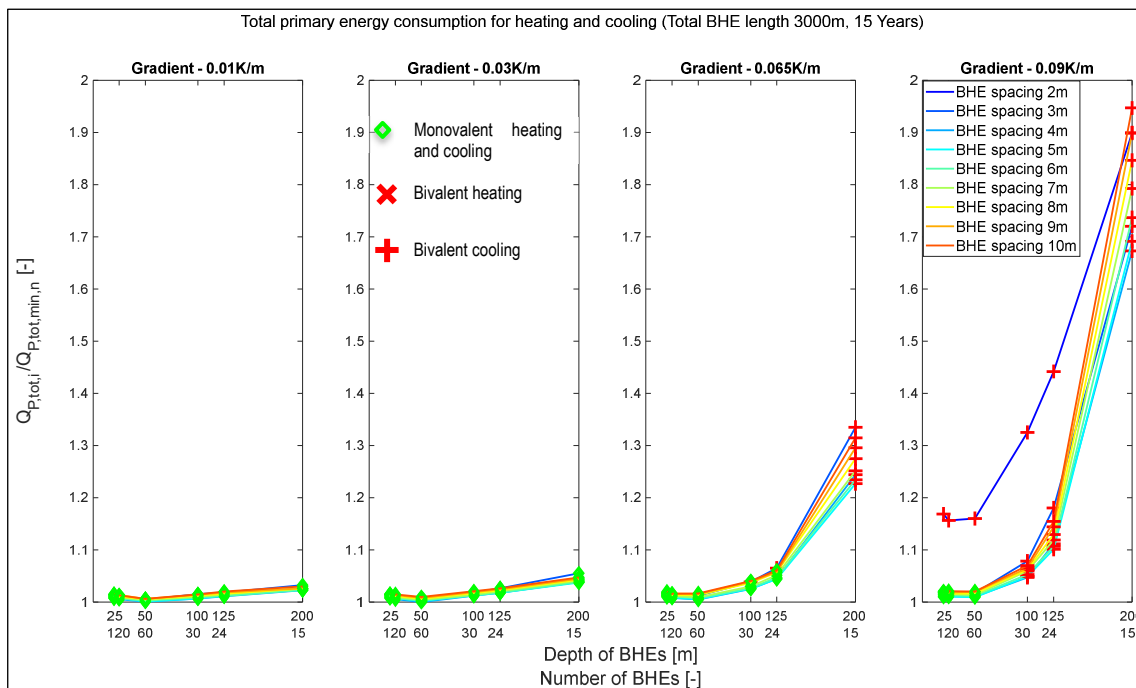


Fig. A-5.9 $Q_{P,tot}$ for parameter studies 2 (3,000 m).

By considering only monovalent variants, variation in total primary energy consumption ($Q_{P,tot}$) accounts for 3 to 6 %. This variation is insignificant similar to the previous building model. But, unlike the previous building model, compact arrangements are possible here. This is obvious because of better regeneration in the ground (equal heating / cooling demand from the building). Better regeneration can be confirmed from evaluation Fig. A-5.13, where annual average fluid outlet temperature from BHEs during heat supply ($\bar{T}_{out,BHE,C}$) does not change significantly. Most of the variants with minimum borehole spacing of 4m are monovalent for heating. But cooling is critical, particularly at higher gradients. Significant variation in $Q_{P,tot}$ occurs only if the variant is bivalent for cooling. Hence, again the primary focus should be on designing monovalent variants, particularly for cooling. For gradients 0.01 K/m and 0.03 K/m, all variants are monovalent for the simulated period. For gradient 0.065 K/m, 200 m deeper BHEs cannot be monovalent, whereas for gradient 0.09 K/m, even 100 m deep BHEs cannot be monovalent. Since the spacious arrangement is not essential for this building type, more BHEs of depth 50 m can be compactly arranged even at the gradient 0.09 K/m. But to secure long-term

monovalent operation, average BHE fluid outlet temperatures have to be analysed. Before that, the following factors are explained with relevant examples. First, primary energy consumption for heating / cooling and its reflection in total primary energy consumption. Second, Variation of primary energy consumption for heating and cooling depending on construction parameters.

Fig. A-5.10 depicts the ratio of primary energy consumption of a particular variant to the minimum primary energy consumption from all variants in gradient 0.065 k/m for 15 years (Y-axis). Three graphs represent total primary energy consumption (A.21), primary energy consumption for heating (A.22), and primary energy consumption for cooling (A.23), respectively. The X-axis represents borehole depth and the corresponding number of boreholes n . Curve parameters are borehole spacing.

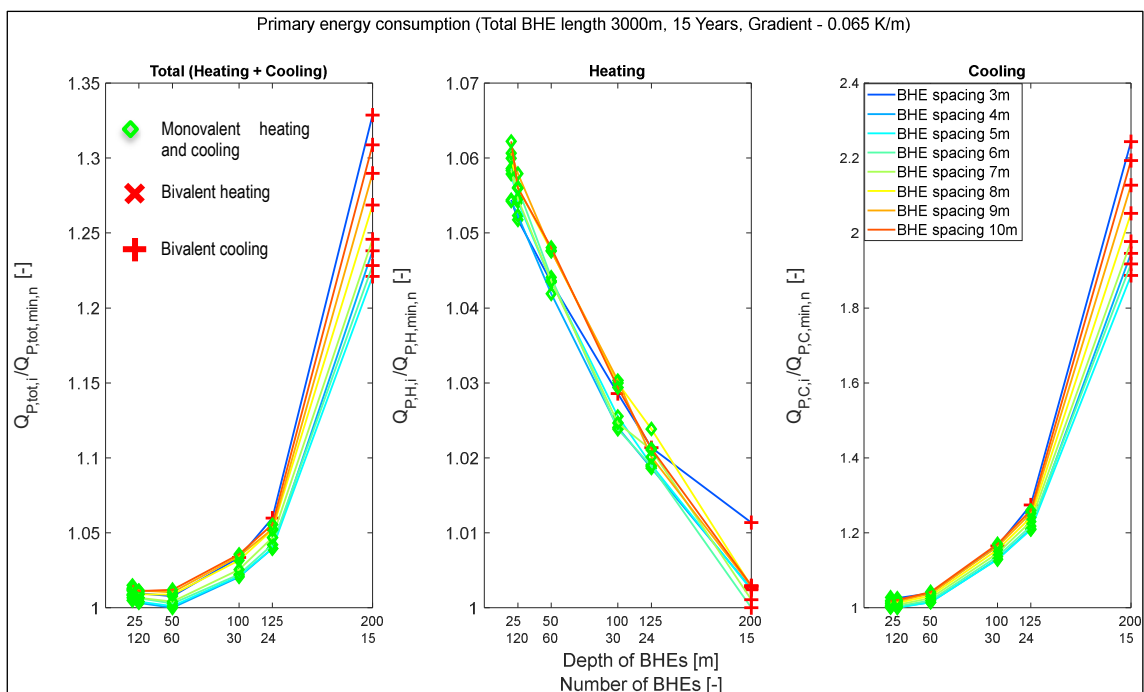


Fig. A-5.10 $Q_{P,tot}$ vs. $Q_{P,H}$ vs. $Q_{P,C}$ for parameter studies 2 (3,000 m, 0.065 K/m).

By considering only monovalent variants, $Q_{P,tot}$ varies around 5%. $Q_{P,H}$ varies around 6%, with deeper BHEs as the minimum point. Here, the influence of favourable operating dominates the influence of pressure drop. This variation is overlaid by $Q_{P,C}$, which varies more than 20% depending on the constructive design. Despite that, significant variation in $Q_{P,C}$ is not reflected in $Q_{P,tot}$. This indicates that a better SPF by cooling system plays a vital role. Variation in $Q_{P,tot}$ is significant, only if addition cooler is used. Overall, it again leads to the suggestion that designing monovalent variants should be the primary concern. To find the variants that secure long term monovalent heating and cooling, average BHE fluid outlet temperatures are evaluated.

Fig. A-5.11 depicts fluid outlet temperature of BHE field averaged over the heat extraction period for 15 years ($\bar{T}_{out,BHE,H}$). Four graphs represent four different gradients. The X-axis represents borehole depth and the corresponding number of boreholes n . Curve

parameters are borehole spacing. As shown in the graph, none of the variants used additional heaters over 15 years of operation. Besides, $\bar{T}_{out,BHE,H}$ lies mostly above 2 °C. Hence, most of the variants unlikely to use the aid of additional heaters in the following years. As cooling is critical for this building model, BHEs field fluid outlet temperature averaged over the heat supply period for 15 years ($\bar{T}_{out,BHE,C}$) is evaluated in the next graph.

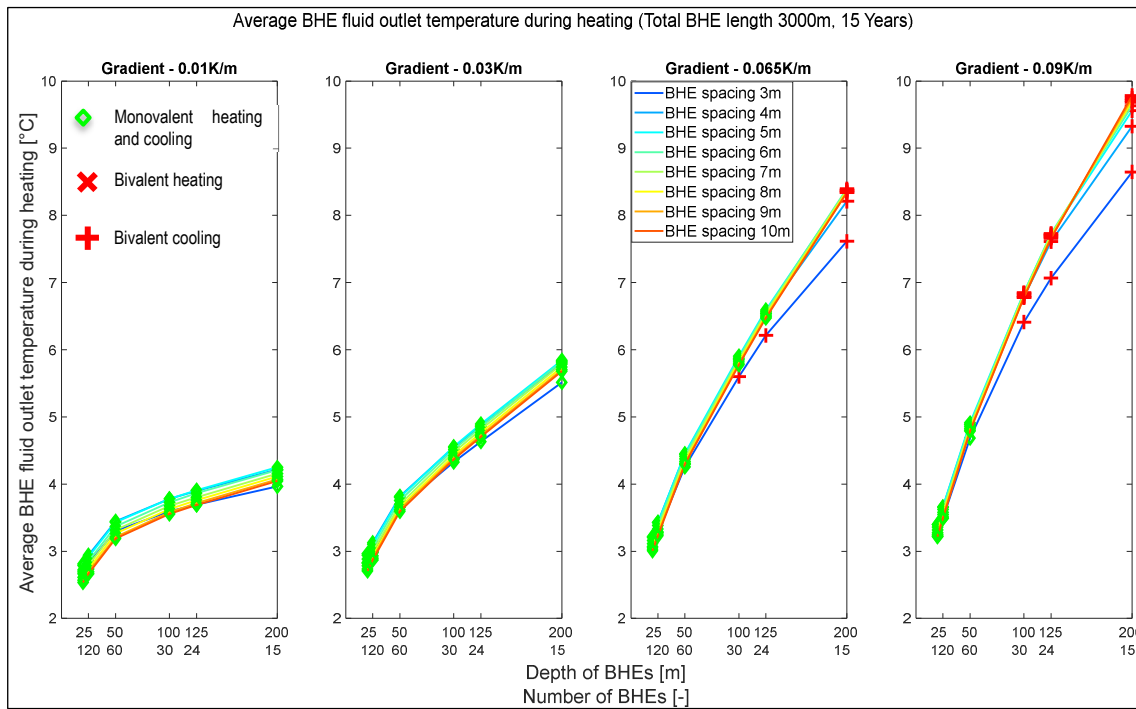


Fig. A-5.11 $\bar{T}_{out,BHE,H}$ (15-year average) for parameter studies 2 (3,000 m).

Fig. A-5.12 depicts fluid outlet temperature BHE field averaged over the heat supply period for 15 years ($\bar{T}_{out,BHE,C}$). Four graphs represent four different gradients. The X-axis represents borehole depth and the corresponding number of boreholes n . Curve parameters are borehole spacing. As shown in the figure, the aid of an additional heater is required mostly if the average temperature is more than 16.5 °C, which occurs mostly by deeper BHEs at gradients 0.065 K/m and 0.09 K/m. 3 m spaced BHEs with gradient is also critical for cooling operation. Though additional cooler was required only for a shorter period, demand might increase in the coming years. Borehole spacing below 4 m poses a high risk of being influenced by short term behaviours. Hence, minimum 4 m borehole spacing is suggested, even for smaller gradients. For gradients 0.01 K/m and 0.03 K/m, all depicted variants were monovalent for the simulated period. For gradient 0.065 K/m, BHEs with depth less than or equal to 125 m and minimum spacing of 4 m is required for monovalent operation. For gradient 0.09 K/m, BHEs with depth less than or equal to 50 m and minimum spacing of 4 m is required for monovalent operation. This evaluation provides information about monovalent variants for the simulated period. To find the variants that secure monovalent operation for a prolonged period, how fast the BHE field cools down or warms up must be analysed. For this purpose, the annual average BHE fluid outlet temperature during the heat extraction period is evaluated in the next graph.

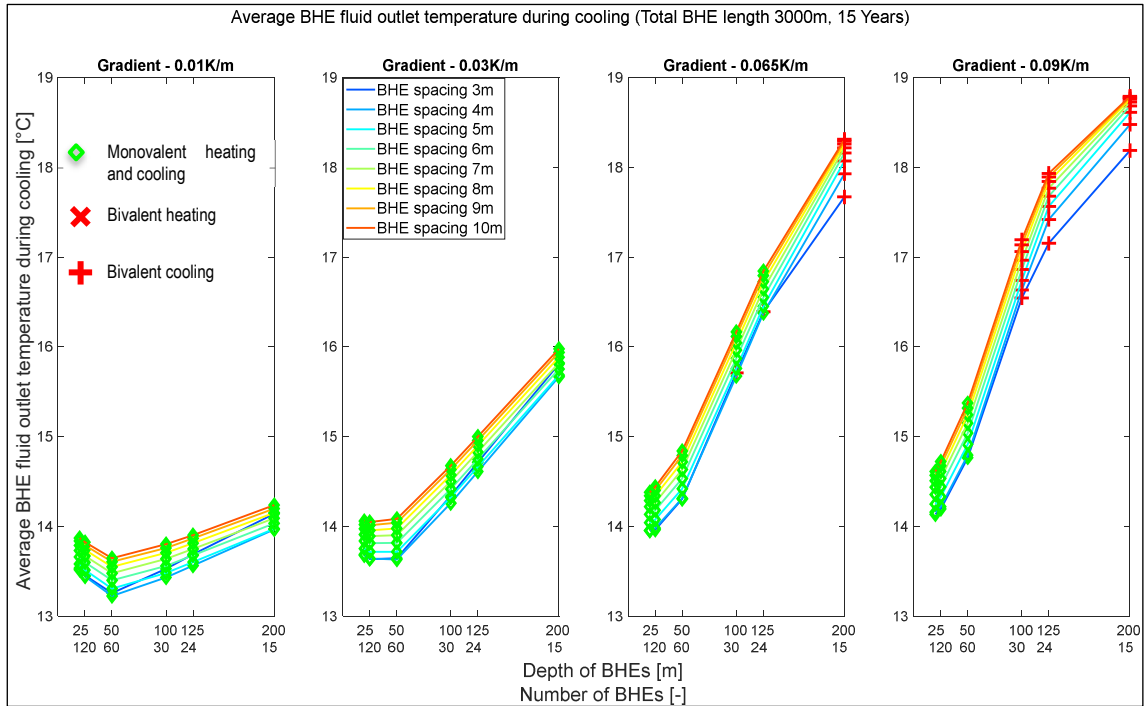


Fig. A-5.12 $\bar{T}_{out,BHE,C}$ (15-year average) for parameter studies 2 (3,000 m).

Fig. A-5.13 depicts BHE field fluid outlet temperature averaged over the heat supply period for a year (total 15 years). From the graph it is clear that operating temperature does not change much over the year. Deeper BHEs have higher $\bar{T}_{out,BHE,C}$ both initially and over year, thus demanding additional cooler to meet the requirement. Hence, all variants which were monovalent during the first 15 years can be monovalent for a prolonged duration.

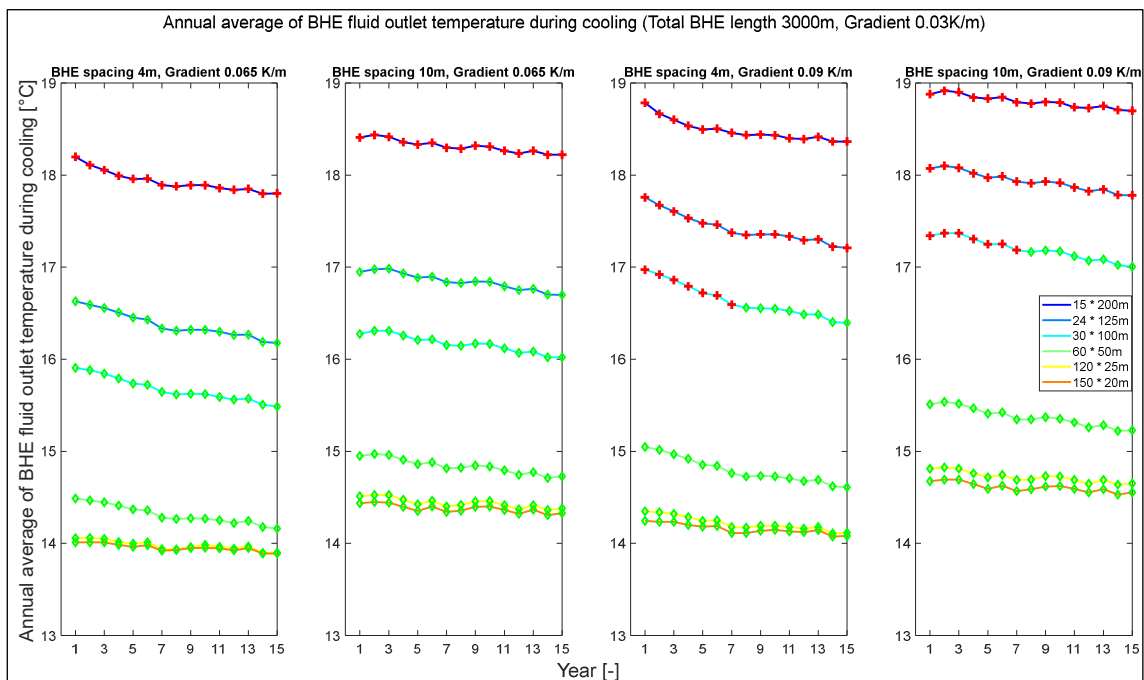


Fig. A-5.13 $\bar{T}_{out,BHE,C}$ (annual average) for parameter studies 2 (3,000 m).

Most bivalent points lie above 16.5 °C for evaluated variants. Hence, to find bivalent points for all simulated variants, the following evaluation, like previous building models, was prepared. In Fig. A-5.14, first graph plots: $\bar{T}_{out,BHE,H}$ averaged over 15 years against the total operating period of the additional heater in 15 years; $\bar{T}_{out,BHE,C}$ averaged over 15 years against the total operating period of the additional cooler in 15 years, Second graph plots: $\bar{T}_{out,BHE,H}$ averaged over a year and operating period of the additional heater in the respective year (total 15 years); $\bar{T}_{out,BHE,C}$ averaged for every year and operating period of the additional cooler in the respective year (total 15 years).

It is clear from the graph that most of the bivalent points lie above 16.5 °C for both 15-year average and annual average values. The aid of an additional cooler is required if the outlet fluid temperature of the BHE field crosses the limit of 20 °C. For the variants with $\bar{T}_{out,BHE,C}$ (averaged over year) more than 16.5 °C, there exists a greater possibility of demanding additional energy from the auxiliary cooler. *Hence, future designing of the BHE field for such a building model can be carried out with simple mathematical models, and the variants in which $\bar{T}_{out,BHE,C}$ stays below 16.5 °C can be considered monovalent variants. But this thesis has to be further analysed to provide plausible conclusions.*

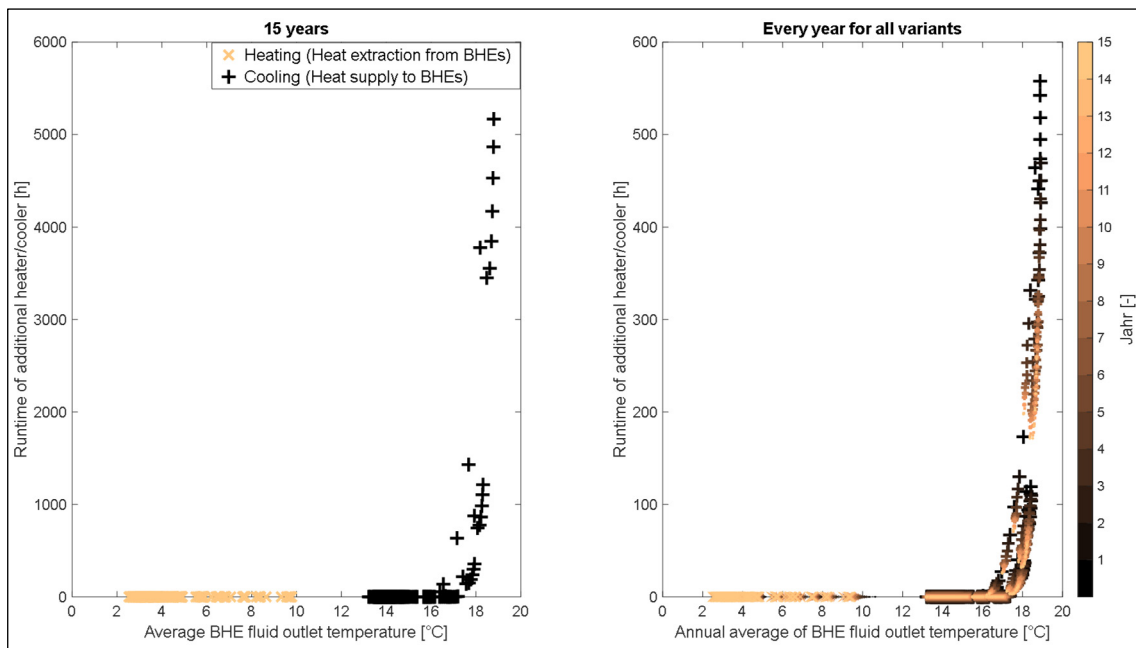


Fig. A-5.14 Bivalent point vs. operation period of auxiliary heater / cooler (parameter studies 2).

5.3 Parameter studies 3

Third parameter studies have been carried out with the building model with predominant cooling demand (building model explained in section 4.5.3). Base constructive design of BHE field is carried out in EED (see section 4.5.3). Initial parameter studies were carried out varying constructive parameters with base design (3,000 m total probe length). Similar to previous parameter studies 1 and 2, this parameter studies had also shown that most variants are bivalent over the simulation period of 15 years. Hence, further parameter studies with an increased total probe length of 4,000 m were carried out. Observation made during these parameter studies is explained in this section with relevant diagrams.

5.3.1 Variant matrix

Tab. A-5.3 Variant matrix for parameter studies 3.

Parameter	Unit	Value					
Total BHE length	[m]	4,000					
Number of BHEs n	[-]	20	32	40	80	160	200
Depth of BHEs	[m]	200	125	100	50	25	20
Borehole spacing	[m]	1, 2, 3, 4, 5, 6, 7, 8, 9, 10					
Geothermal gradient	[K/100 m]	1					
		3 The average value for Germany					
		6,5 At Zittau					
		9					
Hydraulic connections of BHEs in field		parallel					
BHE pipe dimension		32 x 2.9 mm					

$$N_1 = N_2 = N_3 = N_4 = Var1 \cdot Var2 \cdot Var3 \cdot Var4 = 1 \cdot 6 \cdot 10 \cdot 1 = 60 \quad (\text{A.53})$$

$$N = N_1 + N_2 + N_3 + N_4 = 60 + 60 + 60 + 60 = 240$$

5.3.2 Results

Fig. A-5.15 depicts the ratio of primary energy consumption ($Q_{P,tot}$) of a particular variant to the minimum primary energy consumption ($Q_{P,tot,min}$) from all variants (A.21) in respective gradient for 15 years (Y-axis). Four graphs represent four gradients. The X-axis represents borehole depth and the corresponding number of boreholes n . Curve parameters are borehole spacing. Value 1.05 represents 5 % more primary energy consumption than the minimum variant. Note: X-axis does not have the same maximum as previous evaluations. Smaller borehole spacing (less than 3 m) are ignored to avoid inconsistencies in evaluation.

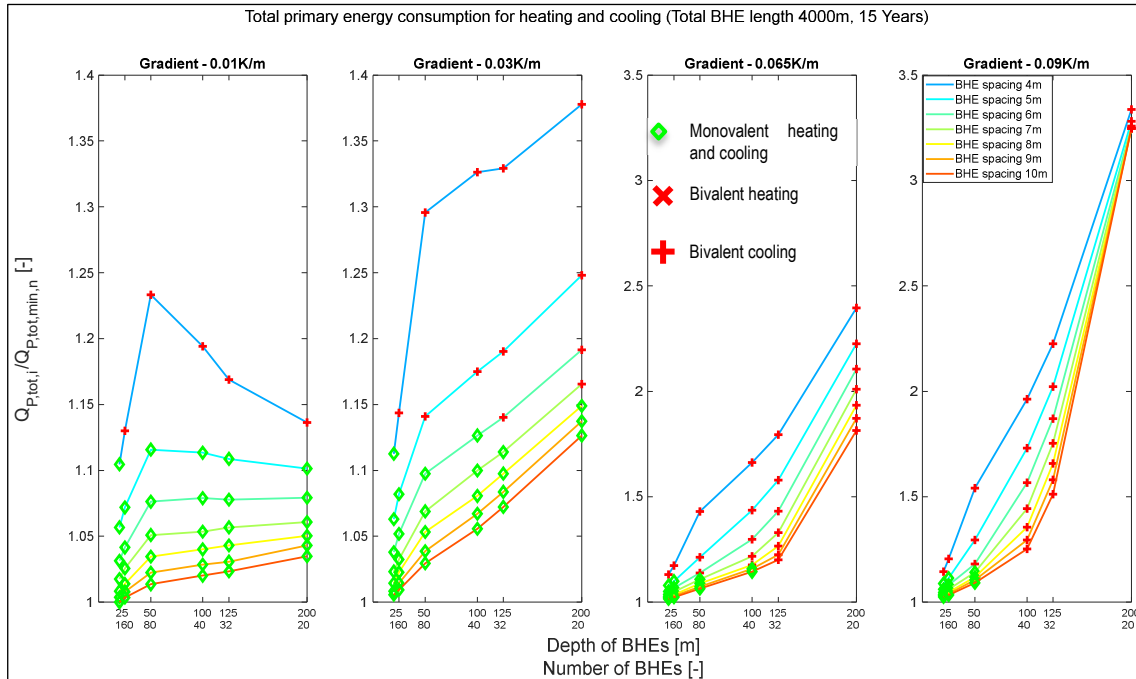


Fig. A-5.15 $Q_{P,tot}$ for parameter studies 3 (4,000 m).

This evaluation shows that the constructive design of BHEs has a significant influence on total primary energy consumption (varies 10 to 14 % depending on gradient) even by considering only monovalent variants. 20 m deep BHEs with larger borehole spacing of 10 m is optimum in all gradients. But, variants with 20 m and 25 m deep BHEs required a gigantic land area. In locations with gradients 0.01 K/m and 0.03 K/m, lack of ground surface can be compensated by deeper BHEs with less borehole spacing. For gradient 0.065 K/m, BHEs with a maximum depth of 100 m and minimum borehole spacing of 8 m is required. For gradient 0.09 K/m, BHEs with a maximum depth of 50 m and minimum borehole spacing of 6 m is required. Though these variants are monovalent for simulated periods, monovalent operation, particularly for cooling, cannot be assured for more prolonged periods. To find the variants that assure monovalent operation for a longer duration, the average fluid outlet temperature of the BHE field during the heat supply period must be evaluated. Before that, the following factors are explained with relevant examples. First, primary energy consumption for heating/cooling and its reflection in total primary energy consumption. Second, Variation of primary energy consumption for heating and cooling depending on construction parameters.

Fig. A-5.16 depicts the ratio of primary energy consumption of a particular variant to the minimum primary energy consumption from all variants in gradient 0.065 K/m for 15 years (Y-axis). Three graphs represent total primary energy consumption (A.21), primary energy consumption for heating (A.22), and primary energy consumption for cooling (A.23), respectively. As shown in the graph, total primary energy consumption ($Q_{P,tot}$) varies more than 100 % considering all variants. Considering only monovalent variants, $Q_{P,tot}$ varies around 12 %. Primary energy consumption for heating ($Q_{P,H}$) varies about 8 %, with 200 m deep BHEs as the minimum point. $Q_{P,C}$ varies more than 250 % by considering all variants, and it varies around 25 % by considering only monovalent variants.

This implicates that the central focus of designing the BHE field is supposed to be both minimum $Q_{P,tot}$, and secured long term monovalent operation. Variants with minimum energy consumption can be predicted from Fig. A-5.15. A secured long-term monovalent operation can be judged only by observing the average fluid outlet temperature of BHEs. Though none of the depicted variants are bivalent for heating over a simulated period, conclusions about long-term monovalent operation can be made only with the average fluid outlet temperature of BHEs during the heat extraction period.

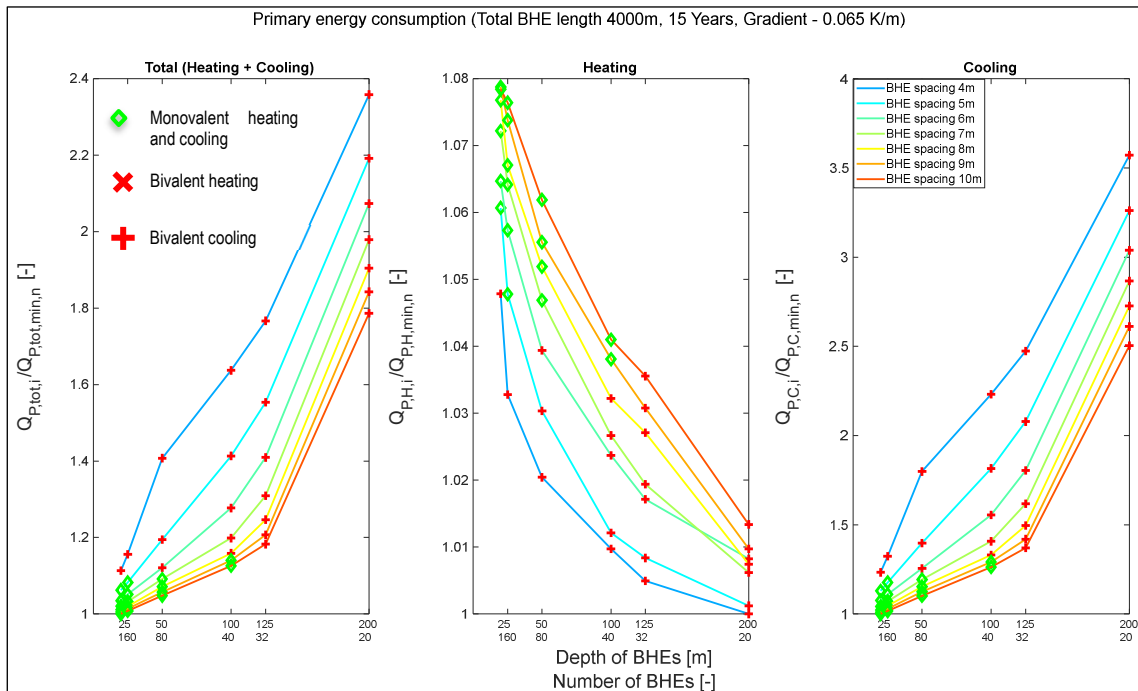


Fig. A-5.16 $Q_{P,tot}$ vs. $Q_{P,H}$ vs. $Q_{P,C}$ for parameter studies 3 (4,000 m, 0.065 K/m).

Fig. A-5.17 depicts fluid outlet temperature of BHE field averaged over the heat extraction period for 15 years ($\bar{T}_{out,BHE,H}$). Four graphs represent four different gradients. The X-axis represents borehole depth and the corresponding number of boreholes n . Curve parameters are borehole spacing. As shown in the graph, none of the depicted variants used additional heaters over 15 years of operation. Besides, $\bar{T}_{out,BHE,H}$ lies mostly above 6 °C. This implies that the depicted variants unlikely to use the aid of additional heaters in the following years. Also, predominant heat supply to the ground leads to a continuous increase in ground temperature over the year, which is favourable for monovalent heating. But cooling is critical for this building model due to the predominant supply to the ground, particularly at larger gradients. To identify the variants that can assure monovalent cooling for a more extended period, the fluid outlet temperature of the BHE field averaged over the heat supply period for 15 years ($\bar{T}_{out,BHE,C}$) is evaluated next figure.

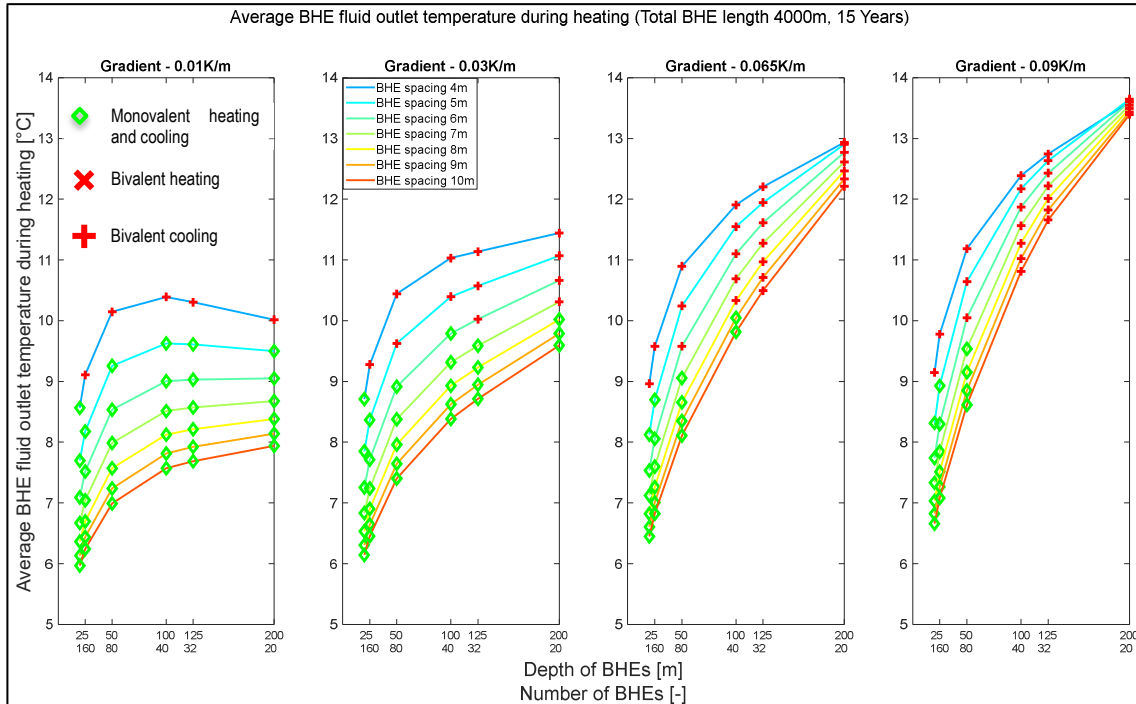


Fig. A-5.17 $\bar{T}_{out,BHE,H}$ (15-year average) for parameter studies 3 (4,000 m).

Fig. A-5.18 depicts fluid outlet temperature of BHE field averaged over the heat supply period for 15 years ($\bar{T}_{out,BHE,C}$). Four graphs represent four different gradients. The X-axis represents borehole depth and the corresponding number of boreholes n . Curve parameters are borehole spacing. As shown in the figure, the aid of an additional cooler is required mostly if $\bar{T}_{out,BHE,C}$ is more than 16.5 °C. This occurs mostly by deeper BHEs and compactly arranged BHEs. In locations with gradient 0.01 K/m and 0.03 K/m, 125 m or less deep BHEs with borehole spacing minimum of 7 m has $\bar{T}_{out,BHE,C}$ less than 16 °C, and 50 m or less deep BHEs has a temperature near to 15 °C. But at higher gradients, only 20 m and 25 m deep BHEs have a temperature below 16 °C. Here, 50 m deep BHEs are still monovalent but in the critical limit. As none of the monovalent variants has $\bar{T}_{out,BHE,C}$ far away from the critical limit of 16.5 °C, secured long term monovalent variant cannot be judged without observing annual average $\bar{T}_{out,BHE,C}$. Temperature development around BHEs at smaller gradients (0.01 K/m and 0.03 K/m) are different from larger gradients (0.065 K/m and 0.09 K/m). Hence, annual average $\bar{T}_{out,BHE,C}$ are compared separately for smaller and larger gradients.

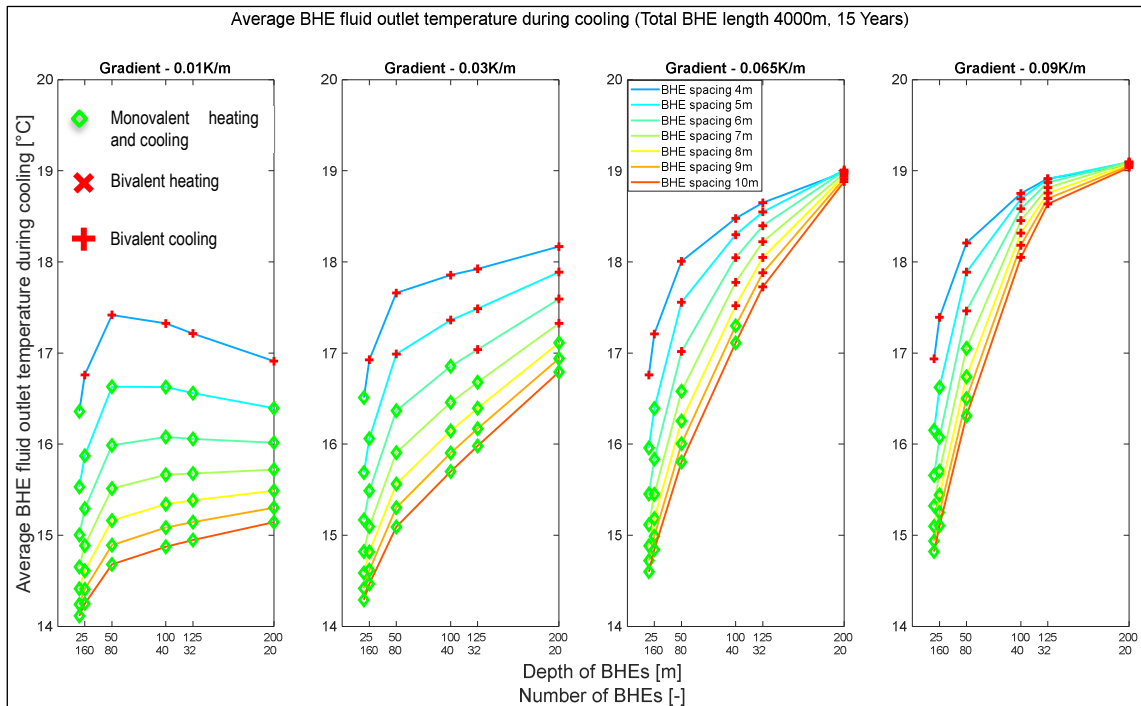


Fig. A-5.18 $\bar{T}_{out,BHE,C}$ (15-year average) for parameter studies 3 (4,000 m).

Fig. A-5.19 depicts annually-averaged $\bar{T}_{out,BHE,C}$ (total 15 years) for two borehole spacings (7 m and 10 m) at gradients 0.01 K/m and 0.03 K/m. Curve parameters are borehole depth and the corresponding number of BHEs. Variants monovalent and bivalent for heating and cooling are marked separately. As shown in the graph, constructions with several BHEs of depth of 20 m and 25 m stabilize fast. If BHEs are arranged with sufficient space between them (10 m), the temperature curve flattens for deeper BHEs. 80 BHEs each of depth 50 m placed 10 m apart from each other sound promising. Still, this construction needs a large ground area, which might not be possible in most cases. Several remaining monovalent variants cannot be judged yet, as $\bar{T}_{out,BHE,C}$ is already near to a critical limit of 16.5 °C.

Fig. A-5.20 depicts annually averaged $\bar{T}_{out,BHE,C}$ (total 15 years) for two borehole spacings (7 m and 10 m) at gradients 0.065 K/m and 0.09 K/m. Again, only for the variants with BHEs of depth 20 m and 25 m placed 10 m apart, the curve flattens around 15 °C. Several remaining monovalent variants have $\bar{T}_{out,BHE,C}$ near the critical limit of 16.5 °C.

It can be summarized that variants which can assure long term monovalent operation are several BHEs of less depth (20 to 25 m in our example). These constructions need vast land area, which is unrealistic. Though there are many realistic constructions with which monovalent heating and cooling are possible for 15 years, the same cannot be assured for a prolonged duration. Hence, this building model conclusion can be made only if realistic variants are simulated for a complete period of system design (50 years).

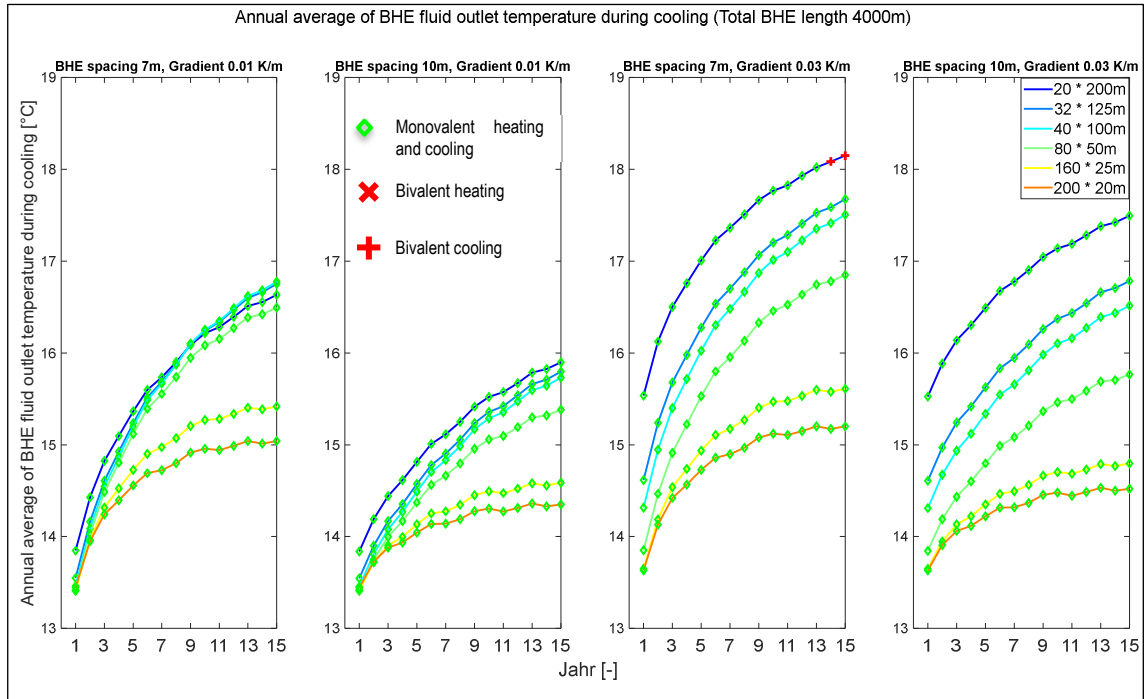


Fig. A-5.19 $\bar{T}_{out,BHE,C}$ (annual average) for parameter studies 3 (4,000 m, 0.01 K/m vs. 0.03 K/m).

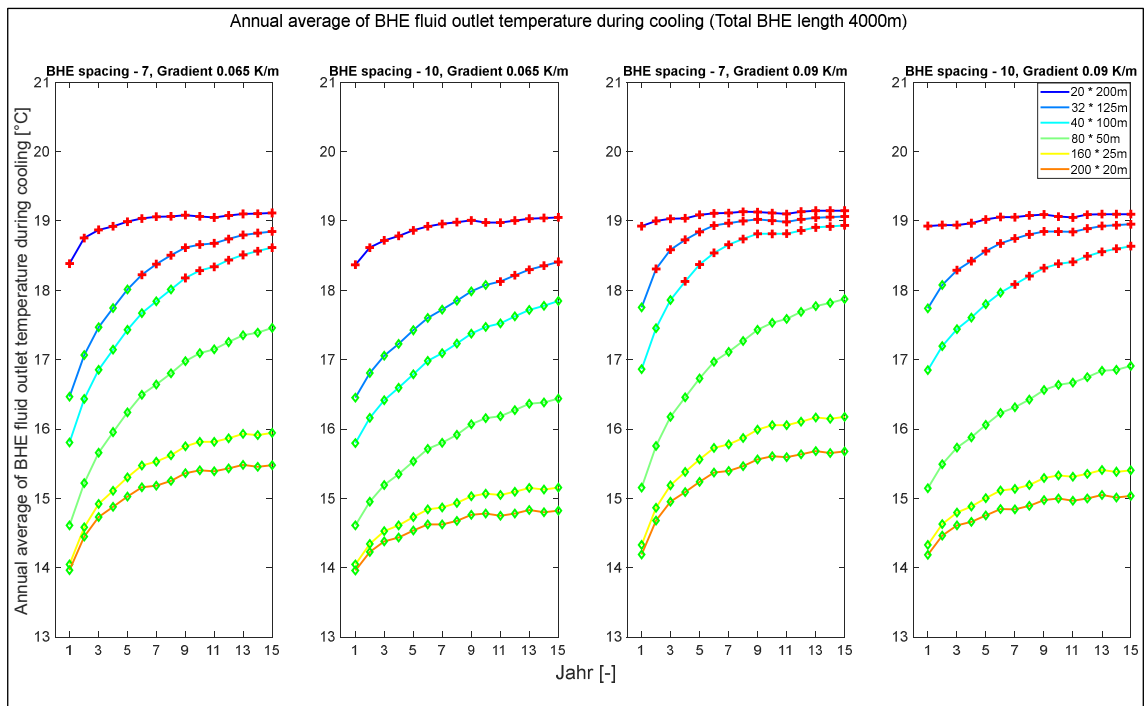


Fig. A-5.20 $\bar{T}_{out,BHE,C}$ (annual average) for parameter studies 3 (4,000 m, 0.065 K/m vs. 0.09 K/m).

Similar to previous building models, evaluation to identify bivalent points from all variants were prepared. In Fig. A-5.21, first graph plots: $\bar{T}_{out,BHE,H}$ averaged over 15 years against a total operating period of the additional heater in 15 years; $\bar{T}_{out,BHE,C}$ averaged over 15 years against a total operating period of the additional cooler in 15 years, Second graph plots: $\bar{T}_{out,BHE,H}$ averaged over a year and operating period of the additional heater in the respective year (total 15 years); $\bar{T}_{out,BHE,C}$ averaged for every year and operating period of the additional cooler in the respective year (total 15 years).

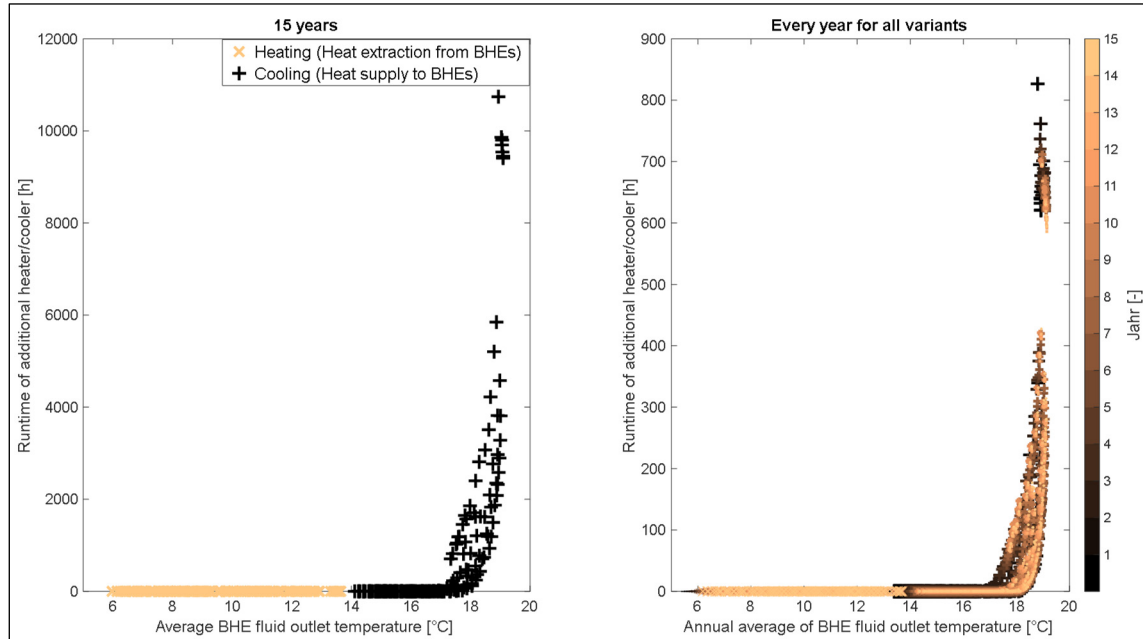


Fig. A-5.21 Bivalent point vs. operation period of auxiliary heater / cooler (parameter studies 3).

It is clear from the graph that most of the bivalent points lie above 16.5 °C for both 15-year average and annual average values for this parameter studies. The aid of an additional cooler is required if the outlet fluid temperature of the BHE field crosses the limit of 20 °C. For the variants with $\bar{T}_{out,BHE,C}$ (averaged over year) more than 16.5 °C, there exists a greater possibility of demanding additional energy from an auxiliary cooler. *As like previous simulation models, in future designing of BHE field for such building can be carried out with simple mathematical models, and the variants in which $\bar{T}_{out,BHE,C}$ stays below 16.5 °C can be considered as monovalent variants. Again, this thesis has to be further analysed to provide plausible conclusions.*

5.4 Summary of parameter studies

Through parameter studies with the building with predominant heating demand, it was observed that designing the variant that assures monovalent heating and cooling for a longer duration is supposed to be the primary goal. Significant variation in primary energy consumption arises because of substantial energy demands from additional heating and cooling system. Using an additional heating/cooling system with better COP will reduce the deviation but cannot be used as an alternate because a ground sourced heating and cooling system has a better SPF than most of the concurrent systems. Among monovalent variants, the potential for energetic optimization is insignificant. For such building models, deep BHEs (100 m to 200 m) with borehole spacing of 10m can assure monovalent heating and cooling. Only at locations with high geothermal gradients (0.09 K/m in our example), 200 m deep BHEs should be avoided as it is unfavourable for cooling, particularly during initial years of system operation. In this case, 125 m deep BHEs with 10 m borehole spacing is suggested.

Through parameter studies with the building with almost similar heating and cooling demand, it is again observed that designing monovalent variants for heating and cooling is essential. Unlike the previous building models, a compact arrangement with a minimum borehole spacing of 4 m is possible. Due to better regeneration, the temperature of the ground does not change much for this building model. Hence, the variants which were monovalent during the simulated period can be monovalent for a longer duration. At locations with smaller gradients (0.01 K/m or 0.03 K/m), all construction with 20 m to 200 m deep BHEs works. Therefore, variants can be chosen based on land availability. At locations with a gradient of 0.065 K/m, BHEs cannot be 200 m deep. Thus, constructions with less borehole depth should be chosen (24 x 125 m deep BHEs from our evaluation). At locations with a gradient of 0.09 K/m, BHEs cannot be 100 m deep or more. Thus, constructions with less borehole depth should be chosen (For example, 50 x 60 m deep BHEs from our evaluation).

Parameter studies with the building that has predominant cooling demand ended up without a conclusion. Variants with 200 BHEs each of depth 20 m and 160 BHEs each of depth 25 m assure monovalent cooling for a prolonged duration. But for these variants, higher borehole spacing is required at locations with higher gradients. These constructive designs cannot be considered sensible due to the requirement of a vast land area. Several other variants were monovalent during the first 15 years. But annual average fluid outlet temperature from the BHE field is near to critical limit. Hence, to assure long-term monovalent operation, simulation over the complete system design period is essential (50 years). Due to time restrictions, 50-year simulations were not possible in the framework of this project. *50-year simulations might be carried out if a follow-up project is generated.*

6 Conclusion

During the project duration, multiple parameter studies were carried out to optimize the constructive design of the BHE field. These parameter studies provided insight into energetic optimization potential for different building models and the importance of designing a BHE field that assures long-term monovalent heating and cooling. With the actual results, judgments about monovalent variants were made for two building models (with predominant heating demand, almost equal heating and cooling demand). It was concluded that to make judgments about monovalent variants for building with predominant cooling demand, a 50-year simulation was essential. Due to time restrictions, these simulations were unachievable during the project duration. Probably, this might be performed in a follow-up project or by Promotion Haack, if required.

In addition to parameter studies, multiple sub-tasks were carried out within the framework of this project. Most of the work revolves around completing the simulation model, widening the scope of parameter studies, and finally automatizing parameter studies. Mathematical models for calculating pressure drop on the primary side of the heat pump and Double depressurized differential manifold (DDV) were developed to complete the simulation model. Finding the building models with different use-energy consumption ratios was essential to widen the parameter studies' scope. The development of macros tools in Microsoft Excel was essential for automatizing parameter studies and arranging the results. Necessary sub-tasks were documented in this report.

Besides, the potential for energetic optimization by using an inverter heat pump (IVHP) was explored. During simulative analysis, it was observed that there is a potential for energy saving by using an inverter heat pump (IVHP). Hence, initially, theoretical optimization potential by IVHP was validated through preliminary investigations. This investigation includes literature research, simulative analysis, and experimental investigation in collaboration with work described in Chapter B. After validating theoretical optimization potential, mathematical modelling of the inverter heat pump was initiated. *The model mathematical model has to be verified with experimental investigation.*

Literature

- BAGARELLA, G.; LAZZARIN, R. & NORO, M. (2016): Sizing strategy of on-off and modulating heat pump systems based on annual energy analysis. – *Int. J. Refrigeration*, 65: 183-193.
- DIN EN 1264-5:2020-02 (Entwurf), Raumflächenintegrierte Heiz- und Kühlsysteme mit Wasserdurchströmung – Teil 5: Heiz- und Kühlflächen in Fußböden, Decken und Wänden – Bestimmung der Wärmeleistung und der Kühlleistung.
- DIN EN 15251:2012-12, Eingangsparameter für das Raumklima zur Auslegung und Bewertung der Energieeffizienz von Gebäuden – Raumluftqualität, Temperatur, Licht und Akustik.
- DIN V 18599, Energetische Bewertung von Gebäuden (13 Teile und 2 Beiblätter).
- DIMPLEX: Wärmepumpenmanager, Operating instructions for technicians. Bestell-Nr.: 452115.66.74; 34 S.
- EnEV 2013, Energieeinsparverordnung. Verordnung über energiesparenden Wärmeschutz und energiesparende Anlagentechnik bei Gebäuden. EnEV vom 24.07.2007 (BGBl. I S. 1519), zuletzt geändert durch Art. 2 des 4. Gesetzes zur Änderung des EnEV vom 04.07.2013 (BGBl. I S. 2197).
- GASSER, L.; FLÜCK, S.; KLEINGRIES, A. & WELLIG, B. (2017): Efficiency Improvements of Brine/Water Heat Pumps through Capacity Control. – 12th IEA Heat Pump Conference 2017, Rotterdam.
- LfU, BAYERISCHES LANDESAMT FÜR UMWELT (Hrsg., 2008): Effiziente Energienutzung in Bürogebäuden, Planungseifaden. – Eigenverlag: 67 S.; Augsburg.
- MADANI, H.; CLAEISSON, J. & LUNDQVIST, P. (2011): Capacity control in ground source heat pump systems. Part II: Comparative analysis between on/off controlled and variable capacity systems. – *Int. J. Refrigeration*, 34: 1934-1942.
- MERKER, O.; PÄRISCH, P. & OBERDORFER, P. (2014): Taktverhalten von Sole/Wasser-Wärmepumpen - Messung der thermischen Zeitkonstanten und ihre Bedeutung für die Jahresarbeitszahl. – Institut für Solarenergieforschung GmbH Hameln/Emmerthal (SFH), BauSIM 2014.
- VDI 4640-2:2015-05, Thermische Nutzung des Untergrundes – Erdgekoppelte Wärmepumpenanlagen (Entwurf).
- WAGNER, W. (2012): Strömung und Druckverlust. – Vogel Communications Group GmbH & Co. KG, 7. Aufl.: 318 S.; Würzburg.